



**US Army Corps
of Engineers®**
Engineer Research and
Development Center

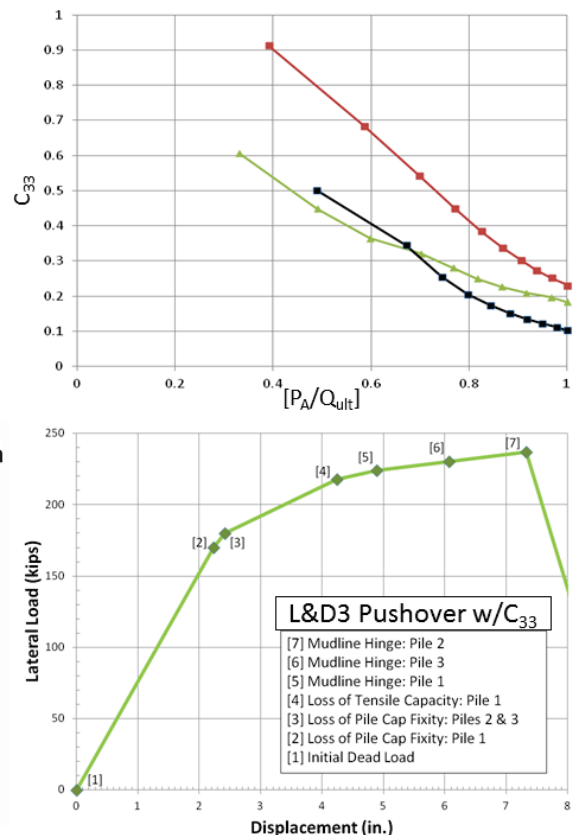
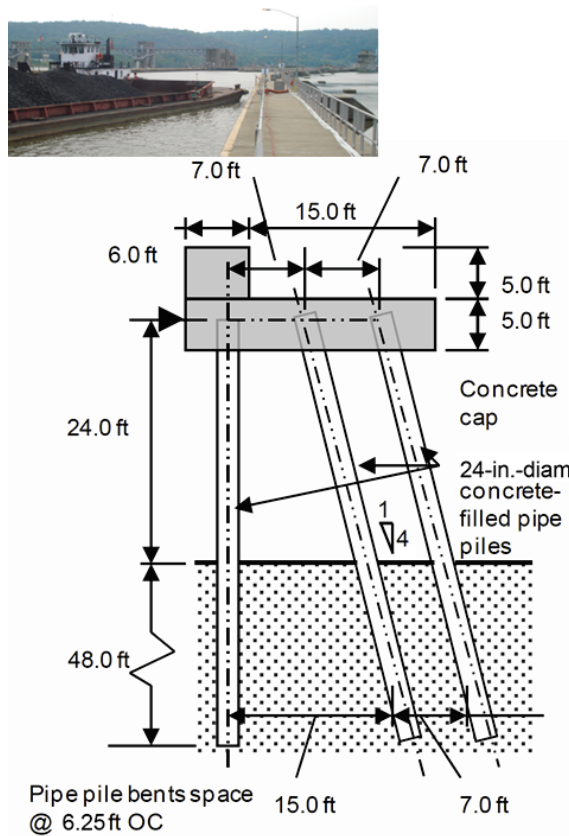
ERDC
INNOVATIVE SOLUTIONS
for a safer, better world

Navigation Systems Research Program

Characterizing Axial Stiffness of Individual Batter Piles with Emphasis on Elevated, Laterally Loaded, Clustered Pile Groups

Robert M. Ebeling and Barry C. White

November 2016



The U.S. Army Engineer Research and Development Center (ERDC) solves the nation's toughest engineering and environmental challenges. ERDC develops innovative solutions in civil and military engineering, geospatial sciences, water resources, and environmental sciences for the Army, the Department of Defense, civilian agencies, and our nation's public good. Find out more at www.erdcl.usace.army.mil.

To search for other technical reports published by ERDC, visit the ERDC online library at <http://acwc.sdp.sirsi.net/client/default>.

Characterizing Axial Stiffness of Individual Batter Piles with Emphasis on Elevated, Laterally Loaded, Clustered Pile Groups

Robert M. Ebeling and Barry C. White

*Information Technology Laboratory
U.S. Army Engineer Research and Development Center
3909 Halls Ferry Road
Vicksburg, MS 39180-6199*

Final report

Approved for public release; distribution is unlimited.

Prepared for U.S. Army Corps of Engineers
Washington, DC 20314-1000

Under Work Unit 448769, "Flexible Approach Walls"

Abstract

This report focuses on an investigation into the engineering characterization of the axial stiffness of individual compression piles embedded within soil. This characterization of axial stiffness is used in the analysis of a clustered pile group's deformation and load distribution response. Its impact on the computed pile group response is most pronounced among a clustered pile group containing batter piles.

This characterization is important because the Corps is moving toward low-cost, pile-founded flexible lock approach walls. These walls absorb kinetic energy of barge-train impacts, which occur as the barge train aligns itself to enter the lock. One type of wall is comprised of an elevated impact deck supported by groups of clustered piles, some with batter. These impact decks are supported tens of feet above the mudline.

A pushover analysis technique is used to establish the potential energy (PE) capacity and displacement capacity of individual batter pile groups accounting for the various pile failure mechanisms. An appropriate axial stiffness characterization will increase the accuracy of this computation. The total stored energy (PE) of the approach wall system will be the sum of the stored energy of all the pile groups reacting to the barge impact. The study concludes with a pushover analysis of a batter pile configuration used at Lock and Dam 3 flexible approach wall extension.

Batter pile groups are constructed of steel pipe or H-piling, which are conducive to in-the-wet construction. This type of construction leads to a cost savings for Corps projects.

DISCLAIMER: The contents of this report are not to be used for advertising, publication, or promotional purposes. Citation of trade names does not constitute an official endorsement or approval of the use of such commercial products. All product names and trademarks cited are the property of their respective owners. The findings of this report are not to be construed as an official Department of the Army position unless so designated by other authorized documents.

DESTROY THIS REPORT WHEN NO LONGER NEEDED. DO NOT RETURN IT TO THE ORIGINATOR.

Contents

Abstract	ii
Figures and Tables.....	v
Preface.....	x
Unit Conversion Factors	xi
1 Introduction: Analysis of Pile Group Deformation and Distribution of Individual Pile Loadings for a Batter Pile Configuration with Respect to a Pushover Analysis	1
1.1 Introduction.....	1
1.2 Background.....	1
1.3 Analyzing massive concrete pile-founded structures	1
1.4 Pile-group founded flexible approach walls.....	2
1.5 Introducing the CPGA software family.....	5
1.6 Analyzing flexible approach walls with CPGA	7
1.7 Using pushover analysis to establish extreme behavior in flexible walls	8
1.8 A criteria for long pile behavior and minimum pile lengths.....	9
1.9 Axial stiffness of piles embedded in soil as input for CPGA.....	12
1.10 Objective	13
1.11 Approach	13
2 The Characterization of Axial Pile Stiffness in CASE software.....	15
2.1 Introduction.....	15
2.2 Introduction to CPGA analysis and coordinate systems (global and pile)	15
2.3 Pile stiffness, pile group stiffness, and local and global force-displacement relationships	19
2.4 Axial pile stiffness b_{33} and axial pile stiffness modifier C_{33}	23
3 Examples of Axial Pile Stiffness Computations for Batter Piles in Stratified and Homogeneous Foundations	30
3.1 Introduction.....	30
3.2 Data reduction of CAXPILE results into values for the CPGA C_{33} parameter for batter piles	31
3.3 Axial pile stiffness characterization of a compression batter pile at the Lock and Dam 3 layered soil site	32
3.4 Axial capacity of a tension batter pile at the Lock and Dam 3 layered soil site.....	35
3.5 Axial pile stiffness characterization of a Lock and Dam 3 type batter pile configuration founded in a hypothetical medium-dense sand	36
3.6 Axial pile stiffness characterization of a Lock and Dam 3 type batter pile configuration founded in a hypothetical dense sand.....	40
3.7 Observations regarding the level of axial compression pile loading, P_A	43
3.8 Concluding remarks	44
4 Using an Axial Pile Stiffness C_{33} Term in a Pushover Analysis of a Clustered Group of Batter Piles	47

4.1	Determination of the axial pile stiffness (C_{33}) term and pushover analysis.....	47
4.2	Example pushover analysis (with C_{33} determination) of the Lock and Dam 3 cluster batter pile configuration	48
4.3	Conclusions.....	56
5	Summary and Conclusions	57
5.1	Summary.....	57
5.2	Conclusions.....	57
	References	61
	Appendix A: Pile Shaft Friction and End Bearing of Driven Pipe Piles.....	64
	Appendix B: Pipe Pile Buckling Evaluation	80
	Appendix C: Axial Capacity of the Concrete-Filled Batter Pile at Lock and Dam 3 and Evaluation of the Value of the CPGA C_{33} Term	93
	Appendix D: Axial Capacity of a Lock and Dam 3 Concrete-Filled Batter Pile Founded in Medium-Dense Sand and Evaluation of the Value of the CPGA C_{33} Term.....	108
	Appendix E: Axial Capacity of Lock and Dam 3 Concrete-Filled Batter Pile Founded in Dense Sand and Evaluation of the Value of the CPGA C_{33} Term	120
	Appendix F: Final CPGA Input Files and Associated Output for Each Incremental Stage of Pushover Analysis Number 1 for a Lock and Dam 3 Approach Wall Batter Pile Group in Its Layered Soil Site.....	132
	Report Documentation Page	

Figures and Tables

Figures

Figure 1.1. Pile layout for soil-founded spillway at Melvin Price Lock and Dam in St. Louis, MO (after Ebeling et al. 2013).	2
Figure 1.2. Idealization of a single group of three, clustered, concrete-filled, 24 in. diameter pipe piles supporting a 6.25 ft tributary section of impact deck of the flexible lock approach wall extension at Lock and Dam 3 on the Upper Mississippi River	4
Figure 1.3. The impact deck supported over clustered pile groups at the flexible lock approach wall extension at Lock and Dam 3 on the Upper Mississippi River.	5
Figure 1.4. Cut-out view of the impact deck and its pile layout for the flexible lock approach wall extension at Lock and Dam 3 on the Upper Mississippi River.	6
Figure 1.5. Idealization of the pile layout for the flexible lock approach wall extension at Lock and Dam 3 on the Upper Mississippi River.	8
Figure 1.6. Resulting load-displacement plot characterizing the pushover capacity of the batter pile configuration for Lock and Dam 3 for fixed-head and free-head boundary conditions at the pile cap (after Ebeling et al. 2012).....	10
Figure 1.7. Load transfer by combined skin friction and tip bearing for an axially loaded compression pile (after Harman et al. 1989).....	13
Figure 2.1. A CPGA global coordinate system centered at the origin, which is located at the center of the rigid pile cap (after Harman et al. 1989).	16
Figure 2.2. A CPGA batter pile group layout and origin specification near the center of the rigid pile cap (after The CASE Task Group on Pile Foundations 1983).....	17
Figure 2.3. Cross-section viewing of an earth retaining wall founded on rows of batter pile groups 3 ft center-on-center along the retain wall (after Hartman et al. 1989).....	18
Figure 2.4. The CPGA local pile head forces, moments, deflections, and rotations (after Harman et al. 1989).	21
Figure 2.5. The CPGA local pile head and global, orthogonal, right-hand coordinate systems (after The CASE Task Group on Pile Foundations 1983).	22
Figure 2.6. Illustration of axial load transfer in a pile with depth (after The CASE Task Group on Pile Foundations 1983).	24
Figure 2.7. Load transfer by combined skin friction and tip bearing for an axially loaded compression pile (after Harman et al. 1989).....	25
Figure 2.8. Load transfers for an axially loaded compression pile (after Harman et al. 1989).	26
Figure 2.9 Compression pile axial load versus deflection curve (after Harman et al. 1989).....	27
Figure 3.1. C_{33} versus axial load expressed as a fraction of the axial capacity of a 4V:1H batter compression pile at Lock and Dam 3 Guidewall extension for the layered soil profile at station 21 + 72, computed using the CAXPILE Soil criteria, WES criteria, and VJ criteria.....	33
Figure 3.2. C_{33} versus axial load expressed as a fraction of the axial capacity of an equivalent vertical batter pile in medium-dense sand for a 4V:1H batter compression pile type configuration used at Lock and Dam 3 guidewall extension, computed using the CAXPILE Soil criteria, WES criteria, and VJ criteria.	37

Figure 3.3. C_{33} versus axial load expressed as a fraction of the axial capacity of an equivalent vertical batter pile in dense sand for a 4V:1H batter compression pile type configuration used at Lock and Dam 3 guidewall extension, computed using the CAXPILE Soil criteria, WES criteria, and VJ criteria.	41
Figure 4.1. Resulting load-displacement plot characterizing the pushover capacity of the batter pile configuration for Lock and Dam 3, given two different values of C_{33}	54
Figure A.1. (a.) Values of α versus undrained shear strength; (b.) values of α_1 α_2 applicable for very long piles (after EM 1110-2-2906, HQUSACE 1991).	71
Figure A.2. Unit side resistance for piles in sand versus relative length (Mosher 1984).	76
Figure A.3. Unit tip resistance for piles in sand versus relative length (Mosher 1984).	77
Figure B.1. Simple interaction diagram for 24 in. diameter, concrete-filled pipe pile (after Ebeling et al. 2012).	84
Figure B.2. Coefficient of critical buckling strength (after Figure 3 Yang, 1966).	85
Figure B.3. Coefficient decrement of buckling strength (after Figure 9 Yang, 1966).	86
Figure B.4. Euler critical buckling loads $P_{CR\Delta}$, translating pile top, pinned-head and fixed-head conditions.	89
Figure B.5. The effective embedment of pile at buckling (after Figure 2, Yang 1966).	90
Figure B.6. The coefficient of horizontal load capacity (after Figure 7, Yang 1966).	91
Figure C.1. Lock and Dam 3 Guidewall extension soil profile.	95
Figure C.2. C_{33} versus axial load expressed as a fraction of the axial capacity of a 4V:1H batter compression pile at Lock and Dam 3 Guidewall extension for Soil profile at station 21 + 72 using the CAXPILE Soil criteria.	103
Figure C.3. C_{33} versus axial load expressed as a fraction of the axial capacity of a 4V:1H batter compression pile at Lock and Dam 3 Guidewall extension for Soil profile at station 21 + 72 using the CAXPILE WES criteria.	105
Figure C.4. C_{33} versus axial load expressed as a fraction of the axial capacity of a 4V:1H batter compression pile at Lock and Dam 3 Guidewall extension for Soil profile at station 21 + 72 using the CAXPILE VJ criteria.	107
Figure D.1. C_{33} versus axial load expressed as a fraction of the axial capacity of an equivalent vertical batter pile in medium-dense sand for a 4V:1H batter compression pile type configuration used at Lock and Dam 3 Guidewall extension computed using the CAXPILE Soil criteria.	116
Figure D.2. C_{33} versus axial load expressed as a fraction of the axial capacity of an equivalent vertical batter pile in medium-dense sand for a 4V:1H batter compression pile type configuration used at Lock and Dam 3 Guidewall extension computed using the CAXPILE WES criteria.	117
Figure D.3. C_{33} versus axial load expressed as a fraction of the axial capacity of an equivalent vertical batter pile in medium-dense sand for a 4V:1H batter compression pile type configuration used at Lock and Dam 3 Guidewall extension computed using the CAXPILE VJ criteria.	119
Figure E.1. C_{33} versus axial load expressed as a fraction of the axial capacity of an equivalent vertical batter pile in dense sand for a 4V:1H batter compression pile type configuration used at Lock and Dam 3 Guidewall extension computed using the CAXPILE Soil criteria.	127
Figure E.2. C_{33} versus axial load expressed as a fraction of the axial capacity of an equivalent vertical batter pile in dense sand for a 4V:1H batter compression pile type configuration used at Lock and Dam 3 Guidewall extension computed using the CAXPILE WES criteria.	129

Figure E.3. C_{33} versus axial load expressed as a fraction of the axial capacity of an equivalent vertical batter pile in dense sand for a 4V:1H batter compression pile type configuration used at Lock and Dam 3 Guidewall extension computed using the CAXPILE VJ criteria.	131
---	-----

Tables

Table 1.1. Constant of horizontal subgrade reaction, n_h [in units of force/length ³] (after Ebeling et al. 2012).....	10
Table 1.2. Correlation of k_{h1} [in units of force/length ³] to the strength of clays and rock (after Ebeling et al. 2012).	11
Table 3.1. Summary of the calculated ultimate compression capacity of a 4V:1H batter pile for the Lock and Dam 3 site using select engineering methodologies and the CASE CAXPILE software.	34
Table 3.2. Summary of the calculated ultimate shaft resistance of a 4V:1H batter pile for the Lock and Dam 3 site in compression or in tension by three engineering methodologies.	36
Table 3.3. Summary of the calculated ultimate compression capacity of an equivalent vertical batter pile in medium-dense sand for a 4V:1H batter compression pile type configuration used at Lock and Dam 3 guidewall extension using select engineering methodologies and the CASE CAXPILE software.	38
Table 3.4. Summary of the calculated ultimate compression capacity of an equivalent vertical batter pile in dense sand for a 4V:1H batter compression pile type configuration used at Lock and Dam 3 guidewall extension using select engineering methodologies and the CASE CAXPILE software.	42
Table 4.1. Global displacements and forces at the impact deck for the Lock and Dam 3 structural system at each incremental analysis step with $C_{33}=0.55$	55
Table 4.2. Axial force, pile cap moment, and mudline moment for the three piles in the Lock and Dam 3 structural system at each incremental analysis step with $C_{33}=0.55$	55
Table A.1. Values for pile-to-soil interface friction δ for driven piles, based on data obtained from Table 4-3 in EM 1110-2-2906 (HQUSACE 1991).	65
Table A.2. API (2000) guidelines for design parameters for cohesionless siliceous soil.	66
Table A.3. Values of lateral earth pressure coefficients and dimensionless bearing capacity factors N_q and N_c , based on data obtained from Table 4-4 and Figure 4-4 in EM 1110-2-2906 (HQUSACE 1991).	66
Table A.4 Values of critical depth in cohesionless soils (HQUSACE 1991).	68
Table A.5. Typical S case shear strength values according to EM 1110-2-2906 (HQUSACE 1991).	72
Table B.1. Euler critical buckling loads P_{CRA} , translating pile top, pinned-head and fixed-head conditions.	88
Table C.1. Lock and Dam 3 Guidewall extension Soil profile at station 21 + 72.	95
Table C.2. Engineering material properties for the soil stratum at station 21 + 72.	96
Table C.3. Summary of the distribution of effective vertical stresses with elevation for an equivalent vertical batter pile soil profile of a 4V:1H batter compression pile at Lock and Dam 3 Guidewall extension for Soil profile at station 21 + 72.	96
Table C.4. Ultimate skin friction capacity calculations of a 4V:1H batter compression pile at Lock and Dam 3 Guidewall extension for Soil profile at station 21 + 72 according to EM 1110-2-2906 (HQUSACE 1991).	98

Table C.5. Ultimate skin friction capacity calculations of a 4V:1H batter compression pile at Lock and Dam 3 Guidewall extension for Soil profile at station 21 + 72 according to API (2000) guidelines.	99
Table C.6. Ultimate skin friction capacity calculations of a 4V:1H batter compression pile at Lock and Dam 3 Guidewall extension for Soil profile at station 21 + 72 according to the Castello sand curves and EM 1110-2-2906 (HQUSACE 1991) criteria for the silt and clay layers.	100
Table C.7. Summary of input data for computing the ultimate skin friction capacity of a 4V:1H batter compression pile at Lock and Dam 3 Guidewall extension for Soil profile at station 21 + 72 using the CAXPILE Soil criteria.	101
Table C.8. Summary of input data for computing the ultimate skin friction capacity of a 4V:1H batter compression pile at Lock and Dam 3 Guidewall extension for Soil profile at station 21 + 72 using the CAXPILE WES criteria.	104
Table C.9. Summary of input data for computing the ultimate skin friction capacity of a 4V:1H batter compression pile at Lock and Dam 3 Guidewall extension for Soil profile at station 21 + 72 using the CAXPILE VJ criteria.	106
Table D.1. Engineering material properties for the riprap and medium-dense sand foundation.	109
Table D.2. Summary of the distribution of effective vertical stresses with elevation of an equivalent vertical batter pile in medium-dense sand for a 4V:1H batter compression pile type configuration used at Lock and Dam 3 Guidewall extension.	109
Table D.4. Ultimate skin friction capacity calculations according to API (2000) guidelines of an equivalent vertical batter pile in medium-dense sand for a 4V:1H batter compression pile type configuration used at Lock and Dam 3 Guidewall extension.	112
Table D.5. Ultimate skin friction capacity calculations according to the Castello sand curves of an equivalent vertical batter pile in medium-dense sand for a 4V:1H batter compression pile type configuration used at Lock and Dam 3 Guidewall extension.	113
Table D.6. Summary of CAXPILE, Soil criteria, input data for computing the ultimate skin friction capacity curves of an equivalent vertical batter pile in medium-dense sand for a 4V:1H batter compression pile type configuration used at Lock and Dam 3 Guidewall extension.	114
Table D.7. Summary of CAXPILE, WES criteria, input data for computing the ultimate skin friction capacity curves of an equivalent vertical batter pile in medium-dense sand for a 4V:1H batter compression pile type configuration used at Lock and Dam 3 Guidewall extension.	116
Table D.8. Summary of CAXPILE, VJ criteria, input data for computing the ultimate skin friction capacity curves of an equivalent vertical batter pile in medium-dense sand for a 4V:1H batter compression pile type configuration used at Lock and Dam 3 Guidewall extension.	118
Table E.1. Engineering material properties for the riprap and dense sand foundation.	121
Table E.2. Summary of the distribution of effective vertical stresses with elevation of an equivalent vertical batter pile in dense sand for a 4V:1H batter compression pile type configuration used at Lock and Dam 3 Guidewall extension.	121
Table E.3. Ultimate skin friction capacity calculations according to EM 1110-2-2906 (HQUSACE 1991) of an equivalent vertical batter pile in dense sand for a 4V:1H batter compression pile type configuration used at Lock and Dam 3 Guidewall extension.	122
Table E.4. Ultimate skin friction capacity calculations according to API (2000) guidelines of an equivalent vertical batter pile in dense sand for a 4V:1H batter compression pile type configuration used at Lock and Dam 3 Guidewall extension.	123

Table E.5. Ultimate skin friction capacity calculations according to the Castello sand curves of an equivalent vertical batter pile in dense sand for a 4V:1H batter compression pile type configuration used at Lock and Dam 3 Guidewall extension.....	124
Table E.6. Summary of CAXPILE, Soil criteria, input data for computing the ultimate skin friction capacity curves of an equivalent vertical batter pile in dense sand for a 4V:1H batter compression pile type configuration used at Lock and Dam 3 Guidewall extension.	126
Table E.7. Summary of CAXPILE, WES criteria, input data for computing the ultimate skin friction capacity curves of an equivalent vertical batter pile in dense sand for a 4V:1H batter compression pile type configuration used at Lock and Dam 3 Guidewall extension.....	128
Table E.8. Summary of CAXPILE, VJ criteria, input data for computing the ultimate skin friction capacity curves of an equivalent vertical batter pile in dense sand for a 4V:1H batter compression pile type configuration used at Lock and Dam 3 Guidewall extension.	130
Table F.1. Global displacements and forces at the impact deck for the Lock and Dam 3 structural system at each incremental analysis step with $C_{33}=0.35$	143
Table F.2. Axial force, pile cap moment, and mudline moment for the three piles in the Lock and Dam 3 structural system at each incremental analysis step with $C_{33}=0.35$	143

Preface

This report was authorized by Headquarters, U.S. Army Corps of Engineers (HQUSACE), and was compiled from January 2015 through September 2015 under the Navigation Systems Research Program. Charles E. Wiggins, USACE Coastal and Hydraulics Laboratory (CHL), was the Program Manager for the Navigation Systems Research Program. Jeff McKee was the HQUSACE Navigation Business Line Manager.

The research was performed by the USACE Information Technology Laboratory (ERDC-ITL) under the general supervision of Dr. Reed L. Mosher, Director, and Patti S. Duett, Deputy Director. Additional general supervision was provided by Dr. Jerrell R. Ballard, Chief, Computational Science and Engineering Division. Jeff Lillycrop (ERDC-CHL) was Navigation Technical Director.

Special appreciation is expressed to consultant Ralph W. Strom for the constructive discussions and insight that he has provided over the years on the general topic of the pushover method of analysis. Strom was a key developer of the pushover method of analysis for capacity-based design for pile-founded flexible approach walls in collaboration with the authors of this report.

COL Bryan S. Green was Commander, ERDC, and Dr. Jeffery P. Holland was Director.

Unit Conversion Factors

Multiply	By	To Obtain
cubic feet	0.02831685	cubic meters
cubic inches	1.6387064 E-05	cubic meters
cubic yards	0.7645549	cubic meters
degrees (angle)	0.01745329	radians
feet	0.3048	meters
foot-pounds force	1.355818	joules
horsepower (550 foot-pounds force per second)	745.6999	watts
inches	0.0254	meters
inch-pounds (force)	0.1129848	newton meters
knots	0.5144444	meters per second
microinches	0.0254	micrometers
microns	1.0 E-06	meters
miles (nautical)	1,852	meters
miles (U.S. statute)	1,609.347	meters
miles per hour	0.44704	meters per second
mils	0.0254	millimeters
pounds (force)	4.448222	newtons
pounds (force) per foot	14.59390	newtons per meter
pounds (force) per inch	175.1268	newtons per meter
pounds (force) per square foot	47.88026	pascals
pounds (force) per square inch	6.894757	kilopascals
pounds (mass)	0.45359237	kilograms
pounds (mass) per cubic foot	16.01846	kilograms per cubic meter
pounds (mass) per cubic inch	2.757990 E+04	kilograms per cubic meter
pounds (mass) per square foot	4.882428	kilograms per square meter
pounds (mass) per square yard	0.542492	kilograms per square meter
slugs	14.59390	kilograms
square feet	0.09290304	square meters
square inches	6.4516 E-04	square meters
square miles	2.589998 E+06	square meters
square yards	0.8361274	square meters
tons (force)	8,896.443	newtons

Multiply	By	To Obtain
tons (force) per square foot	95.76052	kilopascals
tons (long) per cubic yard	1,328.939	kilograms per cubic meter
tons (2,000 pounds, mass)	907.1847	kilograms
tons (2,000 pounds, mass) per square foot	9,764.856	kilograms per square meter
yards	0.9144	meters

1 Introduction: Analysis of Pile Group Deformation and Distribution of Individual Pile Loadings for a Batter Pile Configuration with Respect to a Pushover Analysis

1.1 Introduction

This report summarizes an investigation into the engineering characterization of the axial stiffness of individual compression piles embedded within soil. This characterization of axial stiffness is used in the analysis of a clustered pile group's deformation and load distribution response. Its impact on the computed pile group response is most pronounced among a clustered pile group containing batter piles.

1.2 Background

U.S. Army Corps of Engineers (USACE) designers have long acknowledged that the axial stiffness of piles embedded in soil can affect pile group analysis. To this end, in the primary pile group analysis software developed by the Corps, the Computer-Aided Structural Engineering (CASE) library software Pile Group Analysis (CPGA), a key model input parameter b_{33} was included. This input parameter determines compressive axial deformation of piles under a specified load. This deformation value applied at individual piles affects the computed pile group deformation for a batter pile configured substructure. This report addresses the definition of the b_{33} axial pile stiffness term for use in a batter pile group configuration design.

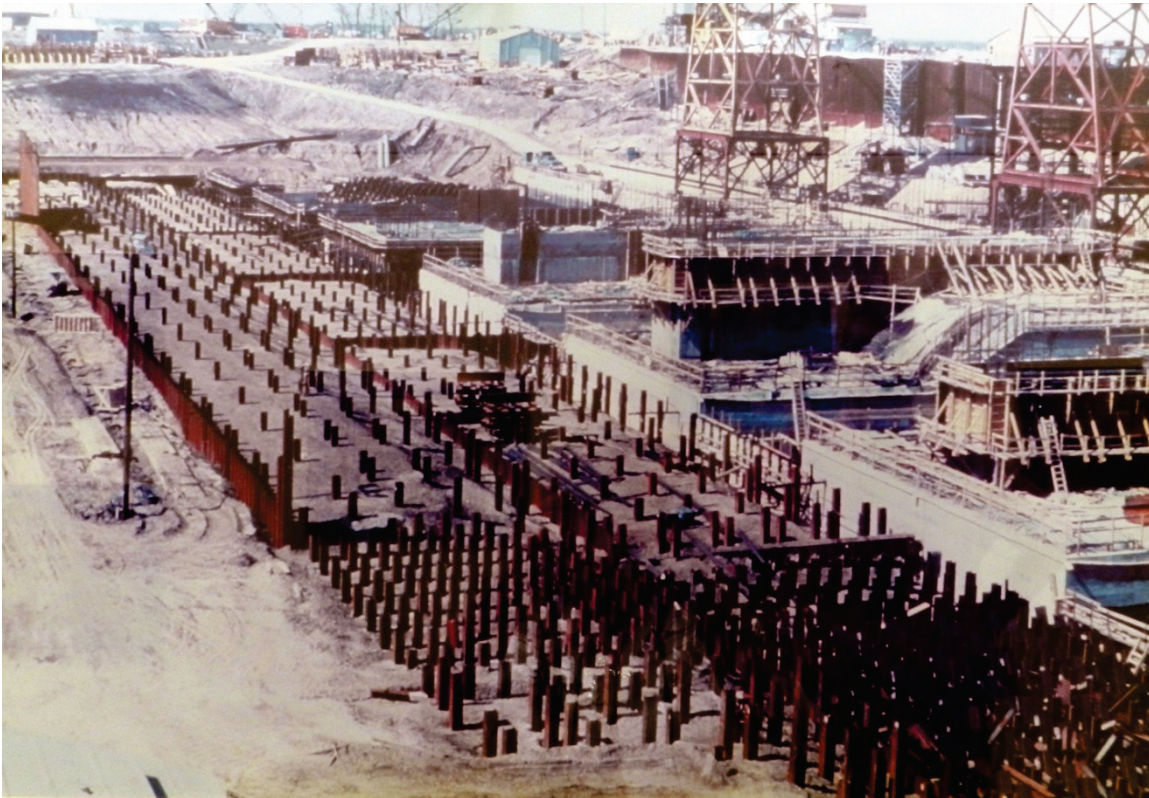
1.3 Analyzing massive concrete pile-founded structures

Figure 1.1 shows the complexity involved in analyzing pile-founded structures. For a number of the Corps' massive hydraulic structures, a foundation was laid on a forest of piles that were either vertical, batter, or some combination of the two.

When the current Corps guidance on the design of pile foundations, EM 1110-2-2906 (HQUSACE 1991), was published in 1991, it reflected the emphasis of the late 1970s and 1980s era of Corps pile foundation designs

involving large groups of piles supporting massive hydraulic lock structures where the load transfer from the hydraulic structure to the pile group soil foundation was at the top of soil foundation. Figure 1.1 shows the pile layout for the soil-founded spillway at Melvin Price Lock and Dam in St. Louis, MO. The load transfer from the hydraulic structure, a spillway for this project feature, into the pile foundation occurs immediately at the top of soil. These structures required a large *forest* of piles and would take a long time to calculate pile response by hand without errors. In order to solve these large-scale structures efficiently, the CPGA was developed and included in the Corps software library, which has since evolved into the CASE software library. CPGA is discussed in a subsequent subsection.

Figure 1.1. Pile layout for soil-founded spillway at Melvin Price Lock and Dam in St. Louis, MO (after Ebeling et al. 2013).



1.4 Pile-group founded flexible approach walls

In recent years there has been more attention paid to the use of pile-group founded, elevated structural systems at Corps projects, particularly with regards to flexible approach walls. Design loads for flexible approach walls are governed by a barge-train impact event to an impact deck (or impact beams).

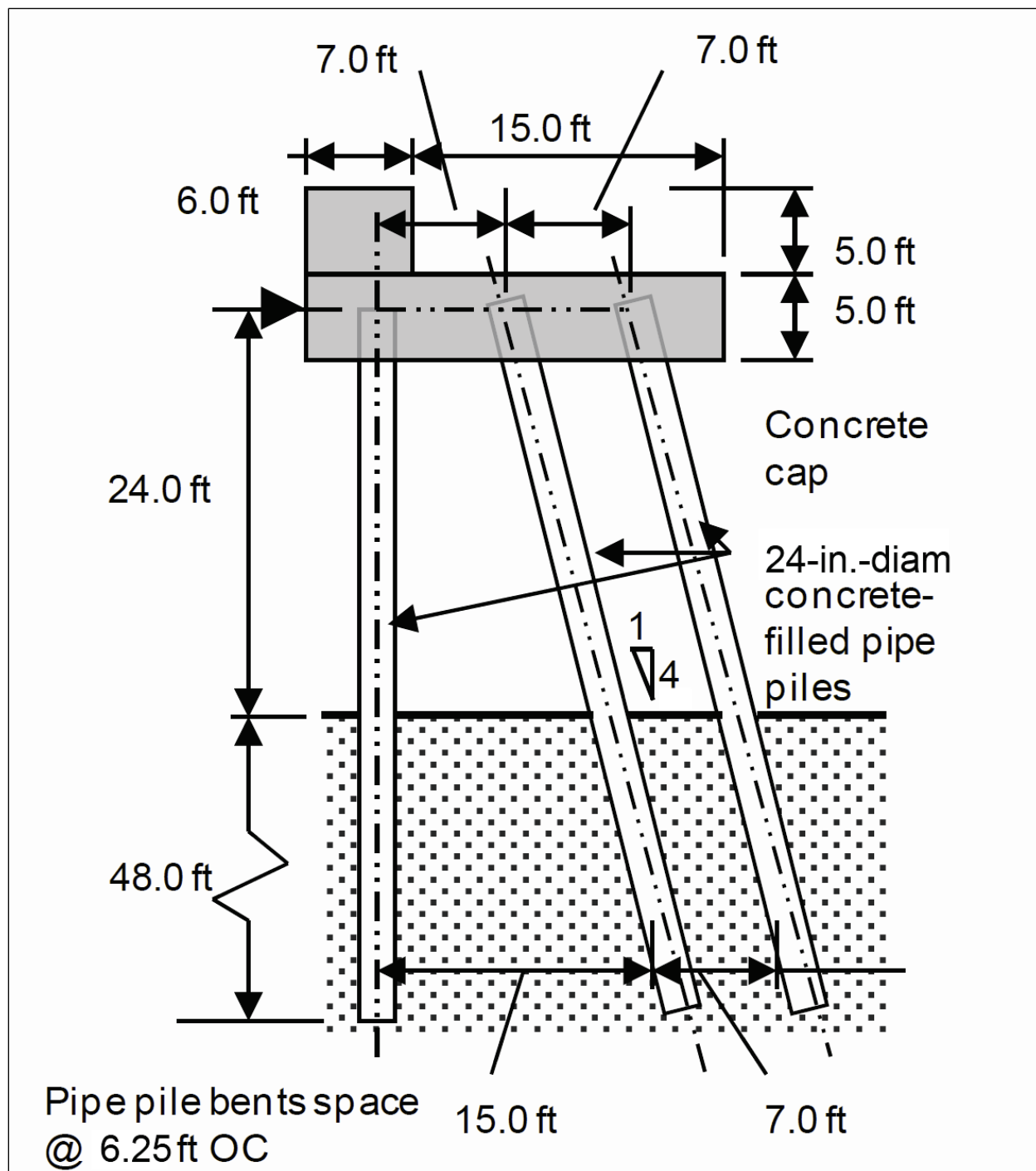
Massive, concrete, pile-founded structures have many contrasts with the Lock and Dam 3 type of elevated flexible approach walls. Since 1991 when EM 1110-2-2906 (HQUSACE 1991) was published, design questions for pile-group founded flexible approach walls have surfaced where there are larger deformations of the pile group due to the use of much smaller pile groups and impact (loading) events occurring tens of feet above the mudline.

In the case of the Lock and Dam 3 flexible approach wall extension of Figure 1.2, this impact occurs approximately 24 ft above the mudline. A glancing-blow impact event of a barge train impacting an approach wall as it aligns itself with a lock is an event of short duration. The contact time between the impact corner of the barge train and the approach wall can range from 1 second to several seconds (Ebeling et al. 2010). In order to reduce construction costs as well as to reduce damage to barges during glancing-blow impacts with lock approach walls, the next generation of Corps approach walls is more flexible than the massive, stiff-to-rigid structures constructed in the past. A flexible approach wall or flexible approach wall system is one in which the wall/system has the capacity to absorb impact energy by deflecting or *flexing* during impact, thereby affecting the dynamic impact forces developing during the impact event (White et al. 2015). Due to their inherent flexibility, pile-founded approach wall structural systems consisting of small numbers of clustered piles are characterized as flexible structures. This opens up the opportunity for analyzing them using deformation-based procedures of analysis.

Figure 1.3 shows an artist's rendering of the Lock and Dam 3 impact deck extension of its flexible approach wall. Figure 1.4 shows a cutaway view of the Lock and Dam 3 impact deck for its flexible approach wall. Note the extensive use of (4V:1H) batter piles in this structure and the impact deck located well above the mudline. Recall from Figure 1.2 that the barge-train impacts occur approximately 24 ft above the mudline. The piles are 2 ft diameter, concrete-filled pipe piles.

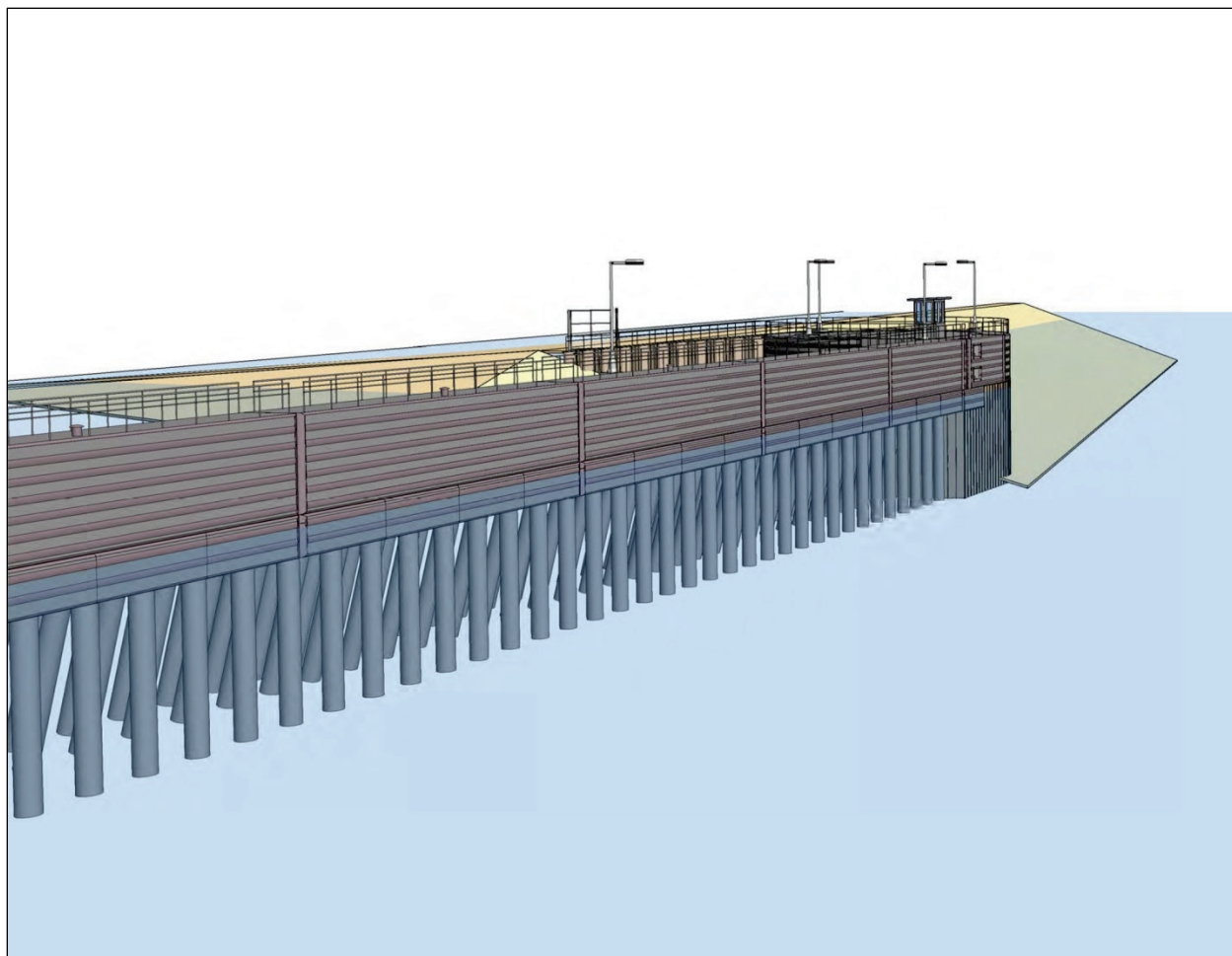
Fortunately, the CPGA software discussed subsequently had enough flexibility to deal with these flexible pile-founded structures. The Ebeling et al. (2012) study of the capacity of the batter pile-founded Lock and Dam 3 flexible approach wall led to the investigation of the details concerning CPGA engineering model parameters that impact the computed pile group deformation. Material from the current reports, from Ebeling et al. (2012) and from White et al. (2015), provide new evaluation procedures and software that contribute important engineering evaluation enhancements to be added during the ongoing revision of EM 1110-2-2906 (HQUSACE 1991).

Figure 1.2. Idealization of a single group of three, clustered, concrete-filled, 24 in. diameter pipe piles supporting a 6.25 ft tributary section of impact deck of the flexible lock approach wall extension at Lock and Dam 3 on the Upper Mississippi River¹.



¹ White, B., J. R. Arroyo, and R. M. Ebeling. In publication. Simplified dynamic structural time-history response analysis of flexible approach wall founded on clustered pile groups using Impact_Deck. ERDC/ITL Technical Report. Vicksburg, MS: U.S. Army Engineer Research and Development Center.

Figure 1.3. The impact deck supported over clustered pile groups at the flexible lock approach wall extension at Lock and Dam 3 on the Upper Mississippi River¹.



1.5 Introducing the CPGA software family

The CPGA program accounts for the effects of pile locations and batters. It can linearly represent any type of pile-soil interaction and can represent fixed or pinned interaction between the pile and pile cap. Piles have a different axial stiffness for tension loads than for compression loads; the program will iterate to a solution using the appropriate stiffness based on the direction of the calculated pile load.

¹ White, B., J. R. Arroyo, and R. M. Ebeling. In publication. Simplified dynamic structural time-history response analysis of flexible approach wall founded on clustered pile groups using Impact_Deck. ERDC/ITL Technical Report. Vicksburg, MS: U.S. Army Engineer Research and Development Center.

Figure 1.4. Cut-out view of the impact deck and its pile layout for the flexible lock approach wall extension at Lock and Dam 3 on the Upper Mississippi River¹.



The user must specify pile and soil properties, pile locations and batters, applied loads, and pile allowable loads. The pile and soil properties are used to calculate the pile stiffness coefficients, or the user can calculate the stiffness by other means and input it directly to the program. Piles of several types may be included in the same analysis. The program is limited to maximums of 2,000 piles and 20 load cases.

CPGA utilizes the stiffness method (Saul 1968) of three-dimensional pile group analysis for user-specified static loadings. The pile foundation consists of a group of piling placed into the soil topped with a reinforced concrete cap. Loads to the cap and the weight of the cap are borne by the piling and then transferred into the soil. The pile cap is assumed to be rigid or nondeformable. Each pile is represented by its calculated stiffness coefficients. The stiffness coefficients of all piles are summed to determine the stiffness matrix for the total pile group. Displacements of the rigid pile cap are determined by multiplying the inverse of the group stiffness matrix

¹ White, B., J. R. Arroyo, and R. M. Ebeling. In publication. Simplified dynamic structural time-history response analysis of flexible approach wall founded on clustered pile groups using Impact_Deck. ERDC/ITL Technical Report. Vicksburg, MS: U.S. Army Engineer Research and Development Center.

by the sets of user-specified, applied loads. Displacements of the rigid cap define displacements of individual pile heads, which are multiplied by the pile stiffness coefficients to determine the force acting on each pile head. These resulting loads are then compared to user-defined allowable loads.

A prerequisite for using CPGA to model a pile group is that this program assumes *long* piles. A commonly used criterion for long-pile behavior is to be discussed subsequently.

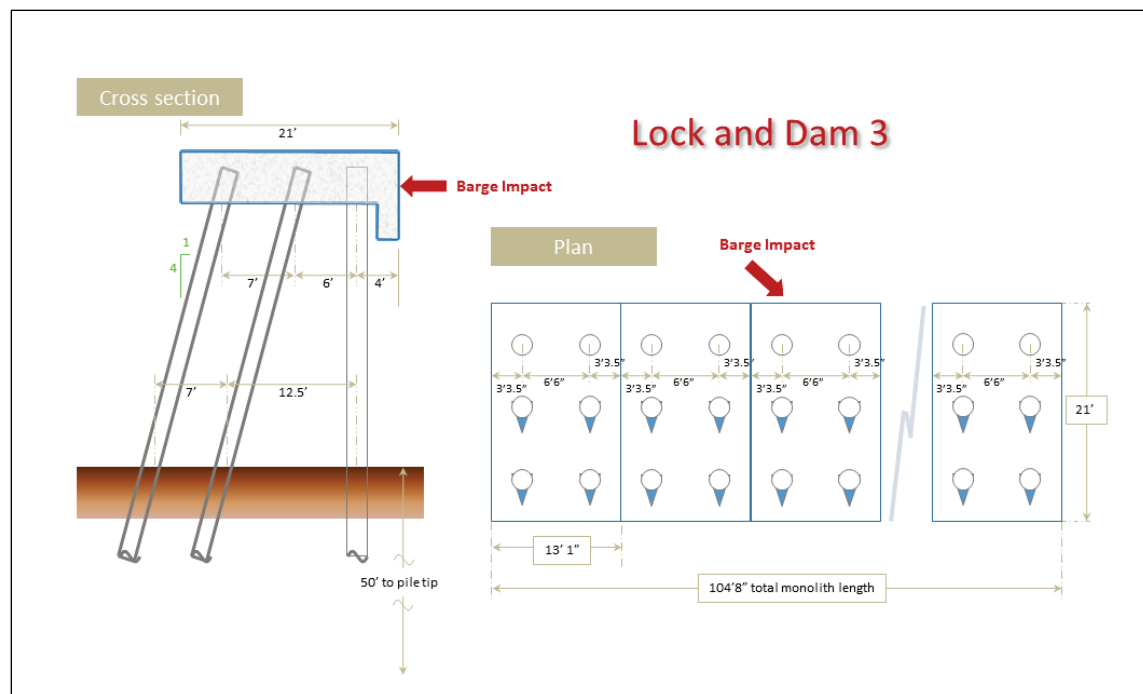
The Corps' CASE repository for software maintains two versions of software for District evaluation of pile groups: the traditional, deterministic version of CPGA for user-specified static loads (Hartman et al. 1989) and a reliability-based version named CPGA-R (Ebeling et al. 2013). CPGA-R may also be executed in a deterministic mode of analysis. CPGA-R also permits input of as many as 2,000 piles and databases of pile and soil properties, as well as a database of loads to be applied to the pile group.

1.6 Analyzing flexible approach walls with CPGA

CPGA is a simplified program used by District engineers to aid in the rapid analysis/design of the Corps hydraulic structures that are founded on groups of piles both vertical, batter, and any combination of the two. CPGA can also evaluate elevated structural systems of the type depicted in Figure 1.5.

This figure shows an idealization of the layout of groups of clustered piles supporting the impact deck of a flexible approach wall extension. This flexible wall extension was constructed at Lock and Dam 3 near Red Wing, MN, on the Upper Mississippi River. Hartman et al. (1989) developed CPGA to help eliminate the engineering inaccuracies inherent in hand-calculation analysis methods. The program assumes the pile cap to be rigid and the piles to be linearly elastic. Soil resistance to pile movement can be input into the model description. This software continues to find usage in the analysis of a wide range of pile-group founded hydraulic structure types used throughout the Corps. CPGA is particularly useful when computing the capacity of flexible approach walls configured with batter pile groups using the engineering evaluation procedure outlined in Ebeling et al. (2012). Specifically, the pushover analysis, as described in Ebeling et al. (2012) is an incremental analysis to determine the energy-absorption capacity of a pile-founded structural system in a performance-based structural design for barge-train impact loading.

Figure 1.5. Idealization of the pile layout for the flexible lock approach wall extension at Lock and Dam 3 on the Upper Mississippi River¹.



1.7 Using pushover analysis to establish extreme behavior in flexible walls

Ebeling et al. (2012) present a structural system capacity calculation methodology centering on a pushover analysis for flexible approach wall systems founded on elevated groups of piles and subjected to barge-train impact. This 2012 study has shown the importance of pile group deformation predictions to the analysis of pile group capacity, especially when these barge-train impacts occur tens of feet above the mudline. A *balance of energy* design procedure for pile-founded substructures is presented based on deformation calculations made for individual impact events. This procedure assumes that all the kinetic energy (KE) of the approaching barge train (normal to the wall) is converted to potential energy (PE), or strain energy, through deformation of the flexible piling. A pushover analysis technique is used to establish the PE capacity and displacement capacity of individual pile groups accounting for various pile failure mechanisms. The total stored energy (PE) of the approach wall system will be the sum of all pile groups reacting to the barge impact. This capacity characterization

¹ White, B., J. R. Arroyo, and R. M. Ebeling. In publication. Simplified dynamic structural time-history response analysis of flexible approach wall founded on clustered pile groups using Impact_Deck. ERDC/ITL Technical Report. Vicksburg, MS: U.S. Army Engineer Research and Development Center.

approach demonstrates the importance of the pile-group deformation calculation. For a flexible structure that is founded on only vertical piles, CPGA is not necessary, and a pushover can be performed with other CASE software (e.g., using COM624G). For batter pile configurations, however, CPGA is a necessity.

The Ebeling et al. (2012) pushover analysis of the Lock and Dam 3 structure to define its energy absorption capacity showed significant deflection occurs at the elevation corresponding to the impact deck as the pile group approaches its ultimate capacity (Figure 1.6). This is attributed to three factors: the use of three, 2 ft diameter piles per clustered group of (three) piles; a spacing (in plan) of 6 ft, 3 in. between clustered groups of piles; and the barge-train impact loading occurring 24 ft above the mudline. The computed deformations are far above those determined for pile-founded spillway and lock structures such as those constructed at Melvin Price Lock and Dam (Figure 1.1).

1.8 A criteria for long pile behavior and minimum pile lengths

One criteria used to establish long pile behavior in the Soil-Structure-Interaction (SSI) modeling procedure implemented in programs like CPGA is that the embedded pile length must be $> 5T$ or $4R$ (as discussed in Hartman [1989]), or $> 4T$ or $4R$ according to Davisson (1970) and discussed in Section 3.3.1 of Ebeling et al. (2012). T and R are the relative stiffness factors of the pile model and have units of length. For granular soils (e.g., sands), T is given by

$$T = \sqrt[5]{EI/n_h} \quad (1.1)$$

for the horizontal subgrade soil modulus $E_s = n_h x$, where the *stiffness* increases with increasing confining pressure with depth, and E and I are the value of Young's Modulus, E , and moment of inertia, I , of the pile. The units for E and I are force/length² and length⁴, respectively. The term E_s has units of force per length² while n_h , referred to as the constant of subgrade reaction (Terzaghi 1955), has units of force per length³. Typical values for n_h are listed in Table 1.1. Observe that the value for n_h is dependent upon if the granular soil is above (i.e., dry or moist) or below (i.e., submerged) the water table and its density (i.e., loose, medium-dense, or dense).

Figure 1.6. Resulting load-displacement plot characterizing the pushover capacity of the batter pile configuration for Lock and Dam 3 for fixed-head and free-head boundary conditions at the pile cap (after Ebeling et al. 2012)

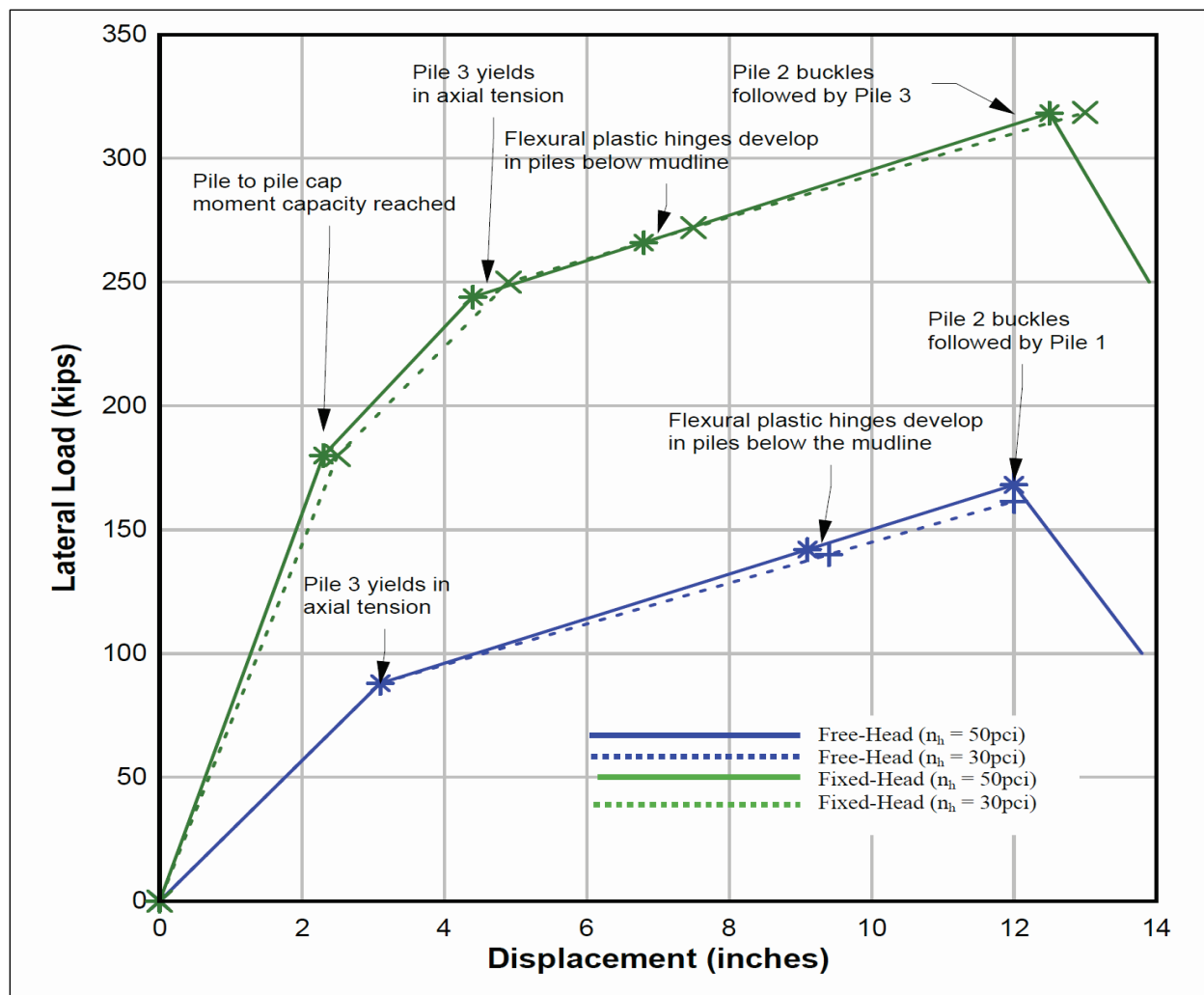


Table 1.1. Constant of horizontal subgrade reaction, n_h [in units of force/length³] (after Ebeling et al. 2012).

Relative Density	n_h			
	Loose	Medium	Dense	Units
Range in values for dry or moist sand, range for n_h	4-10	10-30	30-70	tcf
	8,000-20,000	20,000-60,000	60,000-140,000	pcf
	4.63-11.57	11.57-34.72	34.72-81.02	pci
Dry or moist sand, proposed values for n_h	7	21	56	tcf
	14,000	42,000	112,000	pcf
	8.10	24.31	64.81	pci
Submerged sand, proposed values for n_h	4	14	34	tcf
	8,000	28,000	68,000	pcf
	4.63	16.20	39.35	pci

The relative stiffness factor R is given by

$$R = \sqrt[4]{EI/E_s} \quad (1.2)$$

for the horizontal subgrade soil modulus E_s . The value of E_s is a constant and given by

$$E_s = k_h \cdot d \quad (1.3)$$

with k_h representing the horizontal coefficient of subgrade reaction (Terzaghi 1955) and d being the diameter of the pile. This type of engineering stiffness characterization is often associated with clay or rock strata. Again, the term E_s has units of force per length².

The horizontal coefficient of subgrade reaction (k_h in units of force/length³) for clay and rock follows the equation

$$k_h = k_{h1} \cdot \frac{1}{1.5d} \quad (1.4)$$

where d designates the pile diameter and k_{h1} is the horizontal coefficient of subgrade reaction for a 1 ft square plate (force/length³). After substitution of Equation 1.4 into Equation 1.3, E_s is given by

$$E_s = k_{h1} \cdot \frac{1}{1.5} \quad (1.5)$$

Using the data cited in Terzaghi (1955), the value of k_{h1} for clay is related to the undrained shearing strength S_u . This relationship is given in Table 1.2. The second relationship listed in this table relates the value for k_{h1} to the unconfined compressive strength of rock, q_u .

Table 1.2. Correlation of k_{h1} [in units of force/length³] to the strength of clays and rock (after Ebeling et al. 2012).

	Clay	Rock
k_{h1}	96 S_u	48 q_u

White and Ebeling¹ investigated the minimum required depth of embedment for an example vertical pile bent system founded in a cohesionless sandy soil with two exposed heights (40 ft and 20 ft) and performed a pushover analysis. It has been recognized that as piles are embedded deeper in the soil, the deflection at the top of the pile under a horizontal (impact) load is reduced but that this reduction in deflection approaches a point of diminishing returns for deep pile tip embedment. This property is called long pile behavior. In order to reduce the costs associated with pile placement, the shallowest pile depth that exhibits long pile behavior needs to be computed. Many state-of-practice methods are reported in the technical literature to estimate this depth of long pile behavior. White and Ebeling examined these state-of-practice methods and recommended a new course of action based on the lateral peak loads at the pile tip that lead to a pushover event. This new procedure is named the asymptotic pile tip deflection slope per pile tip embedment inflection point method. From the results of the asymptotic pile tip deflection slope per pile tip embedment inflection point method preferred by the authors, the depths of the pile tip should be 42 ft (for the 40 ft exposed pile), which is $4.26 * T$, or 44 ft (for the 20 ft exposed pile), which is $4.47 * T$. The constant applied to the relative stiffness factor T in cohesionless soils is between 4.26 and 4.47. Using these constant values results in a depth that is 10% to 15% shallower than the $5 * T$ depth suggested in the 1989 CPGA manual.

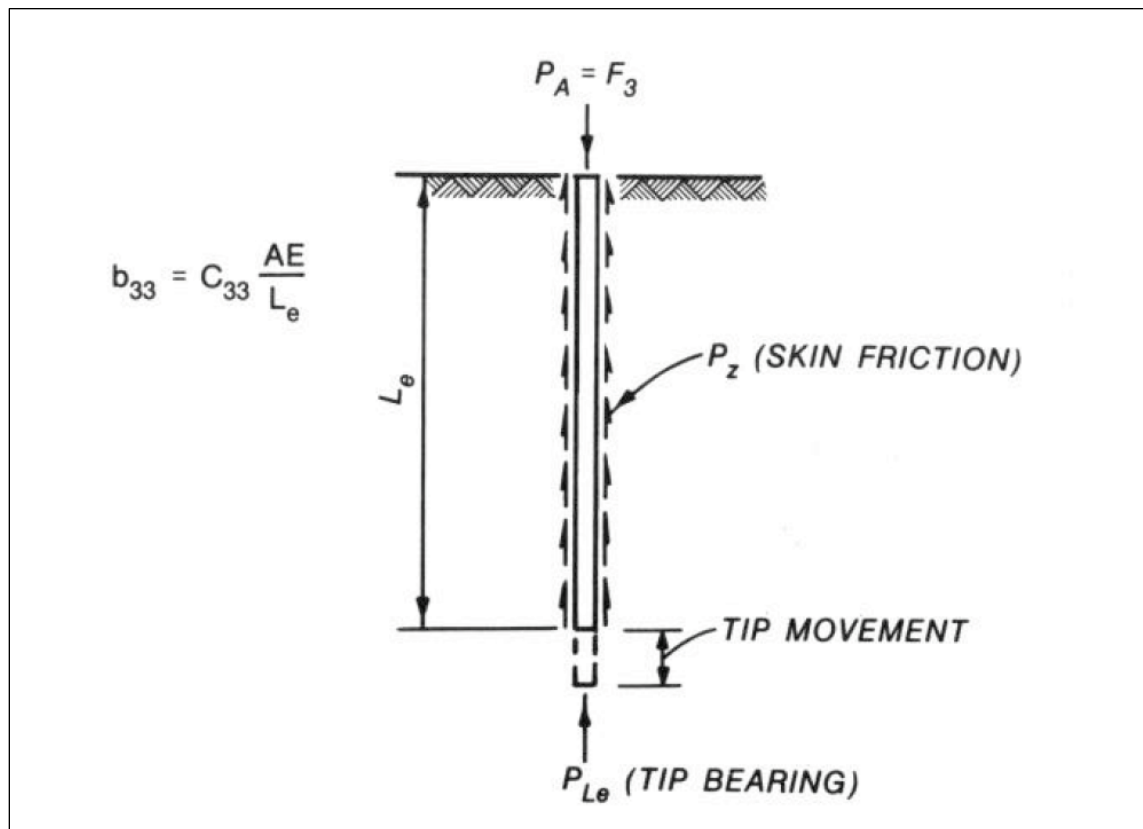
1.9 Axial stiffness of piles embedded in soil as input for CPGA

Recent research by Ebeling et al. (2012) and White et al. (2015) has shown that pile group founded flexible approach walls, which extend tens of feet above the mudline, can develop significant deformations under barge-train loads. Recall that these barge-train impacts occur with an impact deck cast to incorporate the pile cap for each row of the clustered pile groups. For flexible approach walls using impact beams, these precast, pretensioned beams rest on the pile cap bents of the clustered pile groups. For batter pile configurations modeled using CPGA software, the axial stiffness term (b_{33}) dominates the pile group deformation calculation. The Corps approach as implemented within CPGA software accounts for pile-soil interaction effects by applying an empirical factor (C_{33}) to the axial stiffness coefficient of $[AE/L_e]$ of the axially loaded structural (pile) member. Figure 1.7 depicts the

¹ White, B. C., and R. M. Ebeling. In publication. A systematic approach for determining vertical pile depth of embedment in cohesionless soils to withstand lateral barge train impact loads. ERDC/ITL Technical Report. Vicksburg, MS: U.S. Army Engineer Research and Development Center.

pile-soil interaction through load transfer occurring because of skin friction and tip bearing under a compression load of magnitude P_A . L_e in this figure is the length of pile embedment, with A designating the cross-sectional area of the pile and E designating its Young's Modulus.

Figure 1.7. Load transfer by combined skin friction and tip bearing for an axially loaded compression pile (after Harman et al. 1989).



1.10 Objective

A systematic investigation into the batter pile stiffness characterization and user assignment of what is referred to as the C_{33} term was conducted and is summarized in this report.

1.11 Approach

This report focuses on an engineering procedure used to determine an appropriate value to assign to the empirical CPGA model factor (C_{33}) and accurately account for nonlinear pile-soil interaction effects. Representative relationships between values of C_{33} and the fraction of mobilized axial pile capacity in cohesionless soil sites of varying densities are provided. Appendix A discusses various engineering procedures used to compute

axial pile capacity in different soil types. The CASE software CAXPILE (Dawkins 1984) is used to assist in this axial stiffness characterization in this study. An appropriate value for the axial stiffness of batter piles is of particular importance in the CPGA deformation-based computations used in a pushover analysis (Ebeling et al. 2012). Computed results from a pushover analysis are used to define the pile group's structural capacity as a function of the impact-induced deck deformation.

2 The Characterization of Axial Pile Stiffness in CASE software

2.1 Introduction

The CASE software CPGA is used for basic pile group analysis and is especially useful for a batter pile foundation configuration in a pushover analysis (Ebeling et al. 2012). A key input affecting the load distribution among the piles and the pile group lateral deformation is the axial stiffness of the batter pile(s). The CASE software CAXPILE is used to assist in the characterization of axial pile stiffness to be used as input to the CPGA batter pile model. This chapter discusses important details of the CPGA model formulation.

2.2 Introduction to CPGA analysis and coordinate systems (global and pile)

As discussed in Chapter 1, the CPGA software utilizes the stiffness method (Saul 1968) of pile group analysis to solve for pile cap displacement, rotation, and the distribution of forces and moments acting within the individual piles that comprise the pile group. The pile cap is assumed to be rigid or nondeformable. Each pile is represented by its calculated stiffness coefficients. The stiffness coefficients of all piles are summed to determine the stiffness matrix for the total pile group. Displacements and rotations of the rigid pile cap are determined by multiplying the inverse of the group stiffness matrix $[K_{6 \times 6}]$ by the set of six Figure 2.1 user-specified applied loads of magnitude P_x , P_y , and P_z and specified moments of magnitude M_x , M_y , and M_z . The global load vector is denoted by the six-by-one matrix designated $[Q]$ in this figure. Note that in a CPGA analysis, these six user-specified loads and moments are applied at the origin of the global coordinate system. The user defines the origin of this global coordinate system for the CPGA model. In the Figure 2.1, taken from the CPGA user's manual, the origin is specified by a user to be close to the geometric center of the rigid pile cap in this model. The CPGA software then computes the resulting set of three global displacements and three global rotations that are identified in this figure to be of magnitude D_x , D_y , and D_z and R_x , R_y , and R_z , respectively. This global displacement vector is denoted by the six-by-one matrix designated $[U]$ in this figure. Displacements and rotation(s) of the rigid cap are subsequently used to compute the displacements of the individual pile heads. These, in turn, are multiplied by the pile stiffness coefficients to determine the force (and moment, if applicable) acting on each pile head.

Figure 2.1. A CPGA global coordinate system centered at the origin, which is located at the center of the rigid pile cap (after Harman et al. 1989).

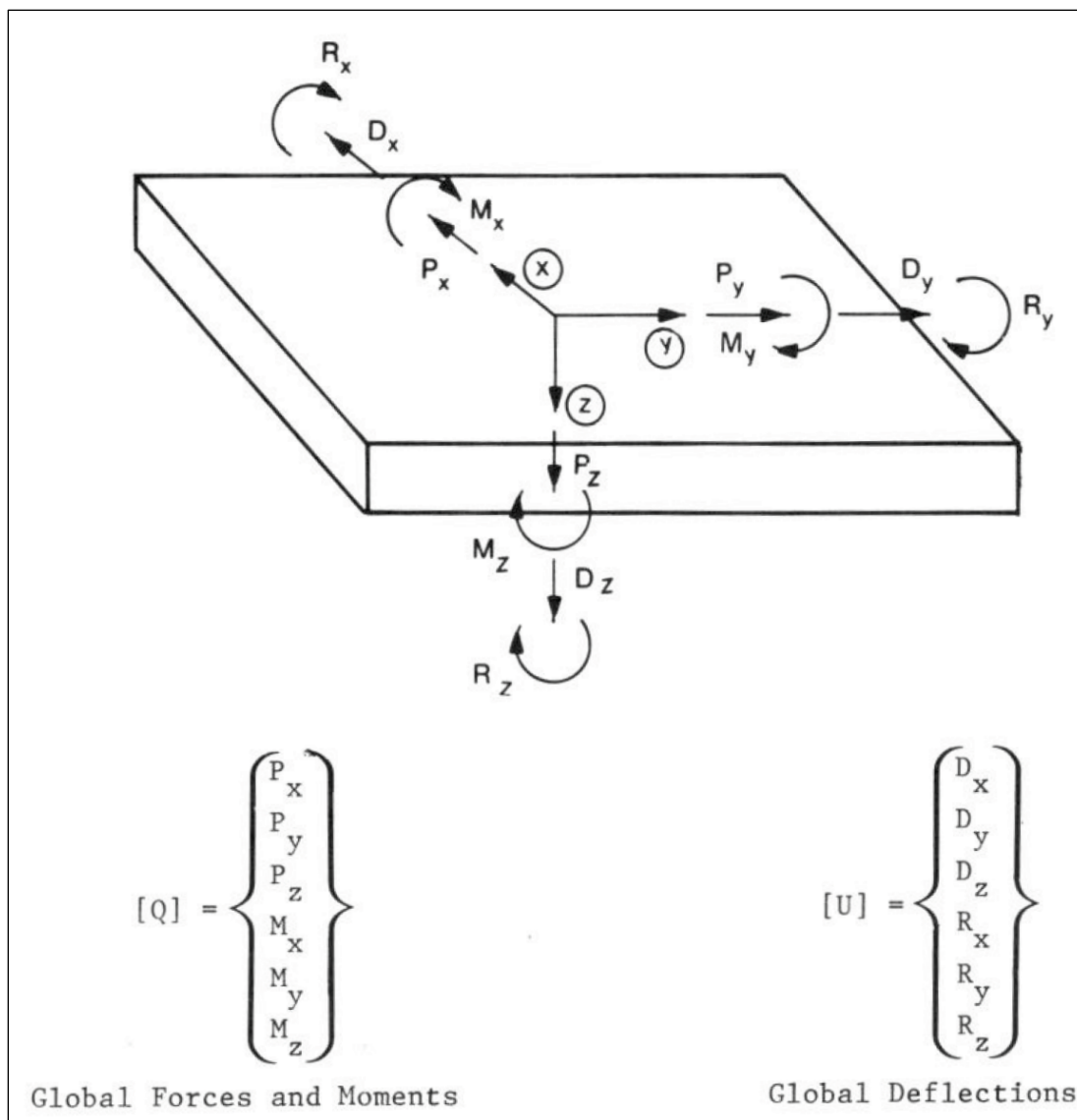


Figure 2.2 shows a second example of a user specification of an origin for the global coordinate system in a batter pile group model configuration problem (Martin et al. 1980 and The CASE Task Group on Pile Foundations 1983). This problem has been analyzed using CPGA software, and results are summarized in Hartman et al. (1989). The forces Q_1 and Q_3 and moment Q_5 act in their positive directions in this figure. This problem was taken from an example given in Hrennikoff (1950) that discusses the analysis of this batter pile founded retaining wall (Figure 2.3). Observe that the user-specified origin in both figures is placed at the intersection of the middle pile (a batter pile labeled no. 3) and the rigid pile cap. It is close to the center of the rigid cap and is being subjected to in-plane forces of

magnitude $Q_1 = -39.375$ kips and $Q_3 = 113.1$ kips and in-plane moment $Q_5 = 173.4$ kip-ft. Each of the clustered pile groups consists of five, 9 in. diameter, 30 ft long timber piles placed 3 ft center to center along the length of the Figure 2.3 retaining wall. The loading specified by Hrennikoff to this 3 ft wide pile foundation, retaining wall section model constitutes a two-dimensional problem. Consequently, there will be no out-of-plane translations (i.e., global displacement vector U_2 ; not depicted in the figure but directed into the paper) nor out-of-plane rotations (i.e., Q_4 and Q_6 ; not depicted in the figure) computed by CPGA for the batter pile configuration in this model.

Figure 2.2. A CPGA batter pile group layout and origin specification near the center of the rigid pile cap (after The CASE Task Group on Pile Foundations 1983).

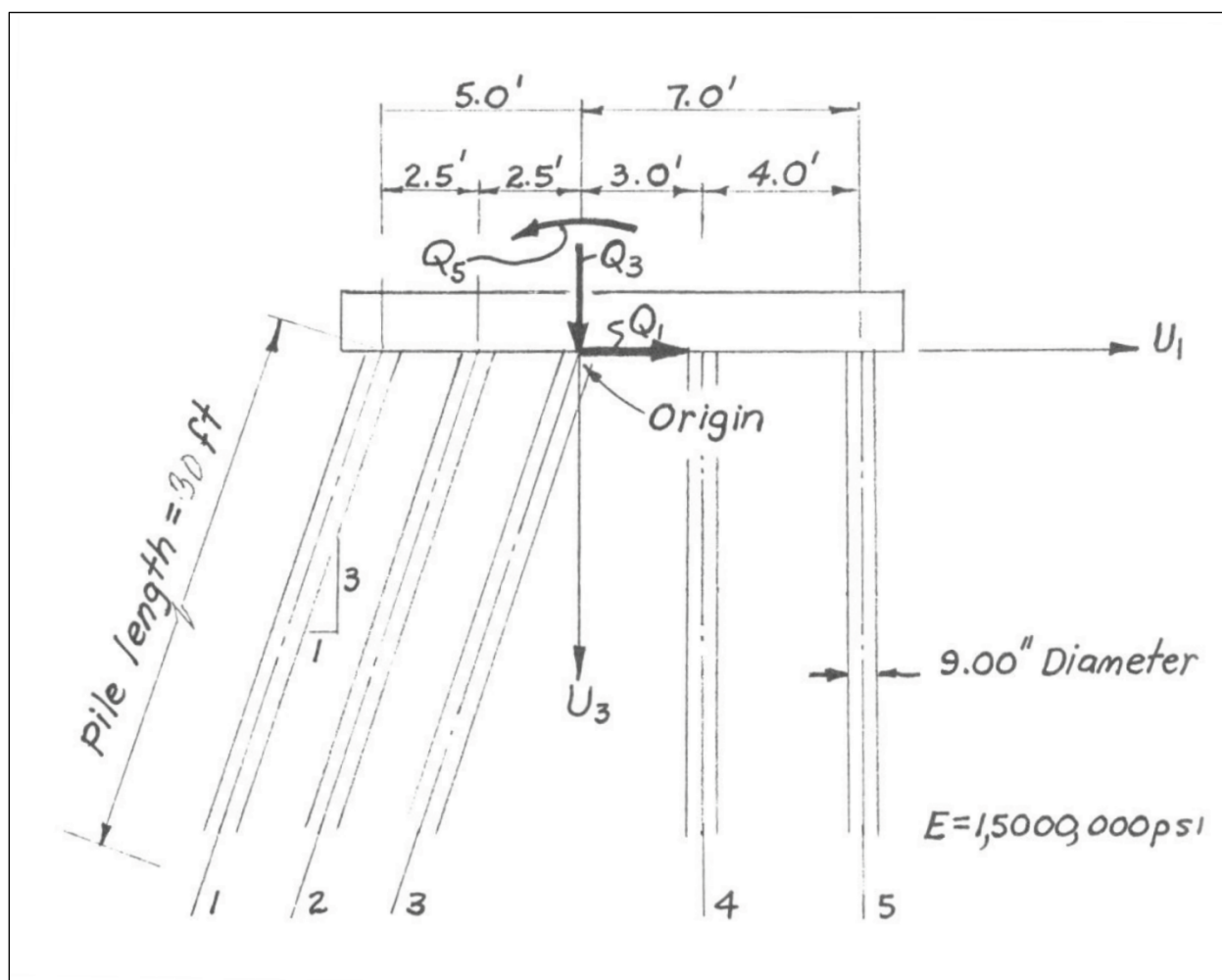
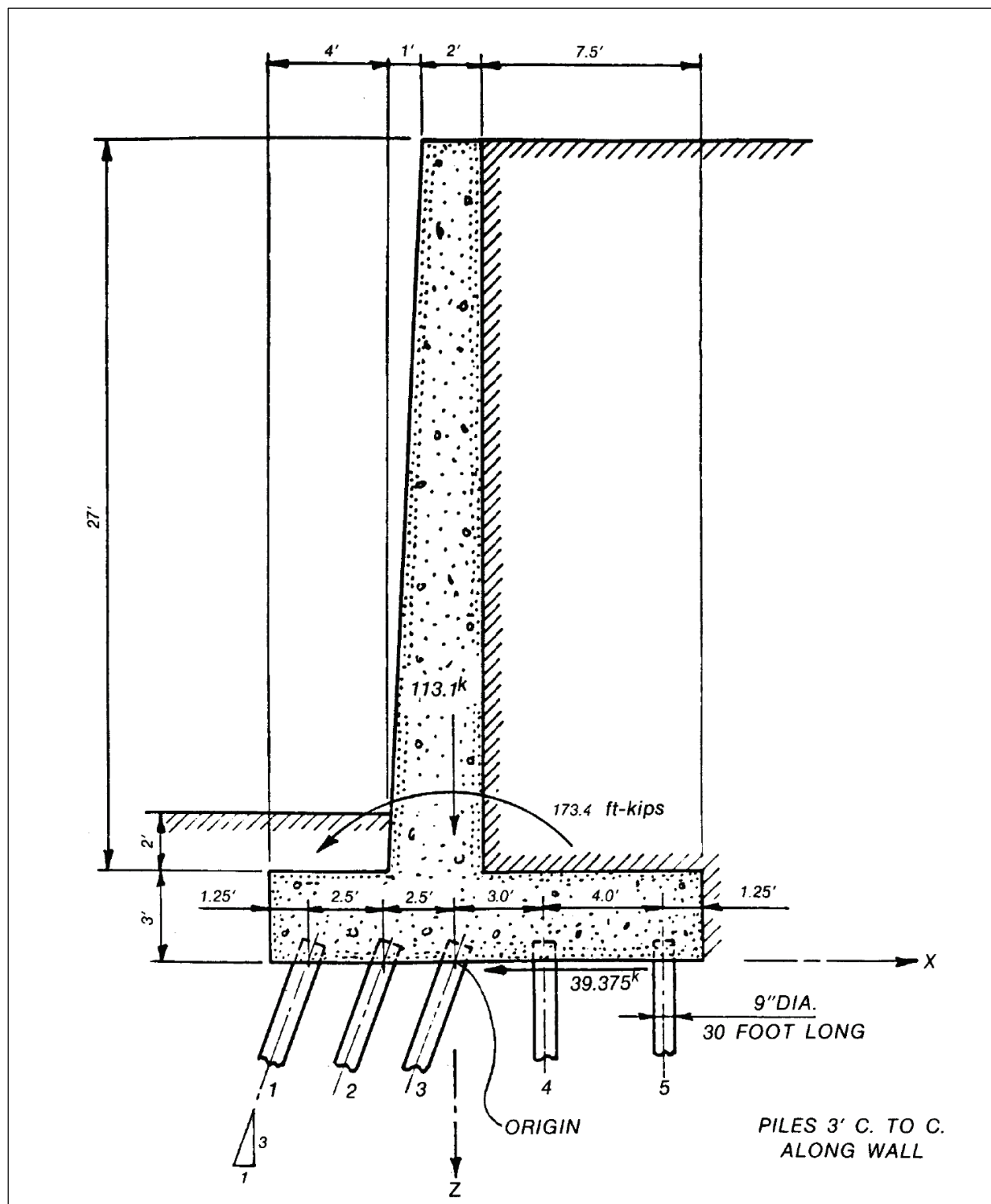


Figure 2.3. Cross-section viewing of an earth retaining wall founded on rows of batter pile groups 3 ft center-on-center along the retain wall (after Hartman et al. 1989)



2.3 Pile stiffness, pile group stiffness, and local and global force-displacement relationships

In the Saul (1968) formulation as implemented in CPGA, each pile is analyzed as a semi-infinite beam on an elastic foundation for flexure, as a modified compression block for axial deformation, and as a modified shaft in torsion. Each pile has 6 degrees of freedom. The pile stiffness is represented by a 6-by-6 matrix of stiffness coefficients $[b_{ij}]$ relating the pile head forces to pile head displacements:

$$\{q_{6 \times 1}\} = [b_{6 \times 6}]\{u_{6 \times 1}\} \quad (2.1)$$

with

$$\begin{Bmatrix} q_1 \\ q_2 \\ q_3 \\ q_4 \\ q_5 \\ q_6 \end{Bmatrix} = \begin{Bmatrix} F_1 \\ F_2 \\ F_3 \\ M_1 \\ M_2 \\ M_3 \end{Bmatrix} \quad (2.2)$$

and

$$\begin{Bmatrix} u_1 \\ u_2 \\ u_3 \\ u_4 \\ u_5 \\ u_6 \end{Bmatrix} = \begin{Bmatrix} u_1 \\ u_2 \\ u_3 \\ \theta_1 \\ \theta_2 \\ \theta_3 \end{Bmatrix} \quad (2.3)$$

The vector $\{q\}$ is a set of three forces and three moments, the vector $\{u\}$ is a set of three translations and three rotations, and the 6-by-6 pile stiffness matrix $[b]$ relates the two vectors. The elastic pile constants matrix (i.e., the pile stiffness matrix) is given as

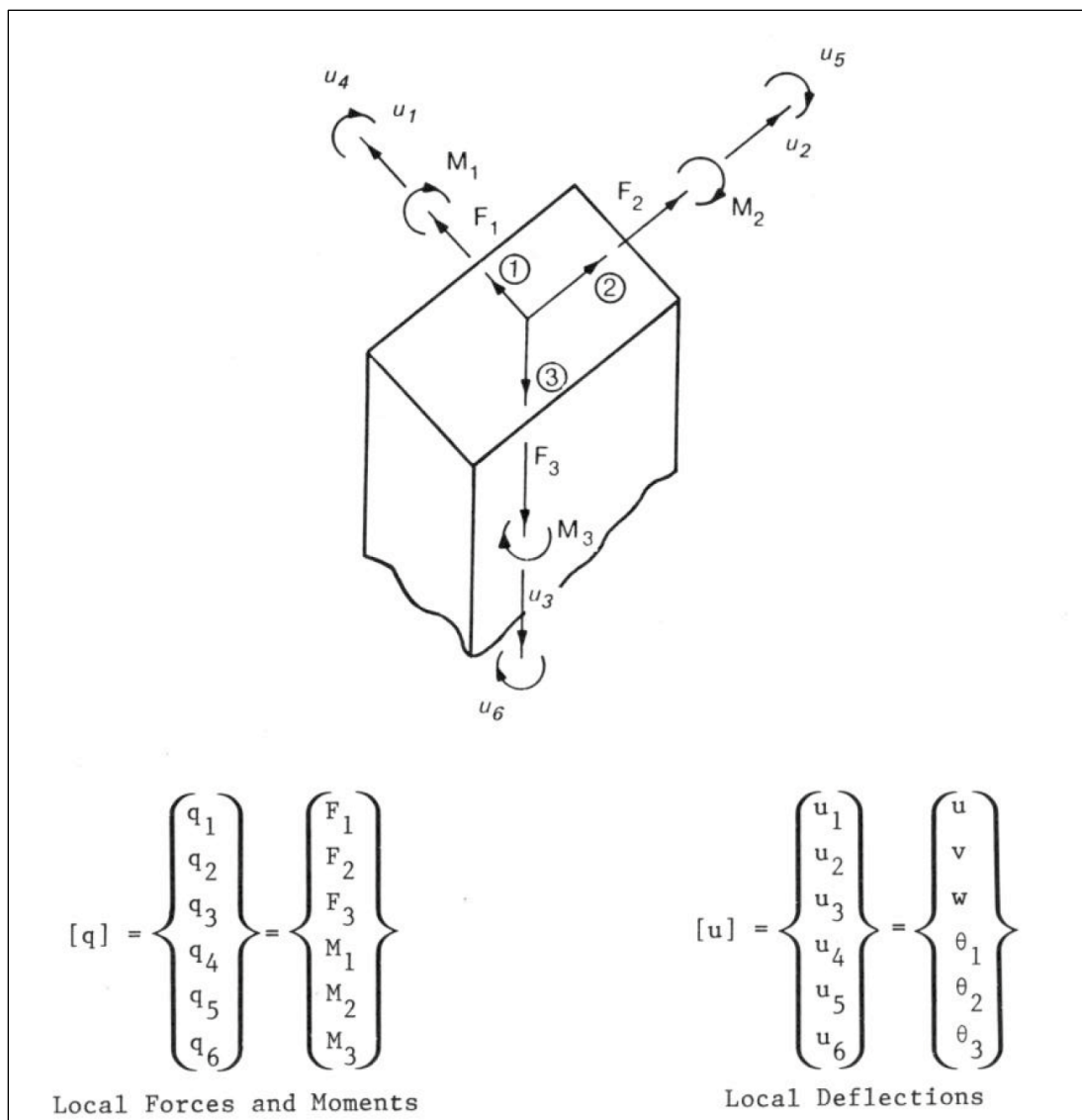
$$[b] = \begin{bmatrix} b_{11} & 0 & 0 & 0 & b_{15} & 0 \\ 0 & b_{22} & 0 & b_{24} & 0 & 0 \\ 0 & 0 & b_{33} & 0 & 0 & 0 \\ 0 & b_{42} & 0 & b_{44} & 0 & 0 \\ b_{51} & 0 & 0 & 0 & b_{55} & 0 \\ 0 & 0 & 0 & 0 & 0 & b_{66} \end{bmatrix} \quad (2.4)$$

where subscripts 1, 2, and 3 refer to the local pile coordinate system axes and 4, 5, and 6 are rotations about those local pile axes, as shown in Figure 2.4. The pile stiffness coefficients are defined as follows:

- b_{11} = Force required to displace the pile head a unit distance along the local 1 axis (force/length)
- b_{22} = Force required to displace the pile head a unit distance along the local 2 axis (force/length)
- b_{33} = Force required to displace the pile head a unit distance along the local 3 axis (force/length)
- b_{44} = Moment required to displace the pile head a unit rotation around the local 1 axis (force*length/radian)
- b_{55} = Moment required to displace the pile head a unit rotation around the local 2 axis (force*length/radian)
- b_{66} = Moment required to displace the pile head a unit rotation around the local 3 axis (force*length/radian)
- * b_{15} = Force required along the local 1 axis to resist lateral movement during a unit rotation of the pile head around the local 2 axis (force/radian)
- * b_{24} = Force required along the local 2 axis to resist lateral movement during a unit rotation of the pile head around the local 1 axis (force/radian)
- * b_{51} = Moment required around the local 2 axis to resist rotation caused by a unit displacement of the pile head along the local 1 axis (force*length/radian)
- * b_{42} = Moment required around the local 1 axis to resist rotation caused by a unit displacement of the pile head along the local 2 axis (force*length/radian)

*Since the stiffness matrix must be symmetric, $b_{15} = b_{51}$ and $b_{24} = b_{42}$. The sign of b_{24} and b_{42} must be negative.

Figure 2.4. The CPGA local pile head forces, moments, deflections, and rotations (after Harman et al. 1989).

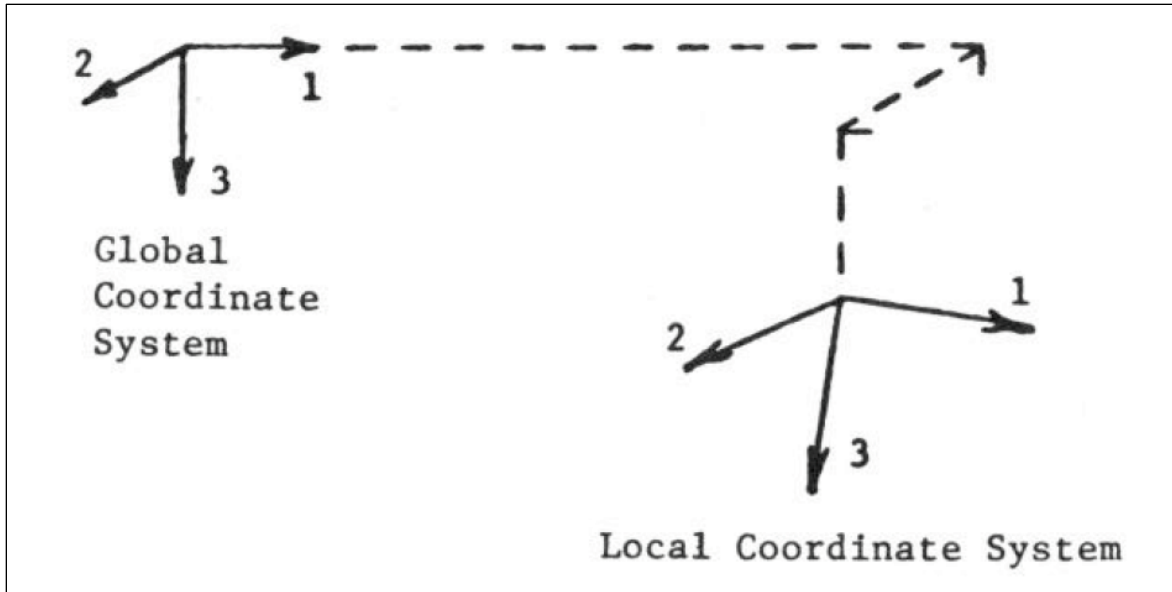


Generally, each stiffness coefficient is influenced by the effects of pile-structure and pile-soil interaction.

Each pile has its own local coordinate system, as depicted in Figure 2.4. The orientation of each local pile system is determined by the user-specified batter and batter direction of each pile. The local pile has three axes labeled 1, 2, and 3, as shown in Figures 2.4 and 2.5. The position of each pile (and its local coordinate system) is located relative to the global coordinate system for the pile group model (Figure 2.5). The forces acting at the local pile are obtained by transferring (i.e., projecting) the global forces (and moments) into forces along the local axes and computation of moments at

the local axis. The 3-axis is positive along the length from head to tip. Recall that the global coordinate system is used for specification of pile locations and orientations, applied forces and moments on the pile cap, for calculation of total pile group stiffness, and for resulting pile cap displacements and rotations.

Figure 2.5. The CPGA local pile head and global, orthogonal, right-hand coordinate systems (after The CASE Task Group on Pile Foundations 1983).



The Equation 2.4 stiffness matrix of each pile is transformed from the local coordinate system to the global coordinate system. Recall the global coordinate system is located at the user-specified origin. All pile stiffness matrices are then summed to form a 6-by-6 matrix representing the stiffness of the entire pile group, $[K_{6 \times 6}]$. Applied loads and moments, $\{Q_{6 \times 1}\}$, are defined at the Figure 2.1 origin. To determine the displacements of the pile cap, $\{U_{6 \times 1}\}$, the following equation is solved by CPGA

$$\{Q_{6 \times 1}\} = [K_{6 \times 6}]\{U_{6 \times 1}\} \quad (2.5)$$

For the vector of global, user-defined forces $\{Q_{6 \times 1}\}$, the Figure 2.1 global displacements $\{U_{6 \times 1}\}$ are computed at the origin. The 6-by-6 matrix $[K_{6 \times 6}]$ is the assembled, global stiffness matrix for the entire pile group foundation. Once these global displacements have been determined, the displacements at the head of each pile can be determined by a geometric transformation based on the location and orientation of that pile. The individual forces in each pile are computed using Equation 2.1 for each pile. This summarizes

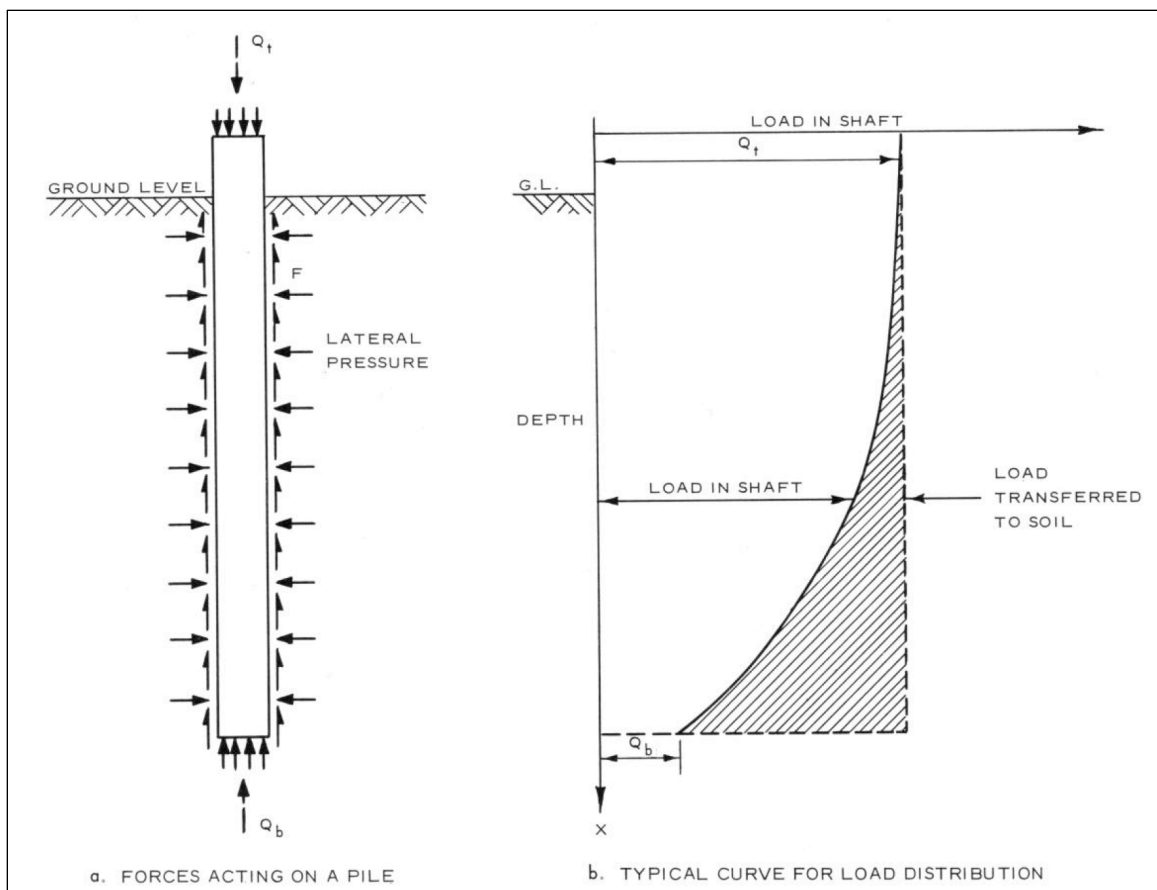
the basic analysis of a pile group by CPGA software. Further details on the equations used are contained in Hartman et al. (1989) and Saul (1968).

2.4 Axial pile stiffness b_{33} and axial pile stiffness modifier C_{33}

The axial stiffness of a batter pile in a pile group like the one used in the Lock and Dam 3 Figure 1.2 configuration can be an important contributor to the lateral resistance of the pile group subjected to an impact load, resulting from a barge-train impact with a flexible approach wall structural system. In the CPGA formulation, the axial compression characteristic of a batter pile is defined by the axial pile stiffness term b_{33} in the individual pile stiffness matrix Equation 2.4. Examination of Equations 2.1 through 2.4 demonstrates that there is no coupling of the axial deformation with any other degree of the 6 (local) degrees of freedom of an individual pile.

The axial stiffness of a pile is defined as the axial force required for displacement of the pile top a unit distance in the axial direction. The axial stiffness of a pile depends on many factors such as the modulus of elasticity of the pile, the pile cross-sectional area, the pile length, the pile tip deflection, the distribution of axial skin friction along the pile, and the percentage of axial load transmitted to the tip. The pile tip deflection under axial load and the manner in which the axial force in the pile is transmitted to the soil are interrelated and can have a great effect on the axial stiffness of the pile. Figure 2.6 is an illustration of the axial load transfer along the length of the embedded portion of the pile. This *load shedding* from the pile into the soil occurs due to mobilization of soil-to-pile skin friction along the length of the pile, progressing from the top of ground surface to the pile tip. Observe the load in the Figure 2.6b shaft of the pile diminishes with depth due to the transfer of load from within the pile to the soil, and Q_b is the magnitude load that is transferred to the soil at the pile tip in this figure. Because of nonlinear soil behavior and SSI effects, the distribution of load transfer along the pile shaft relative to the load transferred at the pile tip varies with the magnitude of the load applied to the top of the pile.

Figure 2.6. Illustration of axial load transfer in a pile with depth (after The CASE Task Group on Pile Foundations 1983).

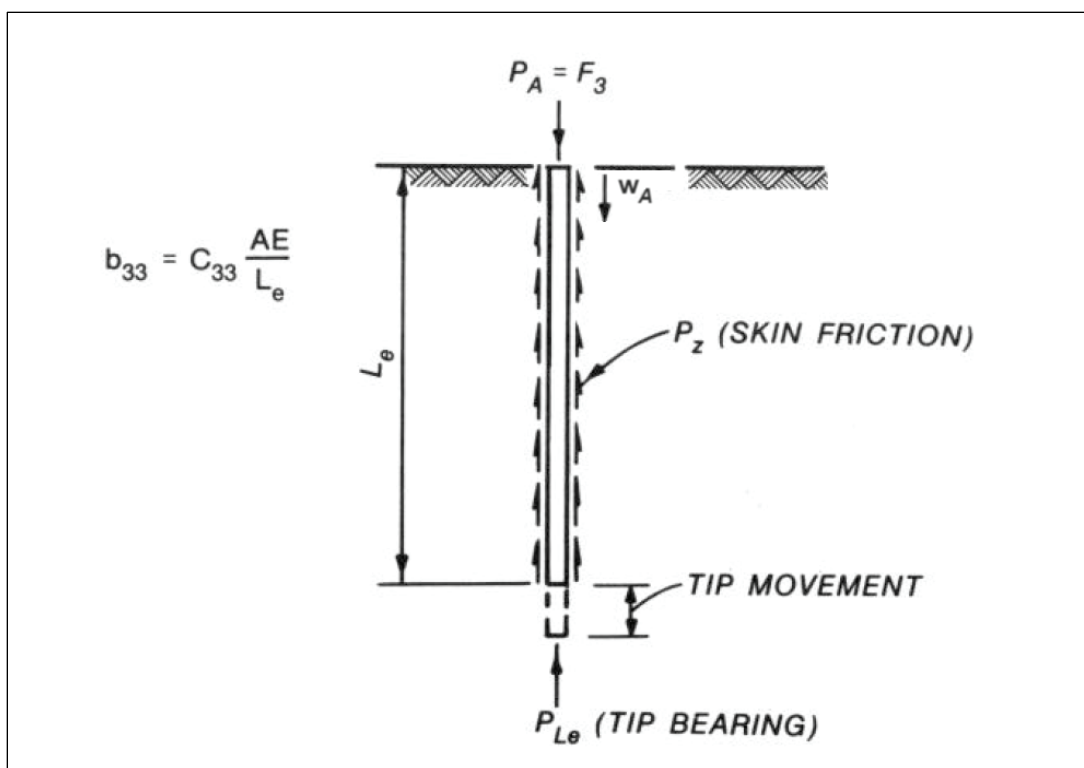


Corps experience has shown that calculation of the axial pile stiffness coefficient for use in pile foundation analysis can best be accomplished using data from axial pile load tests conducted at the project site. When the soil layering and traditional geotechnical engineering material properties have been defined for the site, an alternative method to pile load tests may be used to define a pile's axial stiffness. This alternative approach is an analytical procedure that uses the CASE software CAXPILE to mathematically analyze a single pile. From these computed results, a secant value for axial pile stiffness (i.e., term b_{33} in Equation 2.4 of a CPGA batter pile group analysis) may be computed. Analytical calculations made by the authors of this report as part of this R&D study using CAXPILE confirmed that the magnitude of load shedding along the pile and the magnitude of load reaching the soil foundation below the pile tip (i.e., Q_b) depend upon the movement of the pile relative to that of the soil along the pile as well as the movement developing at the tip of the pile. The distribution of loading between the pile tip and that occurring along the pile is dependent upon the magnitude of the axial load applied to the top

of the pile. Because of this, a secant stiffness approach is recommended for the assignment of the axial pile stiffness, b_{33} term, for use in pile group analysis software such as CPGA.

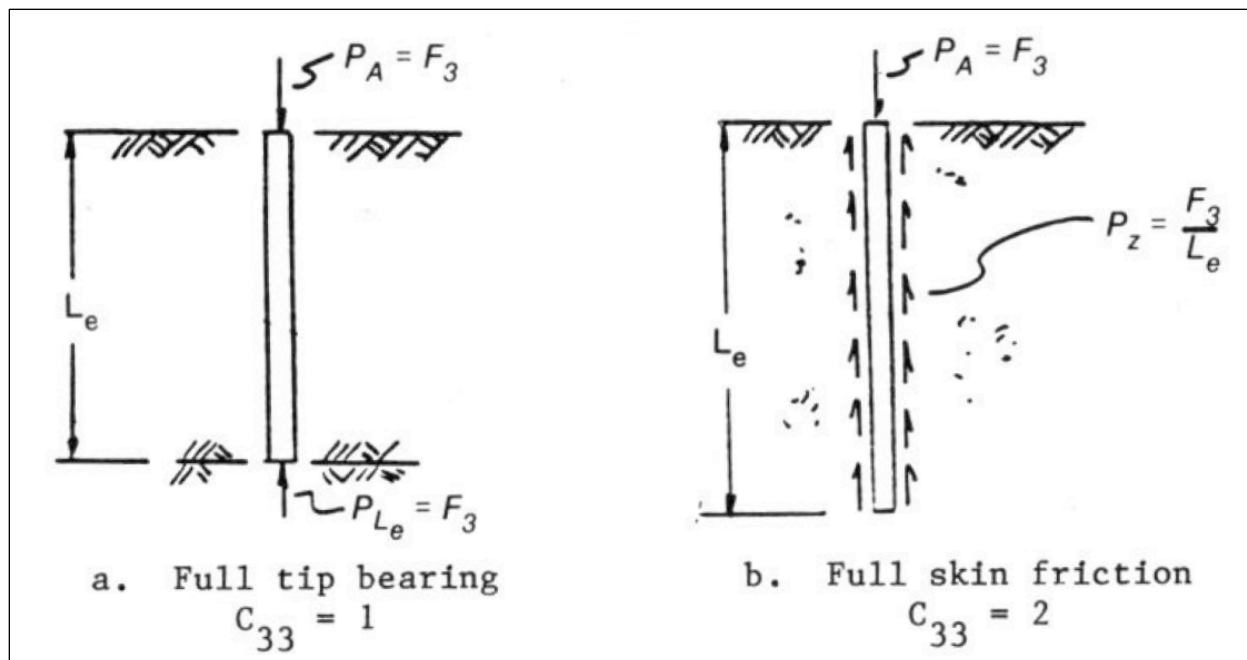
As noted previously, the Corps approach that is implemented in the CPGA software accounts for pile-to-soil interaction by applying the empirical C_{33} factor to the axial pile stiffness coefficient of $[AE/L_e]$ (Figure 2.7). This approach is valid only if the selection of the empirical factor is correlated with either pile load test data or with available geotechnical data for the project site and engineering experience from previous projects. Stiffness coefficients for compression piles and tension piles are addressed separately because their load transfer mechanisms are different. That is to say, the stiffness coefficients will not be equal for identical piles that are equally loaded in tension or compression.

Figure 2.7. Load transfer by combined skin friction and tip bearing for an axially loaded compression pile (after Harman et al. 1989).



An axial stiffness coefficient of $[AE/L_e]$ represents an ideal pile which transfers all its load in tip bearing, as shown in Figure 2.8a. Similarly, an axial stiffness coefficient of $[2*AE/L_e]$ represents an ideal pile which transfers all its load by skin friction uniformly along its length with no tip movement, as depicted in Figure 2.8b.

Figure 2.8. Load transfers for an axially loaded compression pile (after Harman et al. 1989).



Both Hartman et al. (1989) and The CASE Task Group on Pile Foundations (1983) suggested C_{33} values of 1 for compression piles with full tip bearing and 2 for piles with full skin friction, respectively. No engineering derivation/calculation was provided in either document to demonstrate the basis for these recommendations.

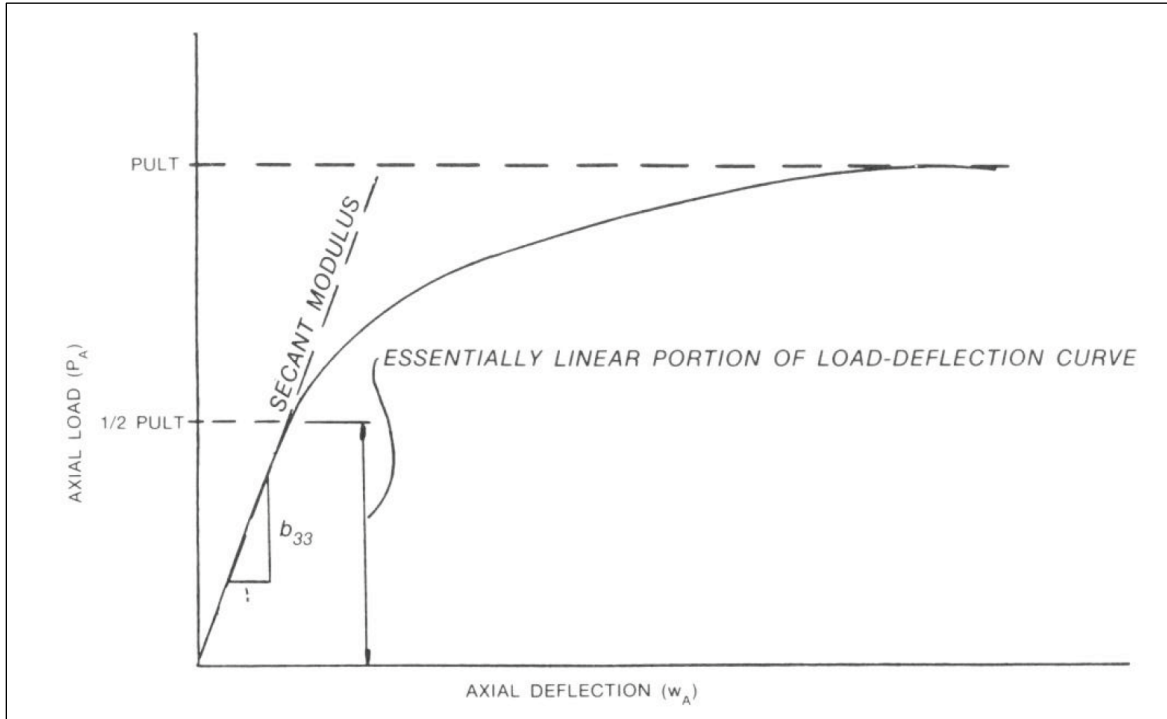
Hartman et al. (1989) observe that the load-versus-deflection (at the top of pile) curve for a compression pile is essentially linear to one-half the ultimate capacity, as depicted in Figure 2.9. Axial compression pile load versus deflection results computed at the top of pile using the Corps CAXPILE software tends to reinforce this generalization. At some stage of axial compression loading above the $[P_{ULT}/2]$ value, this relationship becomes nonlinear¹. Thus, the appropriate value for secant stiffness, b_{33} , will be a function of the deflection of the top of the pile at the ground surface, w_A (Figure 2.9).

The secant axial stiffness term b_{33} is given by a line originating at the Figure 2.9 origin and passing through the specific a point defined by a specific value of load P_A and top of pile displacement w_A :

¹ P_{ULT} is the ultimate axial pile capacity.

$$b_{33} = \frac{P_A}{w_A} \quad (2.6)$$

Figure 2.9 Compression pile axial load versus deflection curve (after Harman et al. 1989)



Observe in Figure 2.9 that each point on the load-deflection curve is unique, defined by a specific P_A value and specific w_A value. Due to the nonlinear relationship between axial load and axial deflection (Figure 2.9), the secant value for b_{33} is a function of the level of axial pile loading P_A . Conversely, since any point on the load-deflection curve is unique and may be defined by either its P_A value or its w_A value, the value for axial stiffness b_{33} may also be stated as a function of the axial deformation of the top of pile at the elevation of the ground surface (i.e., w_A).

Introducing the following equation

$$b_{33} = C_{33} * \frac{A^* E}{L_e} \quad (2.7)$$

into Equation 2.6 and rearranging, results in a secant-based definition of the empirical coefficient,

$$C_{33} = \frac{P_A / w_A}{A^* E / L_e} \quad (2.8)$$

Due to the nonlinear relationship between axial load and axial deflection (Figure 2.9), the value for C_{33} is a function of the level of axial pile loading P_A or the axial deformation of the top of pile at the ground surface (i.e., w_A).

Denoting the deflection of the top of an axially loaded column with no soil present as Δ , the value for Δ is given by

$$\Delta = \frac{P^* L_e}{A^* E} \quad (2.9)$$

The deflection of the top of an axially loaded pile in soil, designated w_A , is obtained by introducing Equation 2.6 into Equation 2.7 and solving for w_A . Performing this substitution and algebraic manipulation results in the relationship

$$w_A = \left(\frac{1}{C_{33}} \right) * \left[\frac{P_A^* L_e}{A^* E} \right] \quad (2.10)$$

Combining Equations 2.9 and 2.10 and solving for C_{33} results in

$$C_{33} = \frac{\Delta}{w_A} \quad (2.11)$$

Thus, the axial pile stiffness modifier is the theoretical deflection of an equivalent column with the same properties as the pile (i.e., length, cross-sectional area, modulus of elasticity) divided by the deflection of the pile due to the same level of load. The CPGA manual (Hartman 1989) suggests that the value for C_{33} falls within the range of 0.5 to 2.0 for compression piles. To provide perspective on the impact of the value assigned to C_{33} , a comparison is made between the displacement at the top of a free-standing column and the top of an axially loaded pile for the same applied load P_A . First, the inter-relationship between the two displacements will be derived.

The inter-relationship between the deflection at the top of an axially loaded pile in soil (w_A) and the deflection of an axially loaded column with

no soil present (Δ) subjected to the same axial load is obtained by rearranging Equation 2.11 as follows:

$$w_A = \left(\frac{1}{C_{33}} \right) * \Delta \quad (2.12)$$

Full tip bearing pile: As reported in Figure 2.8a and according to the CPGA manual (Hartman 1989), a full tip bearing pile possesses a C_{33} value of 1.0. This infers that the displacement at the top of a column with no soil present is the same as at the top of a full tip bearing pile.

Full skin friction pile: As reported in Figure 2.8b and according to the CPGA manual (Hartman 1989), a full skin friction pile with no contribution from tip resistance possesses a C_{33} value of 2.0. This infers that the displacement at the top of a friction pile is one-half of the displacement occurring at the top of column with no soil present. This difference in deflection values reflects the *load-shedding* of the axial load with depth within the pile due to the action of the skin friction of the soil acting on the interface/surface of the pile.

In summary, data obtained from the load-deflection curve resulting from an axial pile load test is ideal for determining the appropriate value for the axial stiffness term b_{33} and the value for the axial stiffness modified C_{33} . Alternatively, a load-transfer analysis using, for example, CAXPILE software is appropriate for defining values for b_{33} and C_{33} . Because of the nonlinear axial compression load versus top-of-pile displacement relationship (e.g., Figure 2.9), a secant stiffness value for the axial stiffness b_{33} is appropriate, as well as for the axial stiffness modifier C_{33} . Thus, the value of b_{33} and C_{33} will be load dependent or dependent on the magnitude of the top-of-pile (at ground elevation [el]) displacement.

Tension pile: It is cautioned that the effect end bearing influences the deflection at the top of a compression pile. This influence will not be present in tension piles. Refer to Harman (1989) for guidance about tension pile axial stiffness. This issue is not part of this study.

One of the failure mechanisms to be concerned with for batter piles is the potential for buckling of a batter pile under compressive load P_A . Appendix B outlines an engineering evaluation process for computing the evaluation of buckling loads of piles.

3 Examples of Axial Pile Stiffness Computations for Batter Piles in Stratified and Homogeneous Foundations

3.1 Introduction

This chapter summarizes an engineering methodology that uses CAXPILE results to assist in the engineering characterization of the axial stiffness of batter piles for use in a CPGA pile group model of flexible approach walls. The flexible approach walls used by the Corps consist of elevated impact decks (or beams) supported by clustered groups of piles. For batter pile configurations modeled using CPGA software, the axial stiffness term (b_{33}) is an important contributor to the pile group deformation calculation, as discussed in Chapter 2. Recall from subsection 2.4:

$$b_{33} = C_{33} * \frac{A * E}{L_e} \quad (2.7 \text{ bis})$$

with C_{33} being an axial stiffness modifier, A designating the cross-sectional area of the concrete-filled pipe pile, E designating the pile's (composite) Young's Modulus, and L_e being the length of pile embedment. As discussed in Subsection 2.4, the CPGA software accounts for pile-to-soil interaction by applying the empirical C_{33} factor to the axial pile stiffness coefficient of $[AE/L_e]$.

Recall that Hartman et al. (1989) and The CASE Task Group on Pile Foundations (1983) suggested a C_{33} value of 1 for compression piles with full tip resistance and a C_{33} value of 2 for piles with full skin friction. The authors of this report observe that no engineering derivation/calculation(s) was provided by CPGA software developers and their supporting CASE Task Group to demonstrate the basis for these two recommendations. Consequently, an engineering investigation into the assignment of an appropriate value for the CPGA C_{33} term was launched. This investigation centers on the analysis of the Figure 1.2 clustered group of three piles configuration used at the Lock and Dam 3 flexible approach wall extension (Figures 1.3 through 1.5).

Different types of soil foundations are investigated for the Figure 1.2 batter pile group: the first axial stiffness investigation discussed involves an

analysis for the seven-layered, soil stratum existing at the site of the Lock and Dam 3 flexible approach wall extension. The soil profile along the guidewall extension is shown in Appendix C (Figure C.1). The submerged layers of soils consist of riprap, interbedded layers of sands at different densities, silts, and clays. No compression pile load tests were conducted at the Lock and Dam 3 site, so the authors of this report reverted to a CAXPILE analysis using site-specific engineering properties made available for this project by Kent Hokens of St. Paul District. This initial series of CAXPILE analyses for the site-specific, stratified soil foundation is augmented by a parametric analysis of the same Figure 1.2 batter pile group CPGA model but founded in homogenous sand foundations, each with a different density. Two different assessments are made of the axial pile stiffness modifier term C_{33} for a batter pile in this Figure 1.2 batter pile group: one for a batter pile group founded in a medium-dense sand site and a second for a batter pile group founded in a dense sand site.

3.2 Data reduction of CAXPILE results into values for the CPGA C_{33} parameter for batter piles

The approach for characterizing axial pile stiffness of batter piles as implemented within CPGA software accounts for pile-soil interaction effects by applying an empirical factor (C_{33}) to the axial stiffness coefficient of $[AE/L_e]$ of the axially loaded structural (batter pile) member of a batter pile configured pile group. Details regarding the CAXPILE analyses made using Lock and Dam 3 site-specific engineering properties are discussed in Appendix C. This appendix includes a summary of relevant engineering material properties and the CAXPILE input for each of the seven soil layers, as well as the processing of CAXPILE results.

Recall Section 2.4 provides a detailed discussion of the engineering methodology being used to assess the axial stiffness of a batter pile for use in a CPGA batter pile group model. The key equation used for processing CAXPILE output into value(s) for C_{33} is Equation 2.8:

$$C_{33} = \frac{P_A / w_A}{A * E / L_e} \quad (2.8 \text{ bis})$$

with P_A designating the applied compression load and w_A designating the displacement of the top of pile (at its start of embedment elevation). The

terms A , E , and L_e are constants. For all CAXPILE analyses discussed in this chapter, the following constants were assigned: the cross-sectional area of the concrete-filled pipe pile is 452.4 in.² (Equation B.1), the composite Young's Modulus is 5,124,000 psi (Equation B.12), and the length of embedded pile L_e , is 53.6 ft.

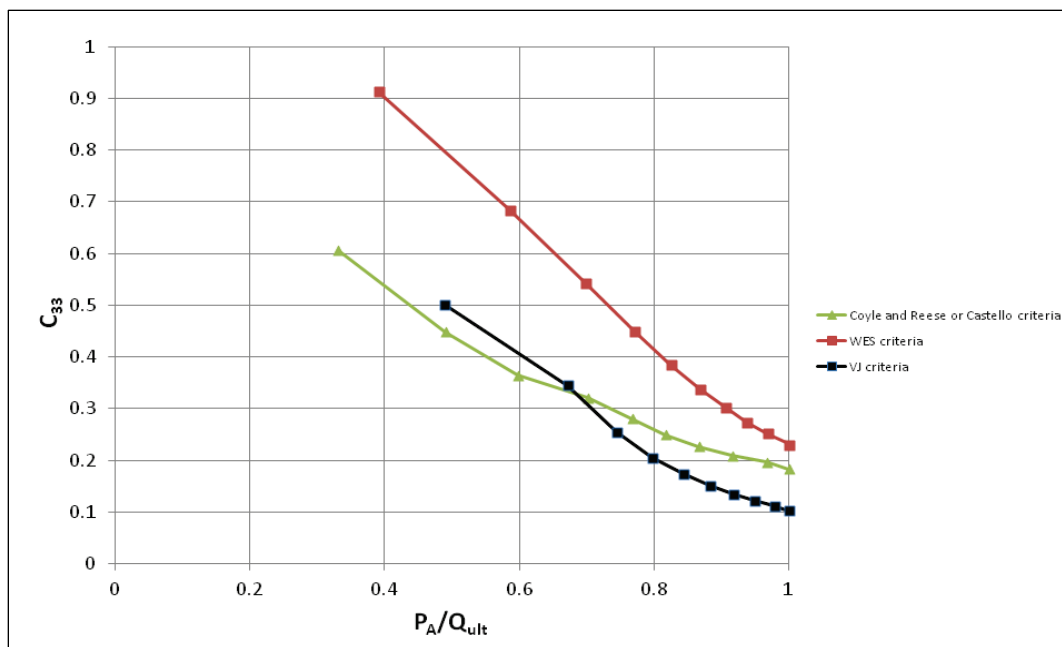
CAXPILE offers three different SSI models to generate the axial load P_A versus top-of-pile axial deformation w_A data (e.g., Figure 2.9) for the user-specified soil site. They are designated as Soil criteria, WES criteria and VJ criteria in the user's manual. All three SSI models were run for each of the Figure 1.2 batter pile foundation models investigated in this study. For the actual soil layering of the site and two hypothetical, isotropic cohesionless soil conditions, a total of nine CAXPILE analyses were conducted. Three of these SSI model results are discussed in detail in Appendix C for the actual soil conditions found at the site. Appendices D and E each discuss three sets of results for the three SSI models used in the CAXPILE batter pile models for the hypothetical medium-dense and dense sand sites, respectively.

The tension pile capacities were also summarized in each of the three appendices. They are based on hand calculations using three independent engineering evaluation procedures.

3.3 Axial pile stiffness characterization of a compression batter pile at the Lock and Dam 3 layered soil site

Figure 3.1 summarizes the axial stiffness modifier C_{33} results from three CAXPILE analyses of a compression batter pipe pile in the Figure 1.2 Lock and Dam 3 clustered group of three piles founded in its layered soil stratum. Engineering material properties used as input to each of the three CAXPILE models are based on Lock and Dam 3 Guidewall extension Soil profile at station 21 + 72, as discussed in Appendix C. The layered soil geometry of Table C.1 and the engineering material properties listed in Table C.2 were used to assemble the three CAXPILE input data files. An important aspect of the site condition is that the batter piles rest on a very dense sand layer. All three SSI models available for use in a CAXPILE analysis (designated as the Soil criteria, WES criteria, and VJ criteria) were run for this 4V:1H batter pile equivalent soil column. A Figure 2.9 type of compression pile load versus deflection plot was generated in each CAXPILE analysis (not shown) and the results processed to obtain the results summarized in this subsection.

Figure 3.1. C_{33} versus axial load expressed as a fraction of the axial capacity of a 4V:1H batter compression pile at Lock and Dam 3 Guidewall extension for the layered soil profile at station 21 + 72, computed using the CAXPILE Soil criteria, WES criteria, and VJ criteria.



The computed results from each of the three CAXPILE analyses are paired P_A and w_A data values at the top of pile (specifically, at its start of embedment elevation). The CAXPILE software analysis has the effect of incrementally increasing the value for axial load P_A until it achieves the compression pile's capacity, Q_{ult} for the pile. The computed P_A and w_A results were postprocessed to generate companion C_{33} values using Equation 2.8. The C_{33} versus normalized axial load [P_A/Q_{ult}] results for the CAXPILE Soil criteria (using Coyle and Reese [1966] for the clay layers and Castello [1980] for the sands) SSI analysis is depicted by the green curve in Figure 3.1. Q_{ult} from the CAXPILE SSI analysis using Soil criteria is computed to be equal to 923.3 kips (Table 3.1). Examination of these computations shows that 83% of Q_{ult} is provided in tip resistance, with 17% provided in skin friction. This indicates that this batter pile is much more of a tip bearing pile rather than a skin friction pile. For a [P_A/Q_{ult}] range in values from 0.35 to 1, C_{33} drops from 0.6 to 0.18. These values for C_{33} from the results of a CAXPILE analysis using a Soil criteria are well below the Hartman et al. (1989) and The CASE Task Group on Pile Foundations (1983) suggested value of 1.0 for full tip bearing. This observation is repeatedly made for each of the analyses performed in this report. Additionally, Figure 3.1 results demonstrate that the value to be assigned to the axial stiffness modifier C_{33} term in a CPGA batter pile group model pushover analysis depends upon the fraction of compression pile capacity being utilized (i.e., [P_A/Q_{ult}]).

Table 3.1. Summary of the calculated ultimate compression capacity of a 4V:1H batter pile for the Lock and Dam 3 site using select engineering methodologies and the CASE CAXPILE software.

Engineering Methodology	Q_s Shaft Resistance of the Pile Due to Skin Friction-Compression (kips)	Q_t Tip Resistance of the Pile Due to End Bearing (kips)	Q_{ult} Ultimate Pile Capacity (kips)	Q_s/Q_{ult}	Q_t/Q_{ult}	Notes
EM 1110-2-2906	172	214.7	386.7	0.44	0.56	Hand calculation; critical depth D_c is 30 ft. ($=15 \cdot D_p$); $\delta' = 0.83 \cdot \phi'$ in sand layers; $N_q = 40$ for tip resistance in dense sand
API*	196.5	472.8	669.3	0.29	0.71	Hand calculation; limiting skin friction in sands of 1,700 psf.; $\delta' = \phi' - 5$ deg in sand layers; $N_q = 50$ for tip resistance in dense sand; limiting unit tip resistance of 250 ksf
Castello sand curves	176.4	785.4	961.8	0.18	0.82	Hand calculation; unit side resistances by Figure A.2 and unit tip resistance by Figure A.3
CAXPILE using Soil criteria	160.3	763	923.3	0.17	0.83	Soil criteria option uses Castello criteria curves for sand layers and Coyle and Reese criteria for clay layers
CAXPILE using WES criteria	137.3	938.8	1,076.1	0.13	0.87	Input specified $\delta' = 0.83 \cdot \phi'$ for sand layers
CAXPILE using VJ criteria	194	472.3	666.3	0.29	0.71	$\delta' = \phi' - 5$ deg in sand layers; $N_q = 50$ for unit tip resistance in dense sand

*Note: API designating the American Petroleum Institute.

Hand calculations were made using the Castello sand curves (i.e., Figure A.2 for unit side resistance and Figure A.3 for unit tip resistance) and the EM 1110-2-2906 (HQUSACE 1991) for the skin friction of the clay and silt layers, resulting in a Q_{ult} value of 961.8 kips (Table 3.1). This computed value for Q_{ult} is within 4% of the 923.3 kips CAXPILE SSI analysis result using the Soil criteria. This hand calculation serves to confirm the CAXPILE Soil criteria result for Q_{ult} .

The C_{33} versus normalized axial load [P_A/Q_{ult}] results computed by the second of three CAXPILE analyses using the WES criteria is depicted by the red curve in Figure 3.1. Q_{ult} from the CAXPILE SSI analysis using WES criteria is equal to 1,076.1 kips (Table 3.1). These computations show that 87% of Q_{ult} is provided in tip resistance, with 13% provided in skin friction. Like the CAXPILE analysis using Soil criteria, this SSI analysis also

indicates that this batter pile is much more of a tip bearing pile rather than a skin friction pile. For $[P_A/Q_{ult}]$ ranging in value from 0.4 to 1, C_{33} drops from 0.91 to 0.23.

The C_{33} versus normalized axial load $[P_A/Q_{ult}]$ results computed by the third CAXPILE analyses using the VJ criteria is depicted by the black curve in Figure 3.1. Q_{ult} from the CAXPILE SSI analysis using VJ criteria, is equal to 666.3 kips (Table 3.1). These computations show that 71% of Q_{ult} is provided in tip resistance, with 29% provided in skin friction. Like the other two CAXPILE SSI analyses, this analysis indicates that this batter pile is more of a tip bearing pile versus a skin friction pile. For $[P_A/Q_{ult}]$ ranging in value from 0.5 to 1, C_{33} drops from 0.5 to 0.1.

Hand calculations made using the API (2000) guidance resulted in a Q_{ult} value of 669.3 kips (Table 3.1). This computed value for Q_{ult} is within 1% of the 666.3 kips CAXPILE SSI analysis result using the VJ criteria. This hand calculation serves to confirm the CAXPILE VJ criteria results for Q_{ult} .

In addition to the previously discussed (five) analyses, a third compression pile capacity (Q_{ult}) computation was made following EM 1110-2-2906 (HQUSACE 1991) guidance. This hand calculation resulted in a value for Q_{ult} equal to 386.7 kips (Table 3.1). This value is far lower than the 666.3 to 1,076.1 kips range computed in the other five analyses. After a careful assessment of the details contained within this last computation, it is deemed by the authors of this report to be a conservative estimate of Q_{ult} . Site-specific compression pile load tests would be the definitive and most reliable method for assessing Q_{ult} at a site. Since that type of field data is not available, a statistical assessment of the six Table 3.1 Q_{ult} values is made. The statistical processing of the Table 3.1 data results in a mean value for Q_{ult} of 780.6 kips, a standard deviation of 253.4 kips, and a coefficient of variation (COV) equal to 0.32. If the result from the EM 1110-2-2906 (HQUSACE 1991) based computation is excluded, the mean Q_{ult} value is 859.4 kips, the standard deviation is 183.7 kips, and the COV equals 0.21.

3.4 Axial capacity of a tension batter pile at the Lock and Dam 3 layered soil site

The tension pile capacity calculations were also made and summarized in Appendix C, with their resulting Q_s values listed in Table 3.2. These results are based on hand calculations using three independent engineering evaluation procedures; EM 1110-2-2906 (HQUSACE 1991), API guidance

for pipe piles and based on the use of Castello skin friction curves given in Figure A.2. The shaft resistance Q_s values computed for compression piles are also listed for comparison purposes. Q_s for a tension pile range in value from a low of 147.5 kips to a high of 196.5 kips. The statistical processing of the Table 3.2 results in a mean value for Q_s (tension) of 173.5 kips, a standard deviation of 24.6 kips, and a COV equal to 0.14.

Table 3.2. Summary of the calculated ultimate shaft resistance of a 4V:1H batter pile for the Lock and Dam 3 site in compression or in tension by three engineering methodologies.

Engineering Methodology	Q_s Shaft Resistance of the Pile Due to Skin Friction-Tension (kips)	Q_s Shaft Resistance of the Pile Due to Skin Friction-Compression (kips)	Notes
EM 1110-2-2906	147.5	172	Hand calculation; critical depth D_c is 30 ft. ($=15 \cdot D_p$); $\delta' = 0.83 \cdot \phi'$ in sand layers; K_h is set equal to 1 for a compression pile in the sand layers and 0.7 for tension piles according to Table A.3
API	196.5	196.5	Hand calculation; limiting skin friction in sands of 1,700 psf.; $\delta' = \phi' - 5$ deg in sand layers; limiting unit skin friction resistance listed in Table A.2 for the sand layers
Castello sand curves	176.4	176.4	Hand calculation; unit side resistances by Figure A.2

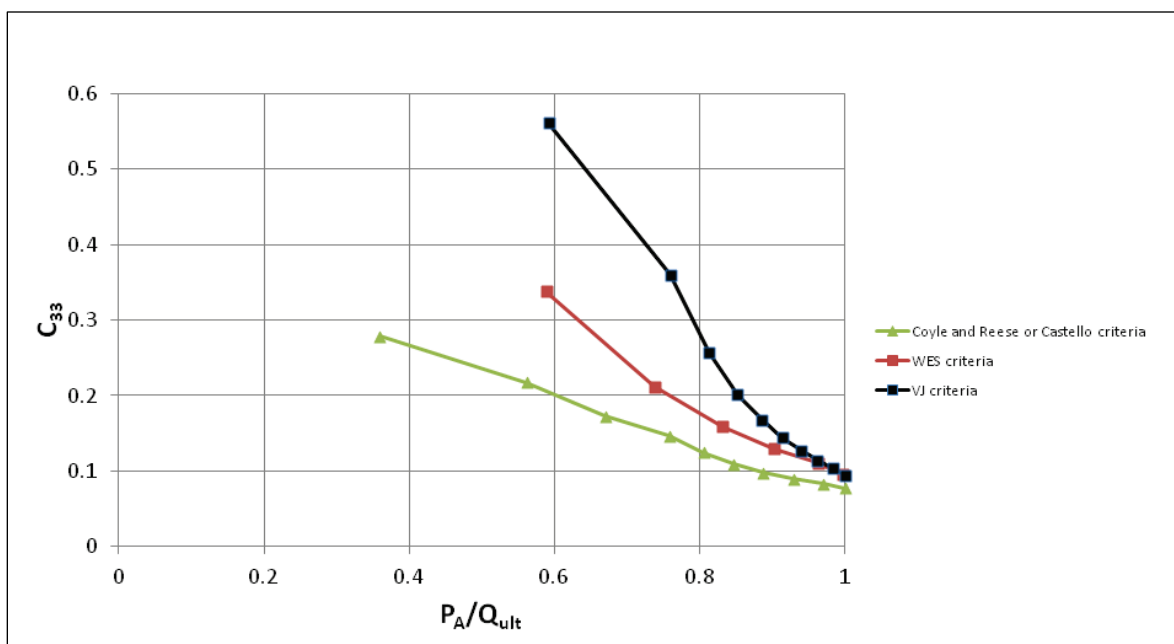
Observe from the pile axial capacity calculations listed in Table 3.2 that the EM 1110-2-2906 (HQUSACE 1991) procedure of analysis results in a lower tensile capacity than its compression capacity contribution due to skin friction.

3.5 Axial pile stiffness characterization of a Lock and Dam 3 type batter pile configuration founded in a hypothetical medium-dense sand

This subsection summarizes CAXPILE results for the first of two parametric analyses conducted of the Figure 1.2 pile-founded, Lock and Dam 3 flexible approach wall configuration. In this first parametric analysis, the upper 5 ft of riprap used in the Subsection 3.4 CAXPILE analyses was maintained, but below that, the layered soil foundation was replaced with homogenous medium-dense sand possessing an effective angle of internal friction equal to 32 degrees.

Figure 3.2 summarizes the axial stiffness modifier C_{33} results from three CAXPILE analyses of a compression batter pipe pile in the Figure 1.2 Lock and Dam 3 clustered group of three piles founded in medium-dense sand. Engineering material properties used as input to each of the three CAXPILE models are discussed in Appendix D. The two-layered soil geometry of Table D.1 and the engineering material properties listed in Table D.2 were used to assemble the three CAXPILE input data files using the Soil criteria, WES criteria, and VJ criteria for this 4V:1H batter pile equivalent soil column.

Figure 3.2. C_{33} versus axial load expressed as a fraction of the axial capacity of an equivalent vertical batter pile in medium-dense sand for a 4V:1H batter compression pile type configuration used at Lock and Dam 3 guidewall extension, computed using the CAXPILE Soil criteria, WES criteria, and VJ criteria.



The computed results from each of the three CAXPILE analyses are paired P_A and w_A data values at the top of pile (at its start of embedment elevation). These P_A and w_A results were then post-processed to generate companion C_{33} values (Equation 2.8). The C_{33} versus normalized axial load [P_A/Q_{ult}] results for the CAXPILE Soil criteria (using Castello for the medium-dense sand) SSI analysis is depicted by the green curve in Figure 3.2. Q_{ult} from the CAXPILE SSI analysis using Soil criteria is computed to be equal to 345.7 kips (Table 3.3). Examination of these computations show that 70% of Q_{ult} is provided in tip resistance, with 30% provided in skin friction. This indicates that this batter pile founded in medium-dense sand behaves more like a tip bearing pile versus a skin friction pile. For a [P_A/Q_{ult}] range in values from 0.36 to 1, C_{33} drops from 0.28 to 0.08.

Table 3.3. Summary of the calculated ultimate compression capacity of an equivalent vertical batter pile in medium-dense sand for a 4V:1H batter compression pile type configuration used at Lock and Dam 3 guidewall extension using select engineering methodologies and the CASE CAXPILE software.

Engineering Methodology	Q_s Shaft Resistance of the Pile Due to Skin Friction-Compression (kips)	Q_t Tip Resistance of the Pile Due to End Bearing (kips)	Q_{ult} Ultimate Pile Capacity (kips)	Q_s/Q_{ult}	Q_t/Q_{ult}	Notes
EM 1110-2-2906	224.9	236.4	461.3	0.49	0.51	Hand calculation; critical depth D_c is 30 ft. ($=15 \cdot D_p$); $\delta' = 0.83 \cdot \phi'$ in sand layers; $N_q = 40$ for tip resistance in medium-dense sand
API	291.1	309.9	601	0.48	0.52	Hand calculation; limiting skin friction in sands of 1,850 psf.; δ' from Table A.2; $N_q = 30$ for tip resistance in medium-dense sand; limiting unit tip resistance of 150 ksf
Castello sand curves	136.6	163.4	300	0.46	0.54	Hand calculation; unit side resistances by Figure A.2 and unit tip resistance by Figure A.3
CAXPILE using Soil criteria	104.3	241.4	345.7	0.3	0.7	Soil criteria option uses Castello criteria curves for sand layers
CAXPILE using WES criteria	92.2	317.2	409.4	0.23	0.77	Input specified $\delta' = 0.83 \cdot \phi'$ for sand layers
CAXPILE using VJ criteria	290.6	309.9	600.1	0.48	0.52	$\delta' = \phi' - 5$ deg in sand layers; $N_q = 30$ for unit tip resistance in medium-dense sand

Changing the site condition from a battered pipe pile embedded within the layered soil strata bearing on a very dense sand layer to one founded in homogenous, medium-dense sand significantly lowered the pile's capacity. The Q_{ult} value dropped from 923.3 kips to 345.7 kips when using the Soil criteria in the two CAXPILE SSI analyses. This change in site conditions also resulted in a lowering of the C_{33} values, ranging in value from 0.6 to 0.18 (Figure 3.1) for the layered site, and to 0.28 to 0.08 (Figure 3.2) for a hypothetical homogenous, medium-dense sand site. A lower CPGA pile model C_{33} value results in more axial batter pile deformation for a given applied axial load.

Hand calculations were made using the Castello sand curves (i.e., Figure A.2 for unit side resistance and Figure A.3 for unit tip resistance), resulting in a Q_{ult} value of 300 kips (Table 3.3). This computed value for Q_{ult} is within 13% of the 345.7 kips CAXPILE SSI analysis result using the Soil criteria.

The C_{33} versus normalized axial load [P_A/Q_{ult}] results computed by the second of three CAXPILE analyses of the hypothetical medium-dense sand site using the WES criteria is depicted by the red curve in Figure 3.2. Q_{ult} from the CAXPILE SSI analysis using WES criteria is equal to 409.4 kips (Table 3.3). These computations show that 77% of Q_{ult} is provided in tip resistance, with 23% provided in skin friction. Like the CAXPILE analysis using Soil criteria, this SSI analysis indicates that for this hypothetical site condition, this batter pile is more of a tip bearing pile rather than a skin friction pile. For [P_A/Q_{ult}] ranging in value from 0.59 to 1, C_{33} drops from 0.34 to 0.06.

These WES criteria SSI results reinforce the observations discussed previously regarding the computed results from the Soil criteria for the two different soil site conditions: the pile's capacity is significantly lowered when the site condition is changed from the layered soil strata with the batter pile bearing on a very dense sand layer to one founded in (and on) homogenous, medium-dense sand. Additionally, this change in site conditions resulted in a lowering of the C_{33} values.

The C_{33} versus normalized axial load [P_A/Q_{ult}] results computed by the third CAXPILE analyses using the VJ criteria is depicted by the black curve in Figure 3.2. Q_{ult} from the CAXPILE SSI analysis using VJ criteria is equal to 600.1 kips (Table 3.3). These computations show that tip resistance and skin friction provide nearly equal contributions to Q_{ult} . For [P_A/Q_{ult}] ranging in value from 0.59 to 1, C_{33} drops from 0.56 to 0.1.

Hand calculations made using the API (2000) guidance resulted in a Q_{ult} value of 601 kips (Table 3.3). This computed value for Q_{ult} agrees with the CAXPILE SSI analysis result using the VJ criteria.

In addition to the previously discussed (five) analyses, a third compression pile capacity (Q_{ult}) computation was made following EM 1110-2-2906 (HQUSACE 1991) guidance. This hand calculation resulted in a value for Q_{ult} equal to 461.3 kips (Table 3.3). Its resulting value is the fourth largest within the 300 to 601 kips range in values computed using the six methods of analysis. Again, site-specific compression pile load tests would be the definitive and most reliable method for assessing Q_{ult} at a site, as recognized by the EM 1110-2-2906 (HQUSACE 1991) guidance. Since that type of field data is obviously not available for this hypothetical site, a statistical assessment of the six Table 3.3 Q_{ult} values is made. The

statistical processing of the Table 3.3 data results in a mean value for Q_{ult} of 452.9 kips, a standard deviation of 126.8 kips, and a COV equal to 0.28. If the result from the hand calculation using the Castello sand curves is excluded, the mean Q_{ult} value is 483.5 kips, the standard deviation is 114.4 kips, and the COV equals 0.24.

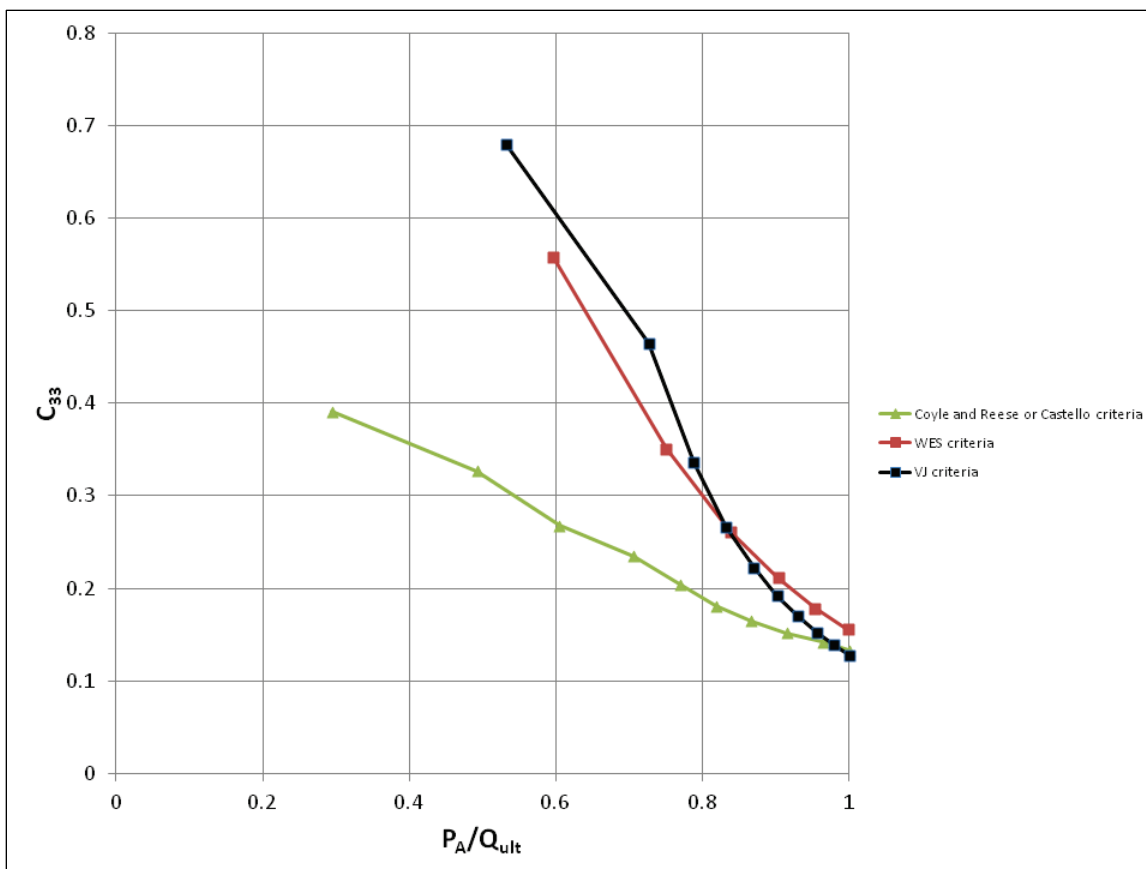
3.6 Axial pile stiffness characterization of a Lock and Dam 3 type batter pile configuration founded in a hypothetical dense sand

This subsection summarizes CAXPILE results for the second of two parametric analyses conducted of the Figure 1.2 pile-founded, Lock and Dam 3 flexible approach wall configuration. In this second parametric analysis, the upper 5 ft of riprap used in the Subsection 3.4 CAXPILE analyses was maintained, but below that, the layered soil foundation was replaced with homogenous dense sand possessing an effective angle of internal friction equal to 36 degrees.

Figure 3.3 summarizes the axial stiffness modifier C_{33} results from three CAXPILE analyses of a compression batter pipe pile in the Figure 1.2 Lock and Dam 3 clustered group of three piles founded in dense sand. Engineering material properties used as input to each of the three CAXPILE models are discussed in Appendix E. The two-layered soil geometry of Table E.1 and the engineering material properties listed in Table E.2 were used to assemble the three CAXPILE input data files using the Soil criteria, WES criteria, and VJ criteria for this 4V:1H batter pile equivalent soil column.

The computed results from each of the three CAXPILE analyses are paired P_A and w_A data values at the top of pile (at its start of embedment elevation). These P_A and w_A results were then postprocessed to generate companion C_{33} values (Equation 2.8). The C_{33} versus normalized axial load $[P_A/Q_{ult}]$ results for the CAXPILE Soil criteria (using Castello for the dense sand) SSI analysis is depicted by the green curve in Figure 3.3. Q_{ult} from the CAXPILE SSI analysis using Soil criteria is computed to be equal to 632 kips (Table 3.4). Examination of these computations shows that 84% of Q_{ult} is provided in tip resistance, with 16% provided in skin friction. This indicates that this batter pile founded in dense sand behaves more like a tip bearing pile versus a skin friction pile. For a $[P_A/Q_{ult}]$ range in values from 0.3 to 1, C_{33} drops from 0.39 to 0.13.

Figure 3.3. C_{33} versus axial load expressed as a fraction of the axial capacity of an equivalent vertical batter pile in dense sand for a 4V:1H batter compression pile type configuration used at Lock and Dam 3 guidewall extension, computed using the CAXPILE Soil criteria, WES criteria, and VJ criteria.



Changing the site condition from a battered pipe pile embedded within a homogenous, medium-dense sand to a homogenous, dense sand increased the pile's capacity. The Q_{ult} value increased from 345.7 kips to 632 kips when using the Soil criteria in the two CAXPILE SSI analyses. This change in site conditions also resulted in an increase in the C_{33} values, ranging in values from 0.28 to 0.08 (Figure 3.2) for a hypothetical homogenous, medium-dense sand site to 0.39 to 0.13 for a hypothetical, homogenous dense sand site (Figure 3.3). The greater the C_{33} value used in the CPGA pile model, the less axial batter pile deformation for a given applied axial load.

Hand calculations were made using the Castello sand curves (i.e., Figure A.2 for unit side resistance and Figure A.3 for unit tip resistance), resulting in a Q_{ult} value of 694.5 kips (Table 3.4). This computed value for Q_{ult} is within 10% of the 632 kips CAXPILE SSI analysis result using the Soil criteria.

Table 3.4. Summary of the calculated ultimate compression capacity of an equivalent vertical batter pile in dense sand for a 4V:1H batter compression pile type configuration used at Lock and Dam 3 guidewall extension using select engineering methodologies and the CASE CAXPILE software.

Engineering Methodology	Q_s Shaft Resistance of the Pile Due to Skin Friction-Compression (kips)	Q_t Tip Resistance of the Pile Due to End Bearing (kips)	Q_{ult} Ultimate Pile Capacity (kips)	Q_s/Q_{ult}	Q_t/Q_{ult}	Notes
EM 1110-2-2906	327.5	334.8	662.3	0.49	0.51	Hand calculation; critical depth D_c is 40 ft. ($=20 \cdot D_p$); $\delta' = 0.83 \cdot \phi'$ in sand layers; $N_q = 40$ for tip resistance in dense sand
API	364.1	465.8	829.9	0.44	0.56	Hand calculation; limiting skin friction in sands of 2,100 psf.; δ' from Table A.2; $N_q = 42$ for tip resistance in dense sand; limiting unit tip resistance of 210 ksf
Castello sand curves	267.3	427.2	694.5	0.38	0.62	Hand calculation; unit side resistances by Figure A.2 and unit tip resistance by Figure A.3
CAXPILE using Soil criteria	103.4	528.6	632	0.16	0.84	Soil criteria option uses Castello criteria curves for sand layers
CAXPILE using WES criteria	101.3	566.2	667.5	0.15	0.85	Input specified $\delta' = 0.83 \cdot \phi'$ for sand layers
CAXPILE using VJ criteria	363.5	465.8	829.3	0.41	0.59	$\delta' = \phi' - 5$ deg in sand layers; $N_q = 42$ for unit tip resistance in dense sand

The C_{33} versus normalized axial load [P_A/Q_{ult}] results computed by the second of three CAXPILE analyses of the hypothetical dense sand site using the WES criteria is depicted by the red curve in Figure 3.3. Q_{ult} from the CAXPILE SSI analysis using WES criteria, is equal to 667.5 kips (Table 3.4). These computations show that 85% of Q_{ult} is provided in tip resistance, with 15% provided in skin friction. Like the CAXPILE analysis using Soil criteria, this SSI analysis also indicates that for this hypothetical site condition, this batter pile is more of a tip bearing pile rather than a skin friction pile. For [P_A/Q_{ult}] ranging in value from 0.6 to 1, C_{33} drops from 0.56 to 0.15.

These WES criteria SSI results reinforce the observations discussed previously regarding the computed results from the Soil criteria for the two different soil site conditions: The pile's capacity increases when the

site condition is changed from a hypothetical, homogenous, medium-dense sand to a dense sand site. Additionally, this change in site condition to a denser sand resulted in an increase in the C_{33} values.

The C_{33} versus normalized axial load [P_A/Q_{ult}] results computed by the third CAXPILE analyses using the VJ criteria is depicted by the black curve in Figure 3.3. Q_{ult} from the CAXPILE SSI analysis using VJ criteria is equal to 829.3 kips (Table 3.4). These computations show that tip resistance contributes 59% of Q_{ult} and skin friction provides 41%. For [P_A/Q_{ult}] ranging in value from 0.68 to 1, C_{33} drops from 0.68 to 0.13.

Hand calculations were made using the API (2000) guidance result in a Q_{ult} value of 829.9 kips (Table 3.4). This computed value for Q_{ult} agrees with the CAXPILE SSI analysis result using the VJ criteria.

In addition to the previously discussed (five) analyses, a third compression pile capacity (Q_{ult}) computation was made following EM 1110-2-2906 (HQUSACE 1991) guidance. This hand calculation resulted in a value for Q_{ult} equal to 662.3 kips (Table 3.4). Its resulting value is just above the lowest of the six values computed for Q_{ult} . Q_{ult} ranges in value from 632 to 829.9 kips. Again, site-specific compression pile load tests would be the definitive and most reliable method for assessing Q_{ult} at a site, as recognized by the EM 1110-2-2906 (HQUSACE 1991) guidance. Since that type of field data is obviously not available for this hypothetical site, a statistical assessment of the six Table 3.4 Q_{ult} values is made. The statistical processing of the Table 3.4 data results in a mean value for Q_{ult} of 719.3 kips, a standard deviation of 87.3 kips, and a COV equal to 0.12.

3.7 Observations regarding the level of axial compression pile loading, P_A

Figures 3.1 through 3.3 show that the axial stiffness modifier C_{33} value is dependent on the value of compression pile axial load, P_A . The value for P_A derived from Appendices C, D, and E CAXPILE analyses has been normalized in this report by the ultimate capacity of the compression pile Q_{ult} , [P_A/Q_{ult}]. Recall that the ratio [P_A/Q_{ult}] will range in value between zero and one. Using information contained in EM 1110-2-2906 (HQUSACE 1991), this subsection introduces a perspective for understanding the ratio [P_A/Q_{ult}].

Paragraph 4-2.c of EM 1110-2-2906 (HQUSACE 1991) summarizes values for the minimum factor of safety for pile capacity. They are dependent upon the loading condition (i.e., Usual, Unusual, or Extreme) and the method used for determining the pile capacity. For example, the minimum values of factor of safety range from a low of 2.0 for a theoretical or empirical compression pile capacity prediction verified by a pile load test up to a value of 3.0 when no load test is used for verification for the Usual load case. This corresponds to levels of normalized axial loading $[P_A/Q_{ult}]$ between 0.5 and 0.33, respectively. For a compression pile, the fraction $[P_A/Q_{ult}]$ is simply equivalent to the inverse of the factor of safety.

The values for the minimum compression pile factor of safety are typically lower for the Unusual and Extreme load cases as compared to the Usual load case. This increases the fraction for $[P_A/Q_{ult}]$ above 0.33. For example, the minimum value of factor of safety is 2.25 for a theoretical or empirical compression pile capacity prediction that is not verified by a pile load test for the Unusual load case. This corresponds to a level of normalized axial loading $[P_A/Q_{ult}]$ of 0.44.

For the Extreme load case, the minimum value of factor of safety is 1.7 for a theoretical or empirical compression pile capacity prediction that is not verified by a pile load test. The corresponding level of normalized axial loading $[P_A/Q_{ult}]$ is equal to 0.59.

The authors of this report observe that when conducting a pushover analysis of a clustered group of batter piles, the level of axial compression pile loading to be developed is likely above the $[P_A/Q_{ult}]$ values mentioned in this subsection. Because the axial stiffness modifier C_{33} value in Figures 3.1 through 3.3 is dependent on the value of $[P_A/Q_{ult}]$, the authors recommend a five-step process to using this data to estimate the value to be assigned to C_{33} for use in a CPGA batter pile pushover analysis. This process is outlined in Chapter 4.

3.8 Concluding remarks

This chapter summarizes an engineering methodology that uses CAXPILE results to assist in the engineering characterization of the axial stiffness of batter piles for use in a CPGA pile group model of flexible approach walls. Recall that the flexible approach walls used by the Corps consist of elevated impact decks (or beams) supported by clustered groups of piles (Figure 1.2). For batter pile configurations modeled using CPGA software,

the axial stiffness term (b_{33}) is an important contributor to the pile group deformation calculation. The approach for characterizing axial pile stiffness of batter piles as implemented within CPGA software accounts for pile-soil interaction effects by applying an empirical factor (C_{33}) to the axial stiffness coefficient of $[AE/L_e]$ of the axially loaded structural (batter pile) member of a batter pile configured pile group:

$$b_{33} = C_{33} * \frac{A * E}{L_e} \quad (2.7 \text{ bis})$$

C_{33} is an axial stiffness modifier, A designates the cross-sectional area of the concrete-filled pipe pile, E designates its (composite) Young's Modulus, and L_e is the length of pile embedment. As discussed in Subsection 2.4, the CPGA software accounts for pile-to-soil interaction by applying the empirical C_{33} factor to the axial pile stiffness coefficient of $[AE/L_e]$.

The authors of this report reverted to a suite of three CAXPILE analyses using site-specific engineering properties made available for the Lock and Dam 3 layered soil site to generate C_{33} values. This initial series of CAXPILE analyses were made of the site-specific, stratified soil foundation (Appendix C). The data generated for the site using CAXPILE was augmented by a parametric analysis of this same Figure 1.2 batter pile group but founded in hypothetical, homogenous sand foundations, each with a different density. One batter pile group was founded in a medium-dense sand site (Appendix D) while the second was founded in a dense sand site (Appendix E). For each of the three sites, a suite of three CAXPILE analyses were conducted using the CAXPILE designated Soil criteria, WES criteria, and VJ criteria.

These CAXPILE results were summarized in terms of computed values for the axial stiffness modifier C_{33} as a function of the axial load, P_A , and P_A was expressed as a fraction of the mobilized axial batter pile capacity Q_{ult} , $[P_A/Q_{ult}]$. Figure 3.1 shows C_{33} versus $[P_A/Q_{ult}]$ for the Lock and Dam 3 layered soil site. The authors of this report observe that this pile group is founded on a very dense sand layer that contributes a substantial portion (i.e., 70% to 80%) of axial pile capacity (Q_{ult}) through pile tip resistance (Q_t). Figure 3.2 show C_{33} versus $[P_A/Q_{ult}]$ results for a hypothetical, homogeneous medium-dense sand site, and Figure 3.3 show C_{33} versus $[P_A/Q_{ult}]$ results for the hypothetical, dense sand site.

- The C_{33} versus $[P_A/Q_{ult}]$ data plots of Figures 3.1, 3.2, and 3.3 provide a convenient and easy-to-use method for assigning a value for the C_{33} term as will be discussed in the subsequent chapter.
- The data shown in Figures 3.1, 3.2, and 3.3 show that the axial stiffness modifier C_{33} decreases with axial load, P_A , or equivalent, with an increasing fraction of the mobilized axial batter pile capacity Q_{ult} , $[P_A/Q_{ult}]$.
- Comparison of the Figures 3.1, 3.2, and 3.2 data trends demonstrate that for a common fractional of mobilized axial pile capacity, the value for the C_{33} axial stiffness modifier increases with increasing density of the sand foundation.

Three sets of analyses were performed for this report: the Lock and Dam 3 layered soil site and two hypothetical homogeneous sand sites with medium-dense and dense sands, respectively. These three sets of analyses gave a range of values for C_{33} from 0.06 to 0.91. These values were consistently below the recommended values given by Hartman et al. (1989) and the CASE Task Group on Pile Foundations (1983). The recommended values were 1.0 for a full tip bearing pile and 2.0 for a full skin friction pile. Given these results, the authors suggest discontinuing the use of the Hartman et al. (1989) and The CASE Task Group on Pile Foundations (1983) recommended values. The authors outline a more suitable procedure for calculating an appropriate C_{33} value in the next chapter.

4 Using an Axial Pile Stiffness C_{33} Term in a Pushover Analysis of a Clustered Group of Batter Piles

4.1 Determination of the axial pile stiffness (C_{33}) term and pushover analysis

This report summarizes an investigation into the engineering characterization of axial stiffness for individual compression piles embedded within soil. This characterization of axial stiffness is used in the analysis of a clustered pile group's deformation and load distribution response. Its impact on the computed pile group response is most pronounced for analysis of a clustered pile group containing batter piles. For batter pile configurations modeled using CPGA software, the axial stiffness term (b_{33}) is an important contributor to the pile group deformation calculation. The approach for characterizing axial pile stiffness of batter piles, as implemented within CPGA software, accounts for pile-soil interaction effects by applying an empirical factor (C_{33}) to the axial stiffness coefficient of $[AE/L_e]$ of the axially loaded structural (batter pile) member of a pile group containing batter piles.

Since the Chapter 3 results show that the axial stiffness modifier C_{33} decreases with increasing fraction of the mobilized axial batter pile capacity Q_{ult} , $[P_A/Q_{ult}]$, the authors of this report recommend a five-step process to estimate the value to be assigned to the axial stiffness modified C_{33} for use in a CPGA batter pile pushover analysis:

1. Compute the ultimate compression pile capacity Q_{ult} using any or all of the six computational procedure(s) summarized in Chapter 3. These computations are outlined in Appendix C for the Layered Lock and Dam 3 site, Appendix D for a hypothetical, homogeneous medium-dense sand site, and Appendix E for a hypothetical, homogeneous dense sand site. Assign a value for a compression batter pile capacity, Q_{ult} . If more than one computational procedure is used to calculate a Q_{ult} value (as was the case for the six Q_{ult} values listed in Tables 3.1, 3.2, and 3.3), a mean estimate may be computed from these values and used as the value for Q_{ult} .
2. Assign a value for $[P_A/Q_{ult}]$. The assignment of a trial value of axial stiffness modifier C_{33} is based on an approximate value for the level of normalized axial loading $[P_A/Q_{ult}]$. $[P_A/Q_{ult}]$ is expressed as a fraction

- (between 0 and 1). P_A is the axial load and is expressed using the Chapter 3 CAXPILE results as a fraction of the mobilized axial batter pile capacity Q_{ult} . A reasonable beginning estimate of $[P_A/Q_{ult}]$ in the range of 0.6 to 0.9 can be used in a pushover analysis assessment of the energy absorption capacity of a pile group.
3. Assign a value for C_{33} . Given a trial value for $[P_A/Q_{ult}]$, a value for C_{33} can be assigned within the band range constrained by the three curves in Figures 3.1, 3.2, or 3.3. Any value for C_{33} within the range for the $[P_A/Q_{ult}]$ trial value is reasonable, and the authors recommend using the midrange value. For a layer soil site with a batter pile group bearing on a very dense sand layer, use Figure 3.1. If the site consists of an approximately homogeneous medium-dense sand site, use Figure 3.2. If the site consists of an approximately homogeneous dense sand site, use Figure 3.3. For all other sites, conduct a CAXPILE analysis to develop a site-specific C_{33} versus $[P_A/Q_{ult}]$ relationship.
 4. Perform a pushover analysis of the batter pile configuration according to Ebeling et al. (2012) using this trial C_{33} value for computation of a P_A value.
 5. Update the value of C_{33} . If the value of C_{33} is not satisfactory, then compute an updated value for $[P_A/Q_{ult}]$ and repeat steps 4 and 5, until sufficient accuracy is attained. Accuracy is measured by a tolerance comparison of $[P_A/Q_{ult}]$ relationships, giving a new value of C_{33} , between successive pushover analyses.

4.2 Example pushover analysis (with C_{33} determination) of the Lock and Dam 3 cluster batter pile configuration

Using the process listed above, a new analysis is performed to determine a new pushover load-displacement curve (similar to Figure 1.6) for the Lock and Dam 3 batter pile group. Changes were made to the 2012 pushover analyses (Ebeling et al. 2012) for more accuracy. These changes are noted in the problem description below.

The Figure 1.2 Lock and Dam 3 batter pile system being modeled consists of three inline piles supporting 100 tons of impact deck (i.e., this 100 tons is based on the Figure 1.2 tributary width of reinforced concrete deck supported by each inline row of three piles). The first pile in the impact deck is vertical, and the next two piles have a 1 horizontal to 4 vertical batter (1H:4V). The vertical elevation from the bottom of the impact deck to the top of the soil is 24 ft. The piles then extend another 48 ft (vertically) down into the soil. In the 2012 report, each pile was estimated to have these values for the unsupported and embedded lengths. In this

pushover analysis model using the CPGA software, the batter is taken into account for the back two piles, giving an unsupported length of 24.7 ft and an embedded length of 49.5 ft.

The piles used at Lock and Dam 3 are 2 ft diameter, concrete-filled pipe piles. The area of the pipe piles is 452.4 in.². The moment of inertia is 16,286 in.⁴. The composite (concrete and steel pipe) modulus of elasticity is given as 5,124 ksi. This value is given with more accuracy than in the 2012 report. For the modulus of elasticity, the value for confined concrete is substituted in place of the value for unconfined concrete as described in Appendix B.

The first step in the five-step process for estimating axial stiffness requires determining the ultimate axial capacity of the soil under compression loading, Q_{ult} . As mentioned before, Chapter 3 details six methods for determining Q_{ult} for piles in compression embedded in layered soils. In Appendix C, these methods are applied to the Lock and Dam 3 layered soil site, resulting in Table 3.4. Because the first entry for Q_{ult} in the table (following EM 1110-2-2906 guidelines) appears to be an outlier, the remaining five entries are averaged to give a mean value for Q_{ult} of 859.6 kips.

In the second step of the process, a trial value for $[P_A/Q_{ult}]$ is assigned with a value in the range from 0 to 1, with a reasonable estimate being between 0.6 and 0.9. Splitting the difference, a reasonable estimate of 0.75 is used for $[P_A/Q_{ult}]$.

In the third step of the process, C_{33} is recovered from Figure 3.1 using the estimate of 0.75 for $[P_A/Q_{ult}]$ because Figure 3.1 is computed using the specified layered soil system for the location of Lock and Dam 3. The midvalue for C_{33} when $[P_A/Q_{ult}] = 0.75$ is approximately 0.35.

With these steps completed, enough data is defined to create the input files for a pushover analysis using the CPGA software. The CPGA pushover analysis process is an incremental process. An initial analysis is performed with dead loads on the structure to determine the initial forces and moments acting on the piles. Each successive run combines their forces and moments with the previous runs. These forces and moments are monitored to determine when failure mechanisms of the structure are engaged. For Lock and Dam 3, the failure mechanisms are as follows:

- **Axial compression failure of the soil:** Q_{ult} gives the ultimate compressive load that the pile can withstand before plunging into the soil. Q_{ult} is given as 859.6 kips. When this capacity has been exceeded, the pile provides no support to the impact deck.
- **Axial tensile failure of the soil:** Section 3.4 describes methods to compute Q_s , the shaft resistance due to skin friction. When these methods are solved, their solutions can be averaged to give an estimated ultimate friction capacity acting along the length of the pile. Tensile loading of the pile is resisted only by this side friction. Table 3.2 provides values for Q_s for the Lock and Dam 3 piles. The average value for Q_s using this table is 173.5 kips for a pipe pile in tension. When a pile has gone into tensile failure, it no longer reacts to the confinement pressure and friction along the length of the pile. This allows the pile to pull free, providing no support against movement of the impact deck.
- **Loss of pile-to-pile cap fixity:** Figure B.1 has an interaction diagram for a pipe pile. The three-line curve reveals the moment capacity of the pipe pile under a specified axial load. The axial load is monitored for each pile, and if the total moment measured at the pile cap exceeds the moment capacity of the pile, then the pile is no longer considered fixed but is changed to a pinned-head condition at the top of pile.
- **Hinging of the pile at the mudline:** Using the Figure B.1 interaction diagram again, the total moment is monitored at a position below the mudline where the pile is expected to hinge. This depth below the pile cap is given by the PMAXMOM calculation presented in Equation B.24. The calculated value for this depth is 335 in. for a pinned-head condition at top of pile.
- **Euler critical buckling of the pile:** As a pile is displaced by lateral loading at the pile cap, the capacity of the pile to withstand an axial compression load before buckling is reduced. This affects both pinned- and fixed-head piles, although fixed-head piles can withstand greater axial compression loads. These relationships are given in Equations B.19 for pinned-head piles and Equation B.21 for fixed-head piles. Equation B.20 relates the displacement in the global x-direction to that displacement occurring normal to the 1H:4V batter pile. A plot of these functions is given in Figure B.4. When a pile has exceeded the capacity for its top of pile boundary condition (either pinned or fixed), then it provides no axial support to the impact deck against further compression loading of the pile.

The complete pushover analysis was completed in seven steps, as described in the following paragraphs. The final incremental analyses results are given in Tables F.1 and F.2. The CPGA software can only return forces and moments at a single point along a pile, assumed to be at the pile cap unless it is specified within a PMAXMOM command line. Until pile cap fixity is lost for all three piles in the pile group, which is expected to occur first, two runs must be made with CPGA so that forces and moments can be collected at the pile cap, to determine loss of fixity or provide cumulative values, and just below the mudline (335 in. depth) to determine hinging or provide cumulative values. After pile cap fixity has been lost due to flexural yielding of the pile at the pile cap, there is no need to monitor conditions at the pile cap.

The pushover analysis accumulates forces and moments at each increment; therefore, the first step is to establish a set of baseline measurements. For the Lock and Dam 3 example, this means analyzing with the dead load that the 100-ton (200 kip) impact deck applies to the pile configuration. Remember that this condition must be run twice to gather forces and moments at the pile cap and the mudline for accumulation. Although there is no lateral load, there is a lateral displacement of -0.253 in. due to moment reactions in the batter piles at the fixed-head, pile cap location.

For the second incremental analysis, the dead load was removed, and a small lateral load was applied to determine the effect loading will have on the pile group. When the load was applied, the first (vertical) pile starts to go into axial tension while the two batter piles start to compress. This effect is pronounced for the second pile, as the impact deck attempts to *pole vault* using that pile. Because piles have a more rapid loss of moment capacity in axial tension than in axial compression according to Figure B.1 and because pile-to-pile cap moments were increasing in magnitude faster than mudline moments, it was assumed that the first failure mechanism to occur would be for hinging of the pile at the pile cap. The lateral load was increased using extrapolation to find a cumulative moment value that was close to the point of rotational failure. Recall from Figure B.1 that as the axial forces change in each pile, the piles resistance to moment changes. While an extrapolation may give a near-to-hinging moment value, it may not be within sufficient accuracy. Therefore, a search for a value in that neighborhood using educated guesses (typically two or three runs) is made. Given that the first pile was increasing in axial tension and the cumulative moment was increasing at the pile cap, it was quickly determined that the first pile would

have a pile cap rotational hinging failure when the incremental lateral load was 170 kips. The incremental lateral displacement was 2.483 in., and the cumulative displacement was 2.23 in. The run was repeated to calculate cumulative forces and moments at the mudline.

For the third incremental analysis, the top of the first pile at the pile cap (i.e., deck) was changed from a fixed-head condition to a pinned-head condition. The load was replaced with a low incremental load. In this case, the assumption was that the accumulated moment at the top of the second and third piles would also develop a hinge due to flexural yielding of the pile. Using the same procedure for finding the load at which the hinge develops, this mechanism developed at the top of the second and third pile occurred at nearly the same incremental (lateral) load, 10 kips. The incremental displacement for this load was 0.1858 in. The cumulative lateral load to this point was 180 kips, and the cumulative lateral displacement was 2.1458 in. The run was repeated to calculate cumulative forces and moments at the mudline. For the following analyses, the only moments captured are at the mudline.

For the fourth incremental analysis, the second and third pile caps were assigned a pinned-head condition. In this case, there was no expectation of which failure mechanism would occur next. A small incremental lateral load was applied to the impact deck, and extrapolation with trial and error was used to determine which of the different potential failure mechanisms developed next. The result was that the cumulative axial tensile force increased in the first pile so as to exceed the limit of 173.5 kips when the lateral load was increased by 38 kips. The incremental lateral displacement of the impact deck was 1.826 in. The cumulative lateral load to this point was 218 kips, and the cumulative displacement was 4.2418 in.

At the fifth stage of incremental analysis, the C_{33} properties for the first pile were changed to an arbitrarily low value of 0.0001. Recall that the C_{33} term adjusts the resistance to axial movement of the pile, so setting this term to a very low value decreases the resistance to movement, effectively freeing the pile to move along its axis. The assumption for this analysis was that some failure would occur in either the second or third pile. Extrapolation using trial and error for the incremental lateral load was applied using this assumption. Unexpectedly, the cumulative moment arose (at a location near the mudline) in the first pile to exceed the capacity before either of the other piles reached a failure condition. The

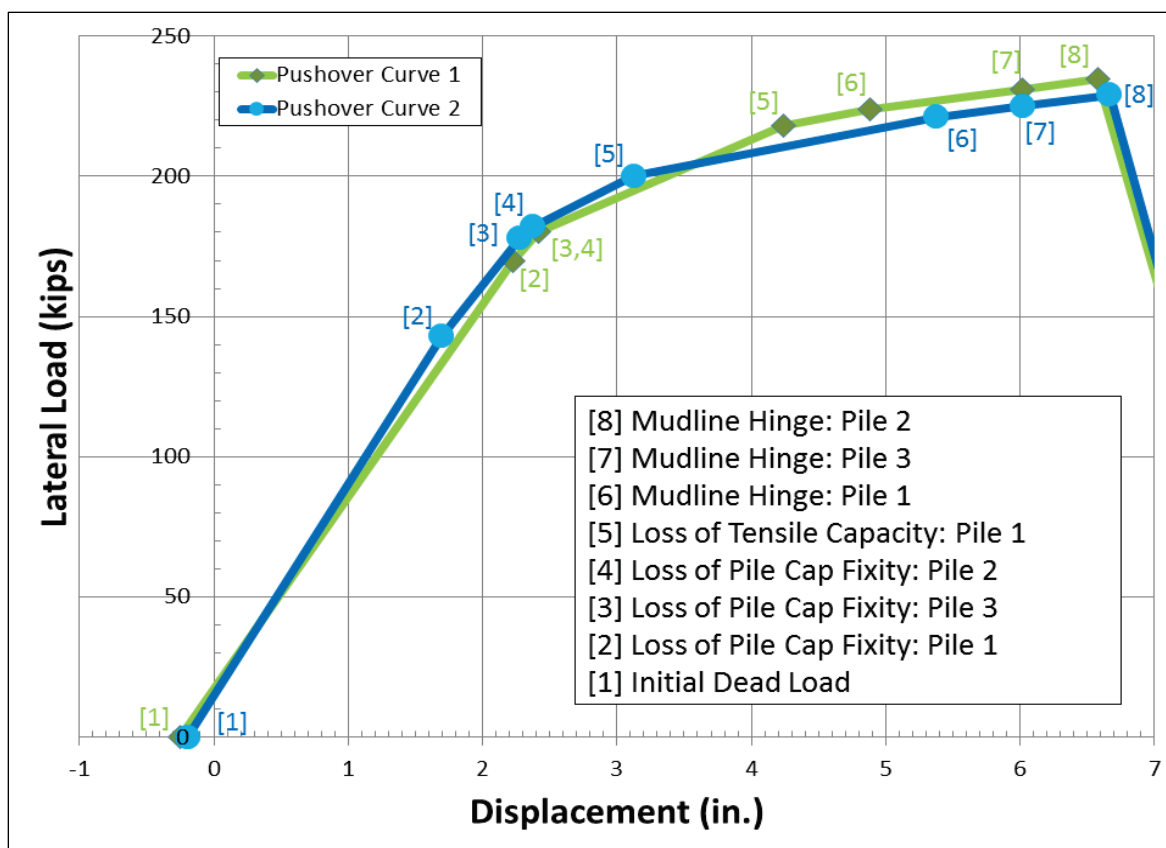
incremental load was then adjusted to find the moment of flexural yielding when the first pile hinged at the mudline. The incremental lateral load at the point of mudline hinging failure was 6 kips, and the incremental displacement was 0.6345 in. The cumulative lateral load to this point was 224 kips, and the cumulative displacement was 4.8853 in.

For the sixth incremental analysis, the first pile was removed from the analysis, since it was no longer providing support for the impact deck. (This is likely a conservative assumption). No assumptions were made regarding which failure mechanism would develop next. The incremental lateral load was applied using trial and error to find which failure mechanism would occur next. The increasing axial compression of the third pile combined with the increasing cumulative moment at the mudline of the third pile led to the third pile hinging at the mudline. The incremental lateral load at the point of mudline hinging of the pile was 7.0 kips, and the incremental displacement was 1.128 in. The cumulative lateral load to this point was 231.0 kips, and the cumulative displacement was 6.0133 in.

Because an impact deck cannot be supported by only one pile, for the seventh incremental analysis, the third pile length was reduced to the length of the pile to the mudline hinge point (335 in.). In this way, the pile provided very little support, and the moment would accumulate at the second pile mudline point. No assumptions were made regarding which failure mechanism would occur next. The incremental lateral load was applied using trial and error to find which failure mechanism that would occur next. The increasing axial compression of the second pile combined with the increasing cumulative moment at the mudline of the second pile led to the second pile hinging at the mudline. The incremental lateral load at the point of mudline hinging failure was 3.5 kips, and the incremental displacement was 0.564 in. The cumulative lateral load to this point was 234.5 kips, and the cumulative displacement was 6.5773 in.

At this point, the accumulation of failure mechanisms meant that the impact deck had no effective support to resist additional increments of lateral loading. Any additional lateral loading would result in the structure being *pushed over*. The resulting diagram of cumulative load versus cumulative displacement is displayed as Pushover Curve 1 in Figure 4.1. Recall the value assigned to C_{33} is set equal to 0.35 for these CPGA analyses. The peak lateral load capacity of the structure is 234.5 kips. The area under the load-displacement curve gives the kinetic energy that can be absorbed from a barge train with that load in a collision with this structural system.

Figure 4.1. Resulting load-displacement plot characterizing the pushover capacity of the batter pile configuration for Lock and Dam 3, given two different values of C_{33} .



By Table F.2, P_A is equal to 481.3 kips in the middle pile at the end of the pushover analysis. With Q_{ult} assigned a value of 859.6 kips (average value for five of the Table 3.1 data values), $[P_A/Q_{ult}]$ equals 0.56. This value is less than the 0.75 value assumed for $[P_A/Q_{ult}]$ prior to starting the pushover analysis. By Figure 3.1, this would lead to a revision of the C_{33} value from 0.35 to 0.55.

A second, complete series of CPGA calculations were performed with the new C_{33} value of 0.55. Using an updated P_A value with a Q_{ult} value of 859.6 kips, $[P_A/Q_{ult}]$ equals 0.59. This value is close to the 0.56 value for $[P_A/Q_{ult}]$ determined after completion of the first pushover analysis. By Figure 3.1, a revision of the C_{33} value from 0.55 is not warranted. The resulting curve is displayed in Figure 4.1 as Pushover Curve 2. The authors observe that these curves are similar to each other, even though the loss of pile cap fixity and the loss of tensile capacity for Pile 1 each happened earlier in the process. The authors also observe that the sequence of members yielding are the same in both pushover analyses. It is worth noticing that although axial loads that could lead to Euler critical buckling (as given in

Table B.1 and Figure B.4) were monitored throughout the analyses, no buckling of either batter pile was observed. Tables 4.1 and 4.2 summarize the process that the second pushover analysis took.

Table 4.1. Global displacements and forces at the impact deck for the Lock and Dam 3 structural system at each incremental analysis step with $C_{33}=0.55$.

Increment Number	Incremental		Cumulative		Notes
	Lateral Load (kip)	Displacement (in.)	Lateral Load (kip)	Displacement (in.)	
1	0.0	-0.193	0	-0.193	-200 kips vertical load
2	143.0	1.89	143	1.697	
3	35.0	0.5836	178	2.2806	
4	4.0	0.0926	182	2.3732	
5	22.0	0.846	200	3.1266	
6	21.0	2.25	221	5.3766	
7	4.0	0.645	225	6.0216	
8	4.0	0.645	229	6.6666	

Table 4.2. Axial force, pile cap moment, and mudline moment for the three piles in the Lock and Dam 3 structural system at each incremental analysis step with $C_{33}=0.55$.

Increment Number	Pile Number	Incremental			Cumulative			Notes
		Axial Force (kips)	Pile Cap Moment (in.-kips)	Mudline Moment (in.-kips)	Axial Force (kips)	Pile Cap Moment (in.-kips)	Mudline Moment (in.-kips)	
1	1	185.3	-176.8	251	185.3	-176.8	251	
	2	36.6	-193	250	36.6	-193	250	
	3	-22.1	-171.3	237	-22.1	-171.3	237	
2	1	-240.1	6383.7	-3468.5	-54.8	6206.9	-3217.5	
	2	269.1	6228.9	-3198.8	305.7	6035.9	-2948.8	
	3	-8.3	6331.1	-3261.5	-30.4	6159.8	-3024.5	
3	1	-62.9		-604.8	-117.7	6206.9	-3822.1	Loss of Pile Cap Fixity for Pile #1
	2	82.8	1980.5	-830.8	388.5	8016.4	-3779.6	
	3	-13.7	2016	-849.4	-44.1	8175.8	-3873.9	
4	1	-8.1		-95.9	-125.8	6206.9	-3918	Loss of Pile Cap Fixity for Pile #3
	2	13	324.6	-133.1	401.5	8341	-3912.7	
	3	-4.3		-94	-48.4	8175.8	-3967.9	
5	1	-56.6		-876.9	-174.3		-4699	Loss of Pile Cap Fixity for Pile #2
	2	117.4		-836.6	505.9		-4616.2	
	3	-57.7		-862.1	-101.8		-4736	

Increment Number	Pile Number	Incremental			Cumulative			Notes
		Axial Force (kips)	Pile Cap Moment (in.-kips)	Mudline Moment (in.-kips)	Axial Force (kips)	Pile Cap Moment (in.-kips)	Mudline Moment (in.-kips)	
6	1	-0.2		-2333.4	-174.5		-7032.4	
	2	2.2		-2271.4	508.1		-6887.6	
	3	1.5		-2271.5	-100.3		-7007.5	
7	1	0		0	0		0	
	2	0.5		-650.0	508.6		-7537.6	
	3	0.5		-650.0	-99.8		-7657.5	
8	1	0		0	0		0	
	2	0.5		-650.0	509.1		-8187.6	
	3	0.5		-650.0	-99.3		-8307.5	

4.3 Conclusions

In this chapter, a five-step method for estimating and evaluating axial stiffness for a pile-founded structural system is introduced. The procedure is then examined with an example problem to show that pushover results give reasonable results for P_A . The authors demonstrate, using the Lock and Dam 3 lock extension structural system, that this five-step procedure can be performed within two complete series of pushover analyses. The resulting pushover results provide the added capability to determine the potential energy that exists within the batter pile-founded structural system, as well as the potential energy that exists until each failure mechanism is engaged.

There are other software packages that make use of the pushover analysis curve for clustered groups of piles. Because the analysis performed in the five-step process produces a batter pile group pushover curve with better batter pile axial parameters that improve the group stiffness characterization, these software packages can then produce more accurate results. For example, the Impact_Deck¹ software computes the dynamic response under barge-train impact of an entire impact deck founded on clustered groups of piles. The pile substructure stiffness for Impact_Deck is modeled using the pushover curve results of the pile groups. The resulting pushover curves of the five-step process can be directly input into Impact_Deck to improve the batter pile performance for these analyses.

¹ White, B., J. R. Arroyo, and R. M. Ebeling. In publication. Simplified dynamic structural time-history response analysis of flexible approach wall founded on clustered pile groups using Impact_Deck. ERDC/ITL Technical Report. Vicksburg, MS: U.S. Army Engineer Research and Development Center.

5 Summary and Conclusions

5.1 Summary

An engineering method has been developed to characterize the axial stiffness of individual piles loaded in compression. This characterization of axial stiffness is used in the analysis of a clustered pile group's deformation and load distribution response. Its impact on the computed pile group response is most pronounced among a clustered pile group containing batter piles, where lateral impact loads drive the batter piles into the soil.

This characterization is important because the Corps is moving toward lower-cost, flexible, pile-founded lock approach walls as compared with rigid approach walls. These walls absorb kinetic energy of the barge-train impacts that occur as the barge train aligns itself to enter the lock. One type of pile-founded approach wall is comprised of an elevated impact deck supported by groups of clustered piles. Some of these walls use batter piles for increased lateral support. These impact decks are supported tens of feet above the mudline.

A pushover analysis technique is used to establish the PE and displacement capacity of individual batter pile groups accounting for the various pile failure mechanisms that can occur in an impact event. An appropriate axial stiffness characterization will increase the accuracy of this computation. The total stored energy (PE) of the approach wall system will be the sum of the stored energy of all the pile groups reacting to the barge impact. The study concludes with a pushover analysis of a batter pile configuration used at Lock and Dam 3 flexible approach wall extension. The pilings for this lock wall extension are founded in layered soil whose engineering properties are discussed in this report.

Batter pile groups are constructed of steel pipe or H-piling, which are conducive to in-the-wet construction. This method of construction leads to a cost savings for Corps projects.

5.2 Conclusions

In order to analyze these batter pile founded flexible lock wall extensions accurately, the axial stiffness of the piles in soil must be computed for CASE software CPGA. A procedure for estimating the axial stiffness using

CASE software CAXPILE and an analysis method using pushover methods with CPGA are introduced.

For batter pile configurations modeled using the Corps CASE software CPGA, the axial stiffness term (b_{33}) is an important contributor to the pile group deformation calculation, as discussed in Chapter 2. Recall from subsection 2.4:

$$b_{33} = C_{33} * \frac{A * E}{L_e} \quad (2.7 \text{ bis})$$

with C_{33} being an axial stiffness modifier, A designating the cross-sectional area of the concrete-filled pipe pile, E designating the pile's (composite) Young's Modulus, and L_e being the length of pile embedment. As discussed in subsection 2.4, the CPGA software accounts for pile-to-soil interaction by applying the empirical C_{33} factor to the axial pile stiffness coefficient of $[AE/L_e]$.

Three sets of analyses were performed for this report: the Lock and Dam 3 layered soil site and two hypothetical homogeneous sand sites with medium-dense and dense sands, respectively. These three sets of analyses gave a range of values for C_{33} from 0.06 to 0.91. These values were consistently below the recommended values given by Hartman et al. (1989) and the CASE Task Group on Pile Foundations (1983). The recommended values were 1.0 for a full tip bearing pile and 2.0 for a full skin friction pile. Given these results, the authors suggest discontinuing the use of the Hartman et al. (1989) and The CASE Task Group on Pile Foundations (1983) recommended values.

A procedure has been outlined in this report to calculate the axial stiffness of batter piles using results from homogenous or layered soil site models using the Corps CASE software CAXPILE. This procedure is iterative and makes use of a pushover analyses.

Using the Lock and Dam 3 layered soil site information, CAXPILE was used to estimate C_{33} . Charts of C_{33} versus normalized axial load $[P_A/Q_{ult}]$ have been developed for this site. If the soil conditions differ from that occurring at the Lock and Dam 3 site and are not a homogenous medium-dense nor a dense sand site, then the procedure outlined in Appendices C,

D, or E would be followed to develop site-specific C_{33} versus normalized axial load $[P_A/Q_{ult}]$ charts.

Since the Chapter 3 results show that the axial stiffness modifier C_{33} decreases with increasing fraction of the mobilized axial batter pile capacity Q_{ult} , $[P_A/Q_{ult}]$, the authors of this report recommend a five-step process to estimate the value to be assigned to the axial stiffness modified C_{33} for use in a CPGA batter pile pushover analysis:

1. Compute the ultimate compression pile capacity Q_{ult} using any or all of the six computational procedure(s) summarized in Chapter 3. These computations are outlined in Appendix C for the Layered Lock and Dam 3 site, Appendix D, for a hypothetical, homogeneous, medium-dense sand site and Appendix E for a hypothetical, homogeneous, dense sand site. Assign a value for a compression batter pile capacity, Q_{ult} . If more than one computational procedure is used to calculate a Q_{ult} value (as was the case for the six Q_{ult} values that listed in Tables 3.1, 3.2, and 3.3), a mean estimate may be computed from these values and used as the value for Q_{ult} .
2. The assignment of a trial value of axial stiffness modifier C_{33} is based on an approximate value for the level of normalized axial loading $[P_A/Q_{ult}]$. $[P_A/Q_{ult}]$ is expressed as a fraction (between 0 and 1). P_A is the axial load and is expressed using the Chapter 3 CAXPILE results as a fraction of the mobilized axial batter pile capacity Q_{ult} . A reasonable beginning estimate of $[P_A/Q_{ult}]$ in the range of 0.6 to 0.9 can be used in a pushover analysis assessment of the energy absorption capacity of a pile group.
3. Given a trial value for $[P_A/Q_{ult}]$, a value for C_{33} can be assigned within the band range constrained by the three curves in Figures 3.1, 3.2, or 3.3. Any value for C_{33} within the range for the $[P_A/Q_{ult}]$ trial value is reasonable, and the authors recommend using the midrange value. For a layer soil site with a batter pile group bearing on a very dense sand layer, use Figure 3.1. If the site consists of an approximately homogeneous medium-dense sand site, use Figure 3.2. If the site consists of an approximately homogeneous dense sand site, use Figure 3.3. For all other sites, conduct a CAXPILE analysis to develop a site-specific C_{33} versus $[P_A/Q_{ult}]$ relationship.
4. Perform a pushover analysis of the batter pile configuration according to Ebeling et al. (2012) using this trial C_{33} value for computation of a P_A value.
5. If the value of C_{33} is not satisfactory, then compute an updated value for $[P_A/Q_{ult}]$ and repeat steps 4 and 5 until sufficient accuracy is attained. Accuracy is measured by a tolerance comparison of $[P_A/Q_{ult}]$ relationships, giving a new value of C_{33} , between successive pushover analyses.

An example using two pushover iterations is provided to illustrate the procedure. Each possible failure mechanism for the pushover of a batter pile founded structure has been described and is monitored during the pushover process. The resulting pushover curves give the potential energy capacity as each failure mechanism is encountered. The accuracy improved over the Ebeling et al. (2012) analyses due to consideration of site-specific soil properties in the axial stiffness and pile capacity terms. This improved procedure of analysis lowered the overall capacity of the structure at Lock and Dam 3. Because site-specific properties are used in this analysis, the authors consider the results to be a more realistic representation of structural capacity.

References

- American Petroleum Institute (API). 1971. *Recommended practice for planning, designing and constructing fixed offshore platforms*. American Petroleum Institute API RP 2A. Washington, DC.
- . 2000. *Recommended practice for planning, designing and constructing fixed offshore platforms-working stress design*. American Petroleum Institute 21st Edition with December 2002 errata and supplement 1. Washington, DC.
- Castello, R. R. 1980. Bearing capacity of driven piles in sand. Ph.D. thesis. Texas A&M University, College Station, TX.
- Coyle, H. M., and R. R. Castello. 1981. New design correlations for piles in sand. *Journal of the Geotechnical Division, ASCE* 107(GT7):965–985.
- Coyle, H. M., and R. R. Castello. 1979. *A new look at bearing capacity factors for piles*. 11th Annual Offshore Technology Conference, OTC 3405, Houston, TX, May 1979, 427–431.
- Coyle, H. M., and L. C. Reese. 1966. Load transfer for axially loaded piles in Clay. *Journal of Soil Mechanics and Foundations Division, ASCE* 92(SM2):1–25.
- Davisson, M. T. 1970. Lateral load capacity of piles. In *Highway Research Record Number 133, Pile Foundations*. Washington, DC: Highway Research Board.
- Dawkins, W. P. 1984. *User's guide: Computer program for soil-structure interaction analysis of axially loaded piles (CAXPILE)*. Instruction Report K-84-4. Vicksburg, MS: U.S. Army Engineer Waterways Experiment Station.
- Duncan, J. M., and A. L. Buchignani. 1976. *An engineering manual for settlement studies*. Geotechnical Engineering Report. Berkeley, CA: Department of Civil Engineering, University of California, Berkeley.
- Duncan, J. M., and A. Bursey. 2007. *Soil and rock modulus correlations for geotechnical engineering*. Center for Geotechnical Practice and Research CGPR #4. Blacksburg, VA: Virginia Polytechnic Institute and State University.
- Ebeling, R. M., B. C. White, A. N. Mohamed, and B. C. Barker. 2010. *Force time-history during the impact of a barge train impact with an approach lock wall using impact force*. ERDC/ITL TR-10-1. Vicksburg, MS: U.S. Army Engineer Research and Development Center.
- Ebeling, R. M., R. W. Strom, B. C. White, and K. Abraham. 2012. *Simplified analysis procedures for flexible approach wall systems founded on groups of piles and subjected to barge train impact*. ERDC/ITL TR-12-3. Vicksburg, MS: U.S. Army Engineer Research and Development Center.
- Ebeling, R. M., B. C. White, and M. T. Fong. 2013. *Simulation and advanced second moment reliability analyses of pile groups using CPGA-R; Formulation, user's guide, and example problems*. ERDC/ITL TR-13-2. Vicksburg, MS: U.S. Army Engineer Research and Development Center.

- Hartman, J. P., J. J. Jaeger, J. J. Jobst, and D. K. Martin. 1989. *User's guide: Pile group analysis (CPGA)*. Technical Report ITL-89-3. Vicksburg, MS: U.S. Army Engineer Waterways Experiment Station.
- Headquarters, U.S. Army Corps of Engineers (HQUSACE). 1991. *Design of pile foundations*. EM 11110-2-2906. Washington, DC.
- Heydinger, A. 1987. *Recommendations: Load-transfer criteria for piles in clay*. Technical Report ITL-87-1. Vicksburg, MS: U.S. Army Engineer Waterways Experiment Station.
- Hrennikoff, A. 1950. Analysis of pile foundations with batter piles. In *Transactions, American Society of Civil Engineers* 76(1) Paper 2401:123–126.
- Hunter, A. H., and M. T. Davisson. 1969. Measurement of pile load transfer. *ASTM Special Technical Publication* 444:106–117.
- Kiousis, P. D., and A. S. Elansary. 1987. Load settlement relation for axially loaded piles. *Journal of Geotechnical Engineering, ASCE* 113(6):655–661.
- Martin, D. K., H. W. Jones, and R. Radhakrishnan. 1980. *Documentation for LMVDPILE program*. Technical Report K-80-3. Vicksburg, MS: U.S. Army Engineer Waterways Experiment Station.
- Mosher, R. L. 1984. *Load-transfer criteria for numerical analysis of axially loaded piles in sand*. Technical Report K-84-1. Vicksburg, MS: U.S. Army Engineer Waterways Experiment Station.
- Pace, M. E., K. Abraham, and R. M. Ebeling. 2012. *Complete soil-structure interaction (SSI) analyses of I-walls embedded in level ground during flood loading*. ERDC/ITL TR-12-4. Vicksburg, MS: U.S. Army Engineer Research and Development Center.
- Radhakrishnan, N., and F. Parker. 1975. *Background and documentation of five University of Texas soil-structure interaction computer programs*. Miscellaneous Paper K-75-2. Vicksburg, MS: U.S. Army Engineer Waterways Experiment Station.
- Rangan, B. V., and M. Joyce. 1992. Strength of eccentrically loaded slender steel tubular columns filled with high-strength concrete. *ACI Structural Journal* 89(6):676–681.
- Reese, L. C., L. A. Cooley, and N. Radhakrishnan. 1984. *Laterally loaded piles and computer program COM624G*. Technical Report K-84-2. Vicksburg, MS: U.S. Army Engineer Waterways Experiment Station.
- Saul, W. E. 1968. Static and dynamic analysis of pile foundations. *Journal, Structural Division, American Society of Civil Engineers* 94(ST5), Proc. Paper 5936.
- Semple, R. M., and W. J. Rigden. 1984. Shaft capacity of driven pile in clay. In *Analysis and Design of Pile Foundations*, ed. J. R. Meyer, 59–79. Reston, VA: American Society of Civil Engineers.

- Strom, R. W., and R. M. Ebeling. 2004. *Simple methods used to estimate the limit-state axial load capacity of spillway invert slabs*. ERDC/ITL TR-04-3. Vicksburg, MS: U.S. Army Engineer Research and Development Center.
- Terzaghi, K. 1955. Evaluation of coefficient of subgrade reaction. *Geotechnique* 5:297–326.
- Terzaghi, K., and R. B. Peck. 1967. *Soil mechanics in engineering practice*. New York: Wiley.
- The CASE Task Group on Pile Foundations. 1983. *Basic pile group behavior, Computer-Aided Structural Engineering (CASE) project*. Technical Report K-83-1 (revision of Technical Report K-80-5). Vicksburg, MS: U.S. Army Engineer Waterways Experiment Station.
- Vesic, A. S. 1970. Tests on instrumented piles, Ogeeche River Site. *Journal of the Soil Mechanics and Foundation Division, ASCE* 96(SM3) Proc. Paper 7170:561–583.
- Vijayvergiya, V. N. 1977. Load movement characteristics of piles. In *Ports '77 4th Annual Symposium of the Waterways, Port, Coastal, and Ocean Division, ASCE*, Long Beach, VA, March 1977, 269–284.
- White, B. C., J. R. Arroyo, and R. M. Ebeling. 2015. *Simplified dynamic structural time-history response analysis of flexible approach walls founded on clustered pile groups using Impact_Deck*. ERDC/ITL TR-15. Vicksburg, MS: U.S. Army Engineer Research and Development Center.
- Yang, N. C. 1966. Buckling strength of pile. In *Bridges and Structures*. Highway Research Record, Number 147. Washington, DC: Highway Research Board.

Appendix A: Pile Shaft Friction and End Bearing of Driven Pipe Piles

A.1 Introduction

This appendix outlines procedures to determine the skin friction capacity and end bearing (i.e., tip capacity) of driven pipe piles, with an emphasis on cohesionless (e.g., in sand) foundation soils. This material was recovered from guidance documents published by both USACE and American Petroleum Institute (API). The offshore petroleum industry makes extensive use of pipe piling in the foundations of their offshore structures. Information provided by Castello (1980) on estimating the ultimate skin friction and tip resistance for piles driven into sand is also included.

The axial capacity of a pile may be represented by the following formula:

$$Q_{ult} = Q_s + Q_t \quad (A.1)$$

$$Q_s = f_s A_s \quad (A.2)$$

$$Q_t = q A_t \quad (A.3)$$

where:

Q_{ult} = ultimate pile capacity

Q_s = shaft resistance of the pile due to skin friction

Q_t = tip resistance of the pile due to end bearing (for a compression pile only)

f_s = average unit skin resistance

A_s = surface area of the shaft in contact with the soil

q = unit tip-bearing capacity

A_t = effective (gross) area of the tip of the pile in contact with the soil.

A.2 Driven pile shaft friction and end bearing

A.2.1 Values for interface friction, earth pressure coefficients, and bearing capacity coefficients

The pile-to-soil interface friction angle δ is less than or equal to the effective angle of friction for the soil, ϕ . Table A.1 provides general guidance for values of pile-to-soil interface friction δ for driven piles. The data contained within this table were interpreted using data obtained from Table 4-3 in EM 1110-2-2906 (HQUSACE 1991).

Table A.1. Values for pile-to-soil interface friction δ for driven piles, based on data obtained from Table 4-3 in EM 1110-2-2906 (HQUSACE 1991)

Pile Material	δ
Steel	0.67ϕ to 0.83ϕ
Concrete	0.9ϕ to 1.0ϕ
Timber	0.8ϕ to 1.0ϕ

In a data reduction of load test results for steel piles driven into sands of different densities, Coyle and Castello (1979, 1981) used a value of δ equal to 0.8 times ϕ , where ϕ is the effective angle of internal friction. This assessment is in agreement with the Table A.1 data. Vijayvergiya (1977) suggested that for steel displacement piles, δ may be estimated as equal to ϕ minus 5 degrees. This relationship is reflected in the API (1971) guidelines for δ in cohesionless soils. The API guidance for δ is reported as a function of soil type and of soil density for cohesionless siliceous soils in Table A.2 of this report. These values of δ have been maintained through several updates up to and including the 2000 version of API recommendations. The API guidelines have a focus on driven pipe piles that are commonly used in the foundations of offshore oil and natural gas platforms. By the δ equal to ϕ minus 5 degrees relationship, δ from Table A.2 varies from a low of 0.75 times ϕ to a high of 0.88 times ϕ . This range is slightly broader than that listed in EM 1110-2-2906 (HQUSACE 1991) Table A.1 values for steel pile material.

Table A.2. API (2000) guidelines for design parameters for cohesionless siliceous soil.

Density	Soil Description	Soil-Pile Friction Angle, δ (degrees)	Limiting Skin Friction Values Kips/ft ² (kPa)	N_q	Limiting Unit End Bearing Values kips/ft ² (MPa)
Very Loose	Sand	15	1.0 (47.8)	8	40 (1.9)
Loose	Sand-Silt				
Medium	Silt				
Loose	Sand	20	1.4 (67)	12	60 (2.9)
Medium	Sand-Silt				
Dense	Silt				
Medium	Sand	25	1.7 (81.3)	20	100 (4.8)
Dense	Sand-Silt				
Dense	Sand				
Very Dense	Sand-Silt	30	2 (95.7)	40	200 (9.6)
Dense	Gravel				
Very Dense	Sand				
		35	2.4 (114.8)	50	250 (12)

Table A.3 provides general guidance for values of lateral earth pressure coefficients $K_{\text{compression}}$ and K_{tension} and dimensionless bearing capacity factors N_q and N_c . The coefficients $K_{\text{compression}}$ and K_{tension} are lateral earth pressure coefficients for compression and tension piles, respectively. The data contained within this table is based on data obtained from Table 4-4 and Figure 4-4 in EM 1110-2-2906 (HQUSACE 1991).

Table A.3. Values of lateral earth pressure coefficients and dimensionless bearing capacity factors N_q and N_c , based on data obtained from Table 4-4 and Figure 4-4 in EM 1110-2-2906 (HQUSACE 1991).

Soil Type	$K_{\text{compression}}$	K_{tension}	N_q or N_c
Sand	1	0.5 to 0.7	40
Silt	1	0.5 to 0.7	10
Clay	1	0.7 to 1.0	9

Notes:

1. The above lateral earth pressure coefficients $K_{\text{compression}}$ and K_{tension} do not apply to piles which are prebored, jetted, or installed with a vibratory hammer.
2. For steel H-piles, pile tip area A_{tip} should be taken as the block perimeter of the pile, and the interface friction δ should be the average friction angles of steel against sand and sand against sand (ϕ).

For open-ended pile piles driven unplugged, API (2000) considers an assumption of K as 0.8 for both tension and compression loadings to be appropriate. Values of K for full displacement piles (plugged or closed end)

may be assumed to be 1.0 according to API. The API compression pile, K-value for pipe piles (of 0.8) is lower than the Table A.3, EM 1110-2-2906 (HQUSACE 1991) value (of 1.0) for all three soil types.

A.2.2 Calculating the skin friction capacity of driven piles

There is a tendency, confirmed with field tests conducted by Vesic (1970), for unit skin friction resistances along the pile-to-soil interface to increase with depth to some limiting value. Vesic noted that even though the rate of increase sharply decreases at some “critical” depth, there is an additional increase with further penetration. According to EM 1110-2-2906 (HQUSACE 1991), the skin friction of piles in cohesionless soils computed using the Equations A.4 through A.6 relationships for cohesionless soils increases linearly to a critical depth, designated D_c , and then remains constant. The unit skin friction acting on the pile shaft may be determined by the following equations:

$$f_s = K\sigma_v' \tan \delta \quad (\text{A.4})$$

and for a submerged site

$$\sigma_v' = \gamma' D \text{ for } D < D_c \quad (\text{A.5})$$

$$\sigma_v' = \gamma' D_c \text{ for } D \geq D_c \quad (\text{A.6})$$

$$Q_s = f_s A_s \quad (\text{A.2 bis})$$

with

K = lateral earth pressure coefficient ($K_{\text{compression}}$ for compression piles and K_{tension} for tension piles)

σ_v' = effective overburden pressure

δ = angle of friction between the soil and the pile

γ' = effective unit weight of soil

D = depth along the pile at which the effective overburden pressure is calculated.

The critical depth has been found to vary between 10 and 20 pile diameters or pile widths (HQUSACE 1991). Pile widths are given as variable B in Table A.4. Table A.4 summarizes this critical depth as a function of density in a cohesionless soil (e.g., sands) and the width of the pile (B).

Table A.4 Values of critical depth in cohesionless soils
(HQUSACE 1991).

D _c	Density
10*B	loose
15*B	medium-dense
20*B	dense

Note that Table A.3 is general guidance to be used unless the long-term engineering practice in the area or the results from pile load tests indicate otherwise. Underprediction of soil strength parameters at load test sites has, at times, produced back-calculated values of K that exceed the values in Table A.3. It has also been found both theoretically and at some test sites that the use of displacement piles produces higher values of K than does the use of nondisplacement piles. Refer to Table 4-5 in EM 1110-2-2906 (HQUSACE 1991) for additional guidance on K values for nondisplacement piles. Batter piles usually involve the use of driven piles versus nondisplacement piles.

The offshore oil and natural gas industry has extensive experience with the use of driven pipe piles to support their offshore platforms. The API provides a recommended practice document for use by engineers to design these structures. API (2000) states that for driven pipe piles developing a plug of soil inside the pile tip, the bearing pressure may be assumed to act over the entire cross section of the pile. For unplugged piles, the bearing pressure acts on the pile wall annulus only. API also states that the shaft friction, f_s , acts on both the inside and outside of the pipe pile. The total resistance is the sum of the external shaft friction, the end bearing on the pile wall annulus, and the total internal shaft friction or the end bearing of the plug, whichever is less.

API's Table A.2 general guidelines may be used for the selection of δ if other data are not available. For long piles, f_s may not indefinitely increase linearly with overburden pressure. In such cases it may be appropriate to limit f_s to values given in Table A.2.

For piles driven in undersized drilled holes, piles jetted in place, or piles drilled and grouted in place, the selection of shaft friction values should take into account the soil disturbance resulting from installation. In general, f_s should not exceed values for driven piles.

Tension capacity: The tension capacity may be computed by applying the appropriate values of K_{tension} from Table A.3 as appropriate for granular soils to the incremental computation for each layer and then combining to yield

$$Q_{\text{ult}} = Q_{\text{s-tension}} \quad (\text{A.7})$$

where $Q_{\text{s-tension}}$ designates the use of K_{tension} to compute the skin friction. Contrasting with Equation A.1 for compression piles, note the absence of the tip resistance, Q_t , in this equation.

Piles in layered soils: The skin friction contributed by different soil types may be computed incrementally and summed to find the ultimate capacity. Consideration should be given to compatibility of strain between layers when computing the unit skin resistance.

$$Q_s = \sum_{i=1}^N f_{s_i} A_{s_i} \quad (\text{A.8})$$

where:

f_{s_i} = unit skin resistance in layer i

A_{s_i} = surface area of pile in contact with layer i

N = total number of layers.

A.2.3 Calculating the end bearing capacity of driven piles

For design purposes, the pile-tip bearing capacity can be assumed to increase linearly to a critical depth (D_c) and then remain constant, according to EM 1110-2-2906 (HQUSACE 1991). The same critical depth (D_c) relationship used for skin friction can be used for end bearing. The unit tip bearing capacity can be determined as follows:

$$q = \sigma'_v \cdot N_q \quad (\text{A.9})$$

where σ'_v is computed for a submerged site using Equations A.5 and A.6, with its value for D_c restricted by those given as a function of density in Table A.4.

For steel H-piles, A_t should be taken as the area included within the block perimeter. EM 1110-2-2906 (HQUSACE 1991) values of the bearing

capacity factor N_q are listed according to soil type in Table A.3. For piles in end bearing for cohesionless soils, the unit end bearing q in lb/ft² (kPa) is computed using Equation A.9 according to API, where σ'_v is the effective overburden pressure lb/ft² (kPa) at the point in question and N_q is a dimensionless bearing capacity factor with values listed in Table A.2.

According to API (2000), the value of unit tip resistance, q , is computed using Equation A.9, but the maximum value is restricted to those listed in Table A.2 by soil type. API indirectly accounts for the critical depth (D_c) concept through the use of this limiting Table A.2 value for q .

Point bearing piles: In some cases, the pile will be driven to refusal upon firm, good-quality rock. In such cases, the capacity of the pile is governed by the lesser of the structural capacity of the pile or the rock capacity.

A.3 Driven pile shaft friction and end bearing in cohesive soils

A.3.1 Pile skin friction and end bearing in cohesive soils according to EM 1110-2-2906

Although called skin friction, the resistance is due to the cohesion or adhesion of the clay to the pile shaft according to EM 1110-2-2906. From this guidance document, the skin friction is computed by

$$f_s = c_a \quad (\text{A.10})$$

$$c_a = \alpha c \quad (\text{A.11})$$

$$Q_s = f_s A_s \quad (\text{A.2 bis})$$

where:

c_a = adhesion between the clay and the pile

α = adhesion factor

c = undrained shear strength of the clay from a Q test.

The values of α as a function of the undrained shear are given in Figure A.1.a.

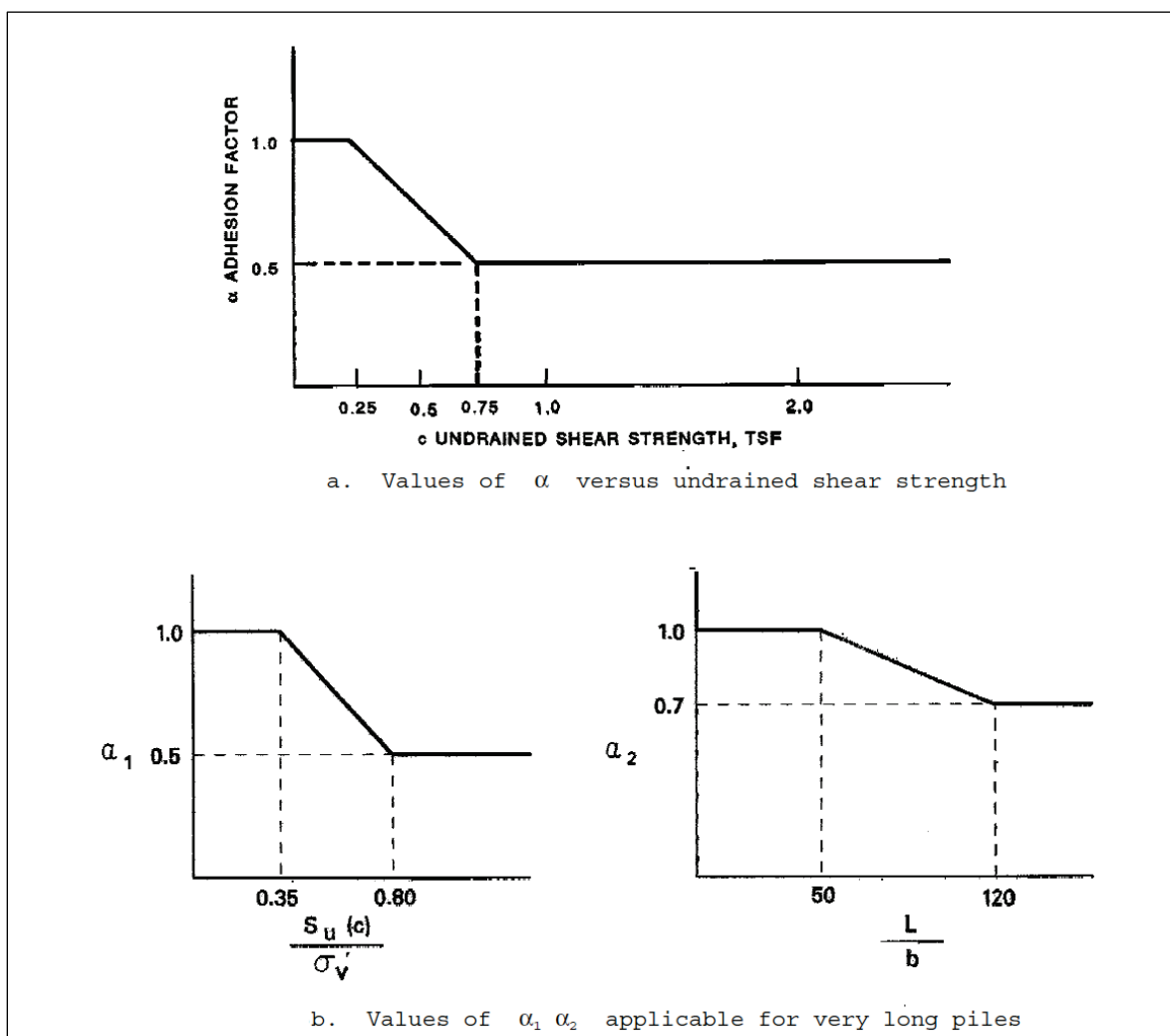
An alternate procedure developed by Semple and Rigden (1984) to obtain values of α which is especially applicable for very long piles is given in Figure A.1.b where

$$a = a_1 a_2 \quad (\text{A.12})$$

and

$$f_s = ac \quad (\text{A.13})$$

Figure A.1. (a.) Values of α versus undrained shear strength; (b.) values of α_1 α_2 applicable for very long piles (after EM 1110-2-2906, HQUSACE 1991).



The pile unit tip bearing capacity for piles in clay can be determined from the following equation:

$$q = 9c \quad (\text{A.14})$$

$$Q_t = A_t q \quad (\text{A.3 bis})$$

However, the movement necessary to develop the tip resistance of piles in clay soils may be several times larger than that required to develop the skin friction resistance.

EM 1110-2-2906 (HQUSACE 1991) provides the following general recommendation: the pile capacity in normally consolidated clays (cohesive soils) should also be computed in the long-term S shear strength case. That is, develop an S case shear strength trend as discussed previously and proceed as if the soil is drained. The computational method is identical to that presented for piles in granular soils, and to present the computational methodology would be redundant. Note, however, that the shear strengths in clays in the S case are assumed to be $\phi > 0$ and $c = 0$. If no laboratory test data are yet available, some commonly used S case shear strengths in alluvial soils can be assumed from Table A.5.

Table A.5. Typical S case shear strength values according to EM 1110-2-2906 (HQUSACE 1991).

S-Case Shear Strength		
Soil Type	Consistency	Angle of Internal Friction ϕ
Fat clay (CH)	Very soft	13° to 17°
Fat clay (CH)	Soft	17° to 20°
Fat clay (CH)	Medium	20° to 21°
Fat clay (CH)	Stiff	21° to 23°
Silt (ML)		25° to 28°

Note: The designer should perform testing and select shear strengths. These general data ranges are from tests on specific soils in site-specific environments and may not represent the soil in question.

It is the opinion of the primary author that the generalized S-case analysis guidance expressed in the preceding paragraph may not be applicable for the short-term barge-train impact loading of a flexible approach wall supported by groups of batter piles. For flexible approach walls, the barge-train impact load case is the governing design load. Ebeling et al. (2010) demonstrate that the impact loading is of very short duration, lasting between 1 and 4 seconds. Considering this short duration of loading, in conjunction with the low permeability of a clay and moderate-to-long drainage paths, it may be argued that an S-case loading condition is not likely to develop.

A.3.2 Pile skin friction and end bearing in cohesive soils according to API

According to API, the unit shaft friction capacity, f_s , in lb/ft² (kPa) for pipe piles in cohesive soils may be calculated by

$$f_s = \alpha \cdot c \quad (\text{A.15})$$

where:

α = a dimensionless factor

c = the undrained shear strength of the soil at the point in question.

API (2000) defines the factor α as being either

$$\alpha = 0.5 \cdot \psi^{-0.5} \text{ when } \psi \leq 1.0 \quad (\text{A.16})$$

or

$$\alpha = 0.5 \cdot \psi^{-0.25} \text{ when } \psi > 1.0 \quad (\text{A.17})$$

with the constraint that α is less than or equal to 1.0

where:

$\psi = c/\sigma'_v$ for the point in question

σ'_v = the effective overburden pressure lb/ft² (kPa) at the point in question.

API (2000) notes that for underconsolidated clays (i.e., clays with excess pore pressures undergoing active consolidation), α can usually be taken as 1.0. Due to a lack of pile load tests in soils having c/σ'_v ratios greater than 3, the above equations should be applied with some engineering judgment for high c/σ'_v values. For very long piles, some reduction in capacity may be warranted, particularly where the shaft friction may degrade to some lesser residual value on continued displacement.

Like EM 1110-2-2906 (HQUSACE 1991), API computes the unit end bearing q in lb/ft² (kPa) for driven piles in cohesive soils by

$$q = 9 \cdot c \quad (\text{A.14 bis})$$

This bearing capacity factor (N_c) of 9 is consistent with the EM 1110-2-2906 (HQUSACE 1991) Table A.3 value for clay material. API emphasizes that the shaft friction f_s acts on both the inside and outside of a pipe pile, and the total resistance is the sum of the total internal shaft friction or the end bearing of the plug, whichever is less. For piles considered to be plugged, the bearing pressure may be assumed to act over the entire cross section of the pile. For unplugged piles, the bearing pressure acts on the pile wall annulus only. Whether a pile is considered plugged or unplugged may be based on static calculations. For example, a pile could be driven in an unplugged condition but act plugged under static loading.

Recall, f_s should not exceed values for driven piles in all soil types, including cohesive soils. However, in some cases for drilled and grouted piles in overconsolidated clays, the value of f_s may exceed these values. In determining f_s for drilled and grouted piles in this type of cohesive soil, the length of the soil-grout interface, including potential effects of drilling mud, should be considered.

A.4 Skin friction and end bearing of piles in silt

According to EM 1110-2-2906 (HQUSACE 1991), the skin friction on a pile in silt may be the result of two component resistances to pile movement contributed by the angle of internal friction (ϕ) and the cohesion (c) acting along the pile shaft. That portion of the resistance contributed by the angle of internal friction (ϕ) is, as with the sand, limited to a critical depth of (D_c), below which the frictional portion remains constant with the limit depths for silt being the same as those stated for sands (Table A.4). That portion of the resistance contributed by the cohesion may require limit if it is sufficiently large, see Figures A-1a and b. The shaft resistance may be computed as follows:

$$f_s = K\gamma' D \tan\delta + ac \quad (\text{A.18})$$

where ($D \leq D_c$)

$$Q_s = A_s f_s \quad (\text{A.2 bis})$$

where:

- Q_s = capacity due to skin resistance
 f_s = average unit skin resistance
 A_s = surface area of the pile shaft in contact with soil
 K = see Table A.2
 γ' = buoyant unit weight for a silts below the water table
 α = see Figures A-1a and b
 D = depth below ground up to limit depth D_c
 δ = limit value for shaft friction angle from Table A.1.

End bearing: The pile tip bearing capacity of silts increases linearly to a critical depth (D_c) and remains constant below that depth. Again, the EM 1110-2-2906 critical depth values of D_c for silts follow the same density criteria listed in Table A.4 for sands.

The unit end bearing capacity of a pile driven into silt soils may be computed using Equations A.4 through A.6. These are the same relationships that are used for sands. The bearing capacity factor N_q for silt is listed in Table A.3, and the critical depth values are those listed in Table A.4.

A.5 Skin friction and end bearing of piles in sand according to Castello

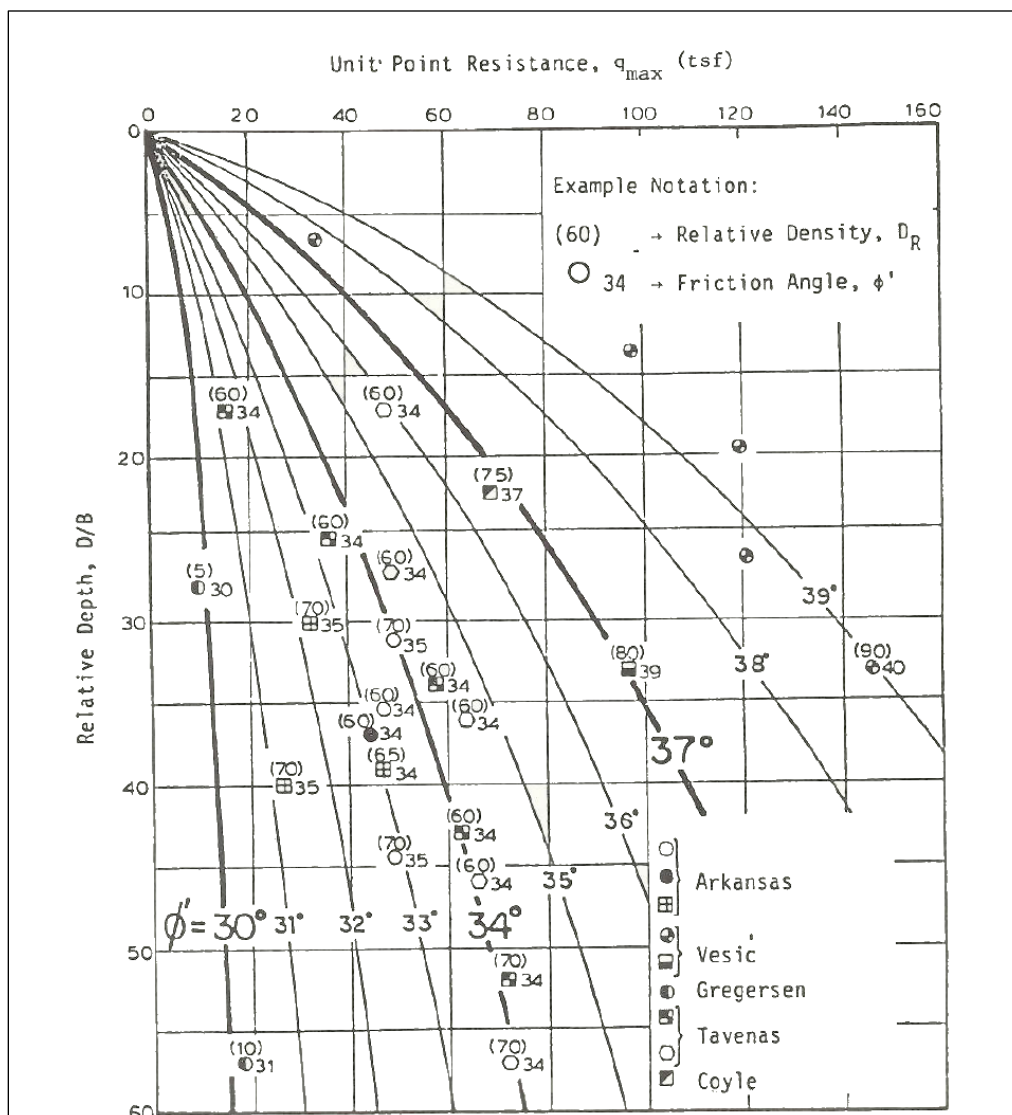
The skin friction capacity of a pile founded in sand may be determined using the procedure recommended by Mosher (1984). Dr. Mosher investigated load-transfer criteria of axially loaded piles in sand. One of the products from his investigation was a pair of charts attributed to the research of Castello (1980) for skin friction capacity and for pile tip capacity (i.e., end bearing). Coyle and Costello (1981) observed that the ground-water level at all of the pile test sites was very close to the ground surface. These charts were identified as Figures 76 and 77 in the Mosher report and are reproduced in Figures A.2 and A.3.

In the Coyle and Castello (1979) discussion of the unit side resistance for piles in sand versus relative length (Figure A.2) data plot and unit tip resistance for piles in sand versus relative length (Figure A.3) data plot in their report, the following three observations were made:

1. The relative depth is probably related in some way to the average effective overburden pressure along the pile.

“residual stresses,” as presented by Castello (1980). However, the average standard error was higher, a value of 32%. This second chart is not included due its higher error.

Figure A.3. Unit tip resistance for piles in sand versus relative length (Mosher 1984).



To determine the skin friction capacity curve of a pile founded in sand using Figure A.2 requires knowledge of the effective angle of internal friction ϕ' for the sand, the embedded length (D) of the pile, and the diameter of the pile (B). The curve will proceed from a relative depth of zero to the relative depth of pile tip and may be calculated by dividing the embedded length of the pile by the diameter of the pile. The value of skin friction capacity (or unit side resistance—with units of tons per square foot [tsf]) for a specified depth of embedment is determined by intersecting the current relative

depth with the curve for the angle ϕ' , which is parabolic with depth. It is possible to approximate this parabolic curve with a piecewise linear definition for the skin friction capacity curve. Interval relative depth values along the pile are determined by dividing the interval depth of embedment by the diameter of the pile. At these regular relative depth intervals, the skin friction capacity can be determined from the figure in the manner described above. The results are more accurate with an increasing number of intervals between the mudline and the total depth of embedment of the pile.

To determine the unit tip resistance of a pile founded in sand using Figure A.3 requires knowledge of the effective angle of internal friction ϕ' for the sand, the embedded length of the pile, and the diameter of the pile. The length of pile embedded in sand is normalized by the pile diameter. It is referred to as the *relative depth*. For this relative depth and a specified value of ϕ' , the unit tip resistance (in units of tsf) is obtained by intersecting the unit tip resistance value with the appropriate curve for ϕ' in Figure A.3. This establishes the unit tip resistance of a pile founded in sand.

As a consequence of the many uncertainties involved with the analysis of pile foundations, it has become customary, and in many cases mandatory, to perform a certain number of full-scale axial pile load tests at the site of important projects to calibrate/verify design assumptions and analytical calculations. For driven (displacement) piles, Coyle and Castello (1979, 1981), along with others, recommend (1) the driven piles be fully instrumented with strain gages along the length of the pile and at the pile tip and (2) that both compression as well as tension tests be conducted on the driven pile in order to adjust the data for residual loads (due to driving stresses). Coyle and Castello suggest the use of a procedure described by Hunter and Davisson (1969) to adjust the pile load data for residual loads in driven piles. This procedure redistributes the recorded compression load data between the side friction load transfer and the tip load transfer of the compression load test using data from the tension load test on the same displacement pile.

A.6 The use of pile load tests

The safest way to deal with design problems has been to use conservative values for bearing factors in preliminary analyses and then to proceed with field load tests for instrumented driven displacement piles at the site. For driven displacement piles, Coyle and Castello (1979, 1981), along with others, recommend that driven piles be fully instrumented with strain gages

along the length of the pile and at the pile tip. It is also recommended that both a compression as well as tension test be conducted on the driven pile in order to adjust the data for residual loads (due to driving stresses). Coyle and Castello suggest the use of a procedure described by Hunter and Davisson (1969) to adjust the pile load data for residual loads in driven piles. This procedure redistributes the recorded compression load data between the side friction load transfer and the tip load transfer of the compression load test using data from the tension load test on the same displacement pile.

Appendix B: Pipe Pile Buckling Evaluation

B.1 Introduction

One of the failure mechanisms to be concerned with for batter piles is the potential for buckling of a batter pile under compressive load. This appendix outlines an engineering evaluation process for computing the evaluation of buckling loads of piles. The method is based on the procedure described in Yang (1966). It is applied to the clustered pile groups that support the impact deck of the flexible approach wall extension at Lock and Dam 3. Figure 1.2 shows an idealization of a single group of three clustered, concrete-filled, 24 in. diameter pipe piles supporting a 6.25 ft tributary section of its impact deck.

B.2 Pipe pile and soil properties for the Lock and Dam 3 site

B.2.1 Pipe pile geometry and engineering properties

The Figure 1.2 pipe pile bent is comprised of 24 in. diameter, concrete-filled pipe piles. The concrete-filled pipe pile geometry and basic engineering properties are presented below:

Outside diameter D_p of concrete-filled pipe pile = 24 in. = 2.0 ft.

Thickness of the steel pipe casing t_{pipe} = 0.375 in.

The steel will have a minimum yield strength of 70,000 psi.

Gross area A_p of concrete-filled pipe pile is given by

$$A_p = \frac{\pi(D_p)^2}{4} = \frac{\pi(24)^2}{4} = 452.4 \text{ in.}^2 \quad (\text{B.1})$$

After rounding, $A_p = 452 \text{ in}^2 = 3.142 \text{ ft}^2$.

Moment of inertia I_p of concrete-filled pipe pile is given by

$$I_p = \frac{\pi(D_p)^4}{64} = \frac{\pi(24)^4}{64} = 16,286 \text{ in.}^4 \quad (\text{B.2})$$

After rounding, $I_p = 16,300 \text{ in}^4 = 0.785 \text{ ft}^4$.

Radius of gyration r is given by

$$r = \sqrt{\frac{I}{A}} = \sqrt{\frac{16,300}{452}} = 6 \text{ in.} = 0.5 \text{ ft} \quad (\text{B.3})$$

Distance from the neutral axis at the center of the pile to extreme fiber,
 $c = 1.0 \text{ ft} = 12 \text{ in.}$

B.2.2 Composite modulus of elasticity of a concrete-filled pipe pile

To obtain an estimate for the modulus of elasticity for the composite concrete filled pipe $E_{\text{composite}}$, the materials science general rule of mixtures is being used. This procedure uses a weighted mean approach to predict a range in values for $E_{\text{composite}}$, considering the composite material to be made up of continuous and unidirectional fibers in a homogenous matrix material.

The estimate for $E_{\text{composite}}$ for loading parallel to the fibers is given by

$$E_{\text{composite}} = f * E_s + (1 - f) * E_c \quad (\text{B.4})$$

where f is the volume fraction of fibers, E_s and E_c are the modulus of elasticity of steel and concrete, respectively.

The secant modulus of elasticity of concrete E_c , in units of psi, at approximately $0.5 * f'_c$, is estimated to be

$$E_c = 33 * (w^{1.5}) * \sqrt{f'_c} \quad (\text{B.5})$$

with w being the unit weight of concrete in lb/ft^3 and the concrete's unconfined compressive strength f'_c expressed in units of psi in this equation. The concrete compressive strength f'_c is assumed to be equal to 4,000 psi in the following computations. For a unit weight of concrete of 145 lb/ft^3 , Equation B.4 becomes

$$E_c = 57,000 * \sqrt{f'_c} \quad (\text{B.6})$$

Again, f_c expressed in units of psi in this equation.

With $f_c = 4,000$ psi and after rounding, the modulus of elasticity of concrete E_c by Equation B.5 is equal to 3,600,000 psi (3,600 ksi, 518,400 ksf).

The modulus of elasticity of steel E_s is equal to 29,000,000 psi (29,000 ksi, 4,176,000 ksf).

In the case of a concrete-filled pipe, the steel is treated as the uniaxial fibers in this idealization, so f is the fraction of steel pipe.

$$f = \frac{V_{steel}}{V_{steel} + V_{concrete}} \quad (B.7)$$

For a unit length of concrete-filled pipe, Equation B.7 simplifies to a ratio of the cross-sectional areas,

$$f = \frac{A_{steel}}{A_{steel} + A_{concrete}} \quad (B.8)$$

The cross-sectional area of a steel pipe (A_s) with an outside diameter of 24 in. and a wall thickness of 0.375 in. is given by

$$A_s = \frac{\pi(D_p)^2}{4} - \frac{\pi(D_p - 2 * t_{pipe})^2}{4} = \frac{\pi(24)^2}{4} - \frac{\pi(24 - 2 * [0.375])^2}{4} = 27.8 \text{ in.}^2 \quad (B.9)$$

The cross-sectional area of the concrete $A_{concrete}$ within the pipe is

$$A_{concrete} = \frac{\pi(D_p - 2 * t_{pipe})^2}{4} = \frac{\pi(24 - 2 * [0.375])^2}{4} = 424.6 \text{ in.}^2 \quad (B.10)$$

By Equation B.8, the volume fraction of fibers (i.e., steel pipe) is computed as

$$f = \frac{27.8}{27.8 + 424.6} = 0.06 \quad (B.11)$$

By Equation B.6, the estimate for $E_{composite}$ in the case of loading parallel to the fibers is

$$E_{\text{composite}} = 0.06 * 29,000,000 + (1 - 0.06) * 3,600,000 = 5,124,000 \text{ psi} \quad (\text{B.12})$$

This value for $E_{\text{composite}}$ is 42% greater than the value of E_c .

B.2.4 Interaction diagram characterizing the capacity of the concrete-filled pipe pile

Ebeling et al. (2012) describe the development of a simple interaction (axial load – moment) diagram to help in assessing the conditions where piles reach their moment or axial load limits. The interaction diagram is based on the ultimate capacity of the pile members. The procedures described in Rangan and Joyce (1992) in conjunction with the simple procedure described in Strom and Ebeling (2004) were used to construct the interaction diagram. The interaction diagram points are

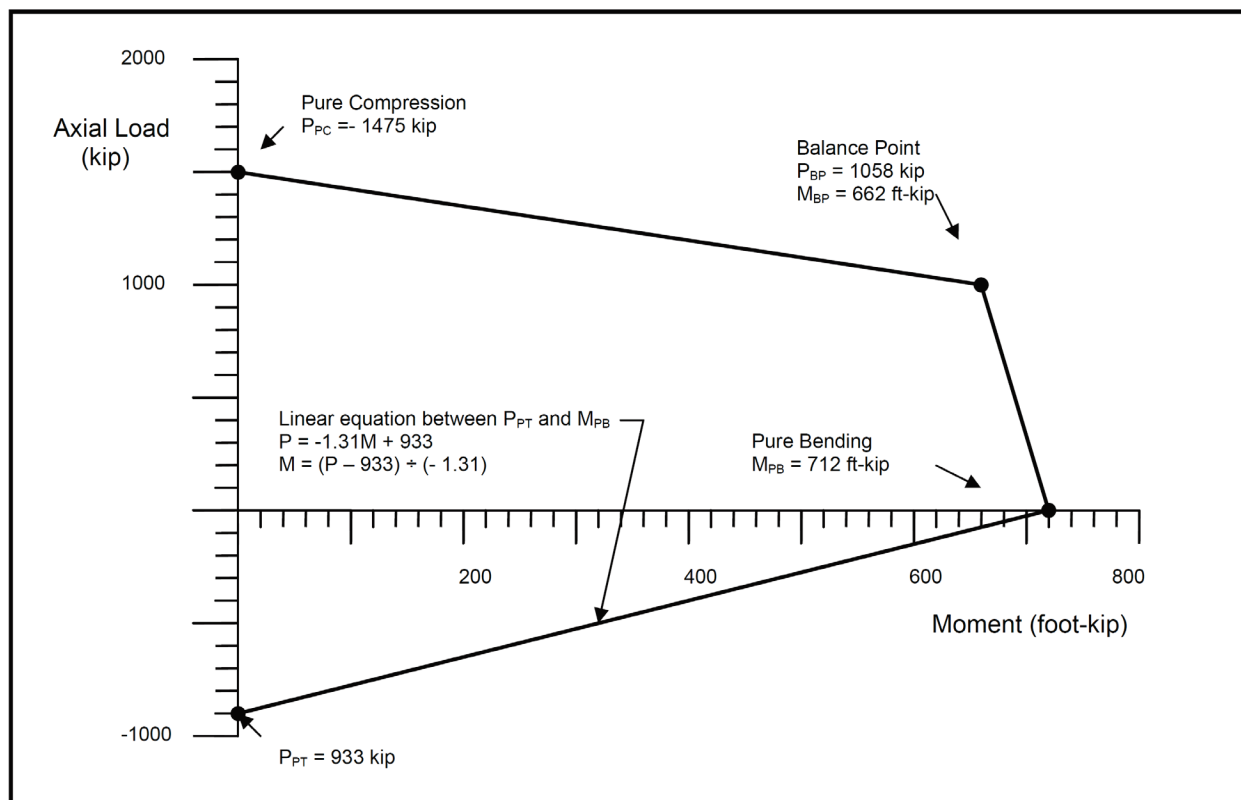
- pure axial compression
- balance condition (axial compression and bending)
- pure bending
- pure axial tension.

The value for pure axial compression is based only on the compressive strength of the concrete. The 0.375 in. thick steel pipe casing was not included in this calculation. The value for pure axial tension is based only on the tensile strength of the steel pipe. Balance point and pure moment conditions assume the contribution only of the concrete in compression on the compressive side of the neutral axis and contribution only of the steel in tension on the tensile side of the neutral axis.

The interaction diagram for a 24 in. diameter concrete-filled pipe pile is presented in Figure B.1.

The interaction diagram assumes that the pipe piles in axial compression fail as a result of the materials (i.e., concrete and steel) reaching their ultimate capacities, rather than by buckling. However, buckling computations will be needed to assure that this is the case. If buckling loads are less than the ultimate axial compressive loads predicted by the interaction diagram, then the buckling loads are to be used in the pushover analysis.

Figure B.1. Simple interaction diagram for 24 in. diameter, concrete-filled pipe pile (after Ebeling et al. 2012).



Ebeling et al. (2012) observe that piles are generally founded in soils that will not allow them to develop their ultimate capacities. It is up to the engineer performing the pushover analysis to consider axial load limitations imposed by the foundation materials. The example discussed in this appendix also considers pile axial capacities that are limited by side friction and tip resistance provided by the soil foundation.

B.2.4 Soil properties for buckling evaluation

The procedure developed by Yang (1966) to evaluate the axial load that induces buckling of a pile assumes a homogenous site model. For this Lock and Dam 3 site example, the soil properties assigned to the buckling evaluation correspond to a homogenous site idealized as a submerged soil with the constant of horizontal subgrade reaction, n_h , set equal to 25 pci. The implication for this homogenous site is that $E_s = n_h x$ so that stiffness increases from the top of the mudline to the tip of the pile (and indirectly, with the confining pressure).

By Equation 1.1, the relative stiffness factor (T) is computed to be

$$T = \sqrt[5]{\frac{E_{\text{composite}} * I_p}{n_h}} = \sqrt[5]{\frac{5,124,000 * 16,300}{25}} = 80.31 \text{ in.} \quad (1.1 \text{ bis})$$

After rounding, $T = 80.3 \text{ in.} = 6.7 \text{ ft.}$

B.2.5 Buckling evaluation of the concrete-filled pipe pile

Ebeling et al. (2012) concluded that buckling loads for the concrete-filled pipe piles may be determined using methods described in Yang (1996). Figures B.2 and B.3, after Figures 3 and 9 of Yang (1966), are provided for use in the analysis.

Figure B.2. Coefficient of critical buckling strength (after Figure 3 Yang, 1966).

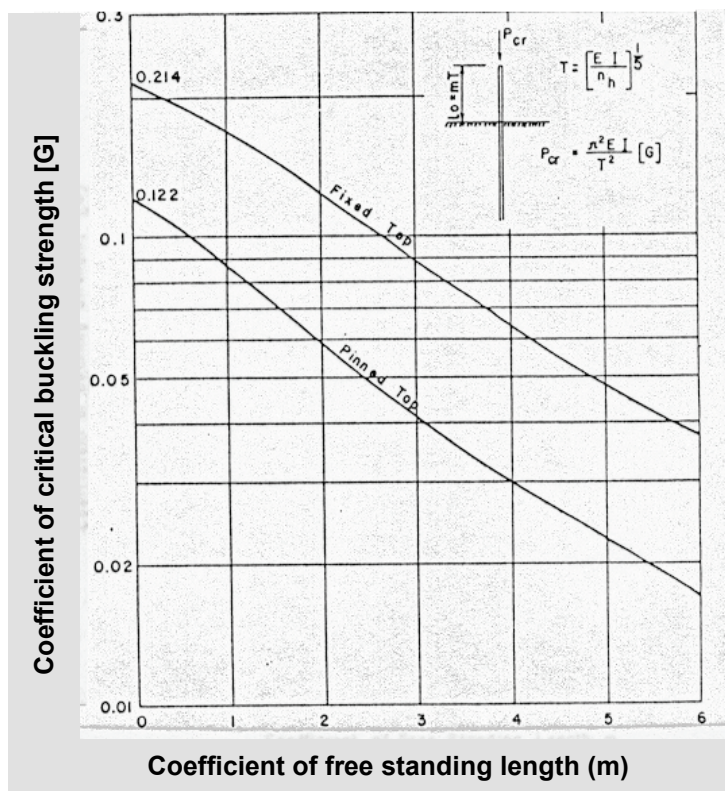
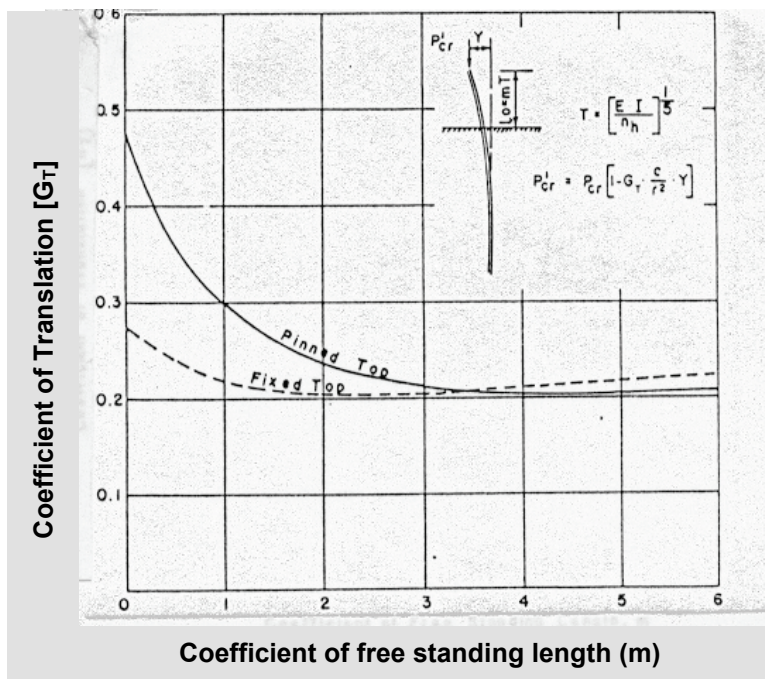


Figure B.3. Coefficient decrement of buckling strength (after Figure 9 Yang, 1966).



The coefficient of free standing length m is equal to the free standing length L_o divided by the relative stiffness factor T :

$$m = \frac{L_o}{T} \quad (\text{B.13})$$

From Figure 1.2, L_o is equal to 24 ft. For the Lock and Dam 3 flexible approach wall extension, Equation B.13 becomes

$$m = \frac{L_o}{T} = \frac{24}{6.7} = 3.58 \quad (\text{B.14})$$

The critical buckling load, assuming no translation, can be determined using Figure B.2 (after Figure 3 in Yang 1966).

For pinned-top nontranslating pile cap, the Euler critical buckling load P_{CR} is given by

$$P_{CR} = \frac{\pi^2 * E_{composite} * I_p}{T^2} [G] \quad (\text{B.15})$$

where $[G]$ is the coefficient of critical buckling strength from Figure B.2.

For a pinned-top, Figure B.2 nontranslating pile cap, the coefficient of critical buckling strength [G] is equal to 0.035, and the Euler critical buckling load is

$$P_{CR} = \frac{\pi^2 * 5,124,000 * 16,300}{(80.3)^2} [0.035] = 4,474,386 \text{ lbs} \quad (\text{B.16})$$

After rounding, the Euler critical buckling load $P_{CR} = 4,474,000 \text{ lb} = 4,474 \text{ kips}$.

For fixed-top, Figure B.2 nontranslating pile cap, the coefficient of critical buckling strength [G] is equal to 0.074 and the Euler critical buckling load is:

$$P_{CR} = \frac{\pi^2 * 4,616,000 * 16,300}{(78.7)^2} [0.074] = 9,460,130 \text{ lbs} \quad (\text{B.17})$$

After rounding, the Euler critical buckling load $P_{CR} = 9,460,000 \text{ lb} = 9,460 \text{ kips}$.

The Euler critical buckling load with translation $P_{CR\Delta}$ is given by

$$P_{CR\Delta} = P_{CR} * \left[1 - G_T \left(\frac{c}{r^2} \right) \Delta \right] \quad (\text{B.18})$$

where P_{CR} is the Euler critical buckling load with no translation (Equation B.15), $[G_T]$ is the coefficient of translation, c is the distance to the extreme fiber from the neutral axis, r is the radius of gyration and Δ is the displacement normal to the axis of the pile. The value for coefficient of translation $[G_T]$ is determined using Figure B.3 (after Figure 9 in Yang 1966).

Entering Figure B.3 with a coefficient of free standing length (m) equal to 3.64, the coefficient of translation $[G_T]$ is approximately equal to 0.21 for both pinned-head and fixed-head piles.

For Lock and Dam 3 pinned-head piles, the Equation B.18 critical buckling load with translation $P_{CR\Delta}$, in units of lb, is

$$P_{CR\Delta} = 4,474,000 * \left[1 - 0.21 \left(\frac{12}{\{6\}^2} \right) \Delta \right] \quad (\text{B.19})$$

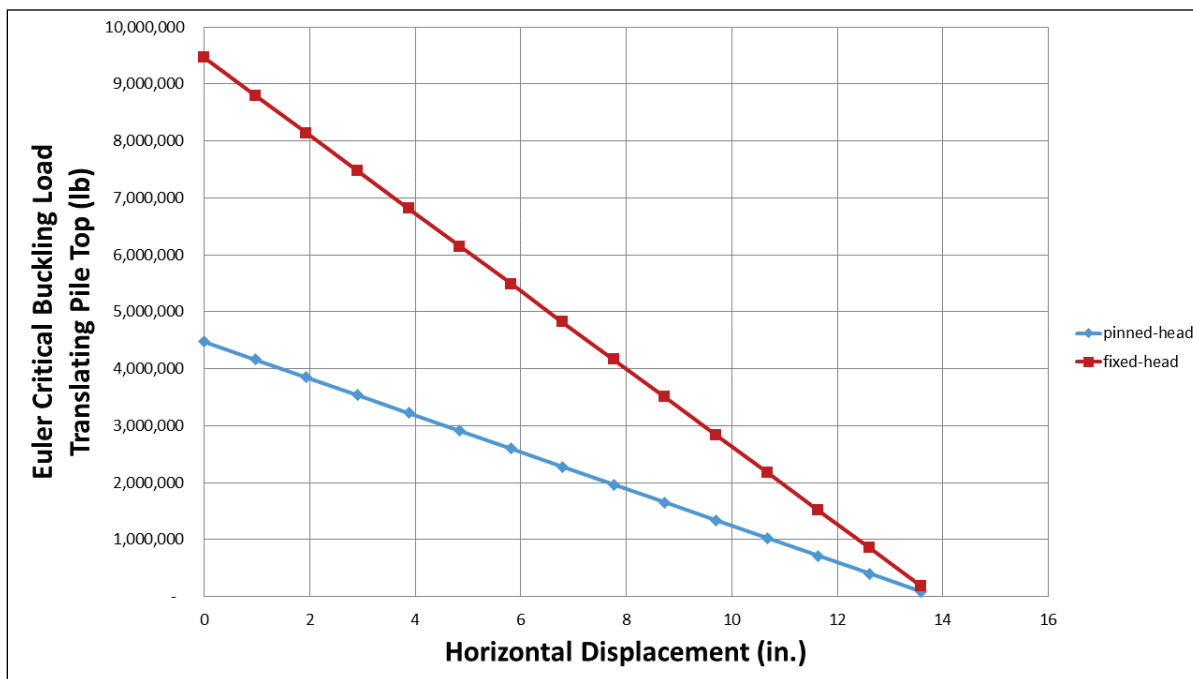
Table B.1 summarizes the resulting values for the Euler critical buckling load with translation P_{CRA} as a function of the movement normal to the axis at the top of the pile, Δ . For pile with a 4V:1H batter, the horizontal component of pile top (and pile cap) deflection Δ_x , in units of inches, is given by

$$\Delta_x = \Delta * \frac{4}{\sqrt{4^2 + 1^2}} = \Delta * \frac{4}{\sqrt{17}} = \Delta * 0.97 \quad (B.20)$$

Table B.1. Euler critical buckling loads P_{CRA} , translating pile top, pinned-head and fixed-head conditions.

Pinned-Head			Fixed-Head		
Δ (in)	Δ_x (in)	P_{CRA} (lb)	Δ (in)	Δ_x (in)	P_{CRA} (lb)
0	0	4,474,000	0	0	9,460,000
1	0.97	4,160,820	1	0.97	8,797,800
2	1.94	3,847,640	2	1.94	8,135,600
3	2.91	3,534,460	3	2.91	7,473,400
4	3.88	3,221,280	4	3.88	6,811,200
5	4.85	2,908,100	5	4.85	6,149,000
6	5.82	2,594,920	6	5.82	5,486,800
7	6.79	2,281,740	7	6.79	4,824,600
8	7.76	1,968,560	8	7.76	4,162,400
9	8.73	1,655,380	9	8.73	3,500,200
10	9.70	1,342,200	10	9.70	2,838,000
11	10.67	1,029,020	11	10.67	2,175,800
12	11.64	715,840	12	11.64	1,513,600
13	12.61	402,660	13	12.61	851,400
14	13.58	89,480	14	13.58	189,200

The horizontal component of deflection Δ_x than Δ) is more directly related (than Δ) to the transverse displacements of the top of piles and pile cap during a pushover analysis using CPGA. The Table B.1 P_{CRA} values as a function of deflection at the top of pile are plotted in Figure B.4 for pinned-head and fixed-head conditions.

Figure B.4. Euler critical buckling loads $P_{CR\Delta}$, translating pile top, pinned-head and fixed-head conditions.

For Lock and Dam 3 fixed-head piles, the Equation B.18 critical buckling load with translation $P_{CR\Delta}$, in units of pounds, is

$$P_{CR\Delta} = 9,460,000 * \left[1 - 0.21 \left(\frac{12}{\{6\}^2} \right) \Delta \right] \quad (B.21)$$

Table B.1 and Figure B.4 also summarize the resulting values for the Euler critical buckling load with translation $P_{CR\Delta}$ as a function of the movement normal to the axis at the top of the pile, Δ .

B.2.6 CPGA input to define a depth below the mudline to monitor a maximum moment within a concrete-filled pipe pile

Ebeling et al. (2012) outline the details regarding the stages of pushover analysis of a flexible approach wall in Appendix B for a pushover analysis conducted of the Figure 1.2 Lock and Dam 3 pile-founded flexible approach wall using CPGA. There are two key pile elevations that need to be monitored for maximum moments and the potential development of a plastic hinge in the piles of the group; the first being at the intersection of the top of piles with the pile cap, and the second is just below the mudline. This elevation data is input into the CPGA analysis so that these elevations can be monitored. Using updated data identified earlier in this appendix,

this subsection defines a revision to the elevation to be monitored in the Lock and Dam 3 elevated impact deck pushover analysis using CPGA.

The CPGA pushover analysis starts out with a fixed-head boundary condition specified at the intersection of the top of pile with the pile cap. For each user-specified load increment applied to the pile cap, the computation of values of the fixed-head moments is automatically made and reported by CPGA for each of the three Figure 1.2 piles. However, to obtain the maximum moment below the mudline, it is necessary to include a FUNSMOM data line to CPGA where

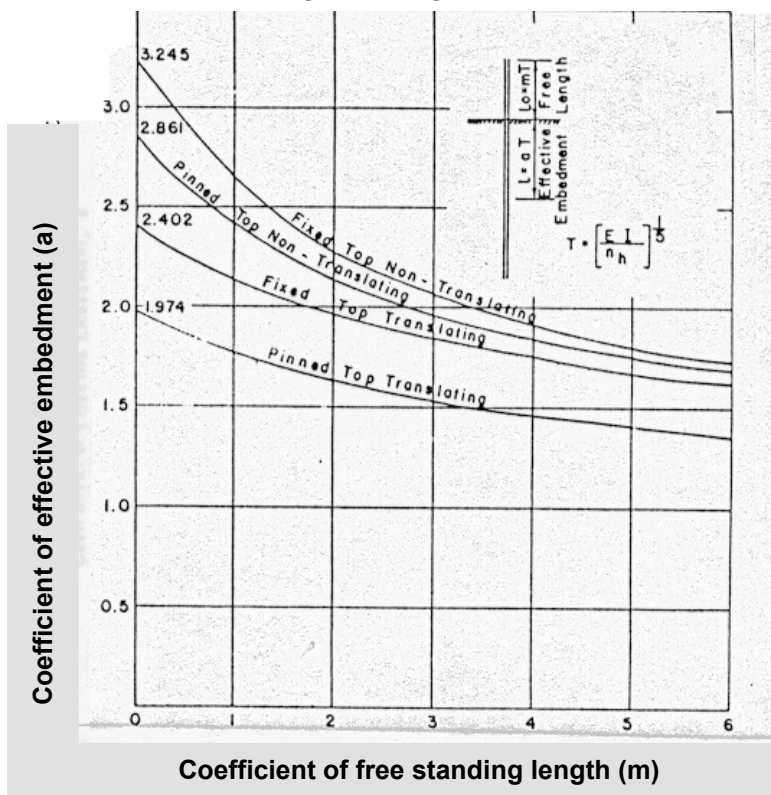
$$FUNSMOM = \frac{T}{H_f} + \frac{L_o + aT}{2} \quad (B.22)$$

where (H_f), the coefficient of horizontal load for fixed-head conditions is obtained from Figure B.5 (after Figure 7 of Yang 1966) and

L_o = free standing length = 24 ft

a = coefficient of effective embedment obtained from Figure B.5 for “fixed to translating” = 1.8.

Figure B.5. The effective embedment of pile at buckling (after Figure 2, Yang 1966).



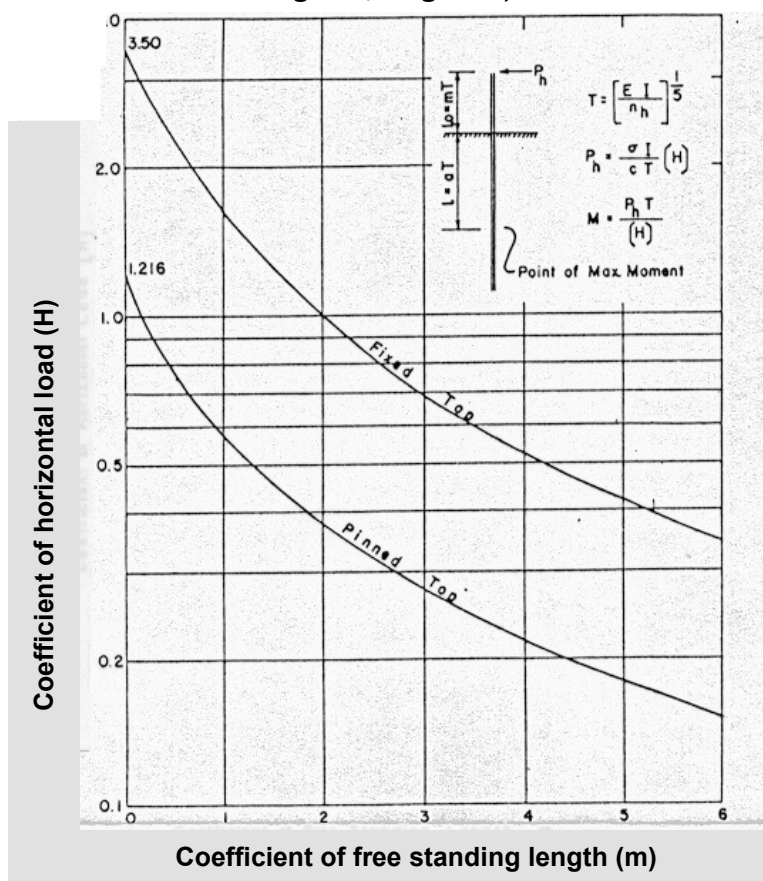
Recall m is equal to 3.58 by Equation B.14 and T , the relative stiffness factor, is equal to 6.7 ft by Equation 1.1 (after rounding). The coefficient of horizontal load for fixed-head conditions (H_f) is obtained from Figure B.6 (after Figure 7 of Yang 1966) and is equal to 0.58.

Therefore, Equation B.22 becomes

$$F_{UNSMOM} = \frac{T}{H_f} + \frac{L_o + aT}{2} = \frac{6.7}{0.58} + \frac{24 + 1.8 * 6.7}{2} = 29.6 \text{ ft} = 355 \text{ in. (B.23)}$$

The maximum moment developing 29.6 ft below the pile cap (i.e., 5.9 ft below the mudline) is monitored during the fixed-head boundary condition, incremental loading stages of the pushover analysis for the potential development of a plastic hinge in the CPGA analysis.

Figure B.6. The coefficient of horizontal load capacity (after Figure 7, Yang 1966).



It is the experience of the authors of this report that plastic hinge development through (moment-induced) yielding of the piles usually occurs first at the pile cap. Once a plastic hinge develops at the top of pile-to-pile cap intersection, the fixed-head boundary condition is changed to a pinned-head boundary condition for use in subsequent incremental load application(s). At that instance, the focus shifts to monitoring an elevation just below the mudline for potential development of a second plastic hinge within each pile(s). To obtain the value for the maximum moment below the mudline for a pinned-head condition, it is necessary to include a PMAXMOM data line where

$$PMAXMOM = \frac{T}{H_p} \quad (B.24)$$

And (H_p), the coefficient of horizontal load for pinned-head conditions, is obtained from Figure B.6 (after Figure 7 of Yang 1966) for a value of m equal to 3.58 (Equation B.14) and is equal to 0.24.

With T , the Relative stiffness factor, equal to 6.7 ft (by Equation 1.1 and after rounding), PMAXMOM for the pinned-head condition is

$$PMAXMOM = \frac{T}{H_p} = \frac{6.7}{0.24} = 27.9 \text{ ft} = 335 \text{ in.} \quad (B.25)$$

Appendix C: Axial Capacity of the Concrete-Filled Batter Pile at Lock and Dam 3 and Evaluation of the Value of the CPGA C_{33} Term

C.1 Introduction

This appendix discusses a series of axial capacity calculations made for concrete-filled, batter pipe piles in compression. These calculations were performed for the Figure 1.2 Lock and Dam 3 clustered group of three piles founded in layered soil stratum.

Six axial capacity calculations are made for batter pipe piles in compression for Lock and Dam 3. Hand calculations are made for axial compression capacity following three different engineering methodologies: EM 1110-2-2906 (HQUSACE 1991), API (2000), Castello (1980), and Coyle and Castello (1981) curves for skin friction and tip resistance for cohesionless soils. These capacity calculations define the compression capacity as the sum of the skin friction capacity along the side of the pile-to-soil interface plus the ultimate tip resistance of the pile due to end bearing. The other three pile compression capacity calculations were made using the CASE software CAXPILE (Dawkins 1984) with the Soil criteria, the WES criteria, and the VJ criteria. This software also separates the pile compression capacity calculation into the sum of the skin friction plus the tip resistance of the pile due to end bearing.

Data generated by these three CAXPILE analyses provide a basis for determining the value of the C_{33} term to be used for batter piles in a CPGA (Hartman et al. 1989) software analysis of the Figure 1.2 batter pile groups supporting the elevated impact deck of the Lock and Dam 3 flexible approach wall.

Results for pile-to-soil tension capacity calculations are also reported in this appendix, made by three different hand calculation procedures. These tension capacity calculations define the capacity as equal to the skin friction capacity along the side of the pile. For a pipe pile being subjected to tension loading, the tip resistance of the pile due to end bearing is not engaged.

C.2 Foundation soils profile and engineering property characterization at the site of the Lock and Dam 3 Guidewall extension

Figure C.1 shows the Lock and Dam 3 Guidewall extension soil profile. The soil deposits can be generalized to consist of an upper stratum of loose sand (QF upper) which forms the river bottom, overlying relatively soft lacustrine and glaciolacustrine soils (QL) of lean-to-fat clay, silt, and occasional organic soil, with occasional interbedded sand (QF middle), which in turn overlie medium-dense fluvial sand (QF lower) to varying elevations. A potentially discontinuous glacial outwash (QO) stratum of dense sand and gravel can be found generally at approximately el 605 to 600 ft. This dense outwash stratum is approximately 5 to 12 ft thick. Below the medium-dense sands, and below the dense outwash, the borings penetrated a major stratum of generally medium-dense to dense glacio-fluvial sand to approximately elevations 565 to 530 ft where dense sand and gravel was encountered to the bedrock surface. The bedrock is reported as siltstone of the St. Lawrence Formation found at depths of approximately 130 to 135 ft below the river bottom. The intent of the designers of the Lock and Dam 3 flexible approach wall extension (i.e., guidewall) was to drive the closed-end pipe piles to bear on, or within, the dense glacial outwash stratum (QO), found in the borings at approximately elevation 605 to 600 ft.

The new Lock and Dam 3 guidewall extension was constructed by extending the existing guidewall from the upstream end for a distance of 862 ft. Recall from Figure 1.2 that it is a pile-supported structure constructed of precast concrete. The impact deck structure has three rows of piles. The leading row (closest to the river channel) is vertical; the other two rows were driven inclined at an angle of 4 vertical to 1 horizontal (4V:1H), angled toward shore. Prior to pile driving, the river bottom was dredged, or filled if needed, to elevation 650 ft. After pile driving, riprap was placed around the piles to elevation 655 ft.

The soil boring B-06-109M located at station 21+72 was the soil profile used in the axial capacity evaluation discussed in this subsection. The soil layer elevations and engineering material properties used by the designers are listed in Tables C.1 and C.2, respectively. This soil profile delineation includes consideration of the dredging to elevation 650 ft and placement of 5 ft of riprap (to el 655 ft).

Figure C.1. Lock and Dam 3 Guidewall extension soil profile.

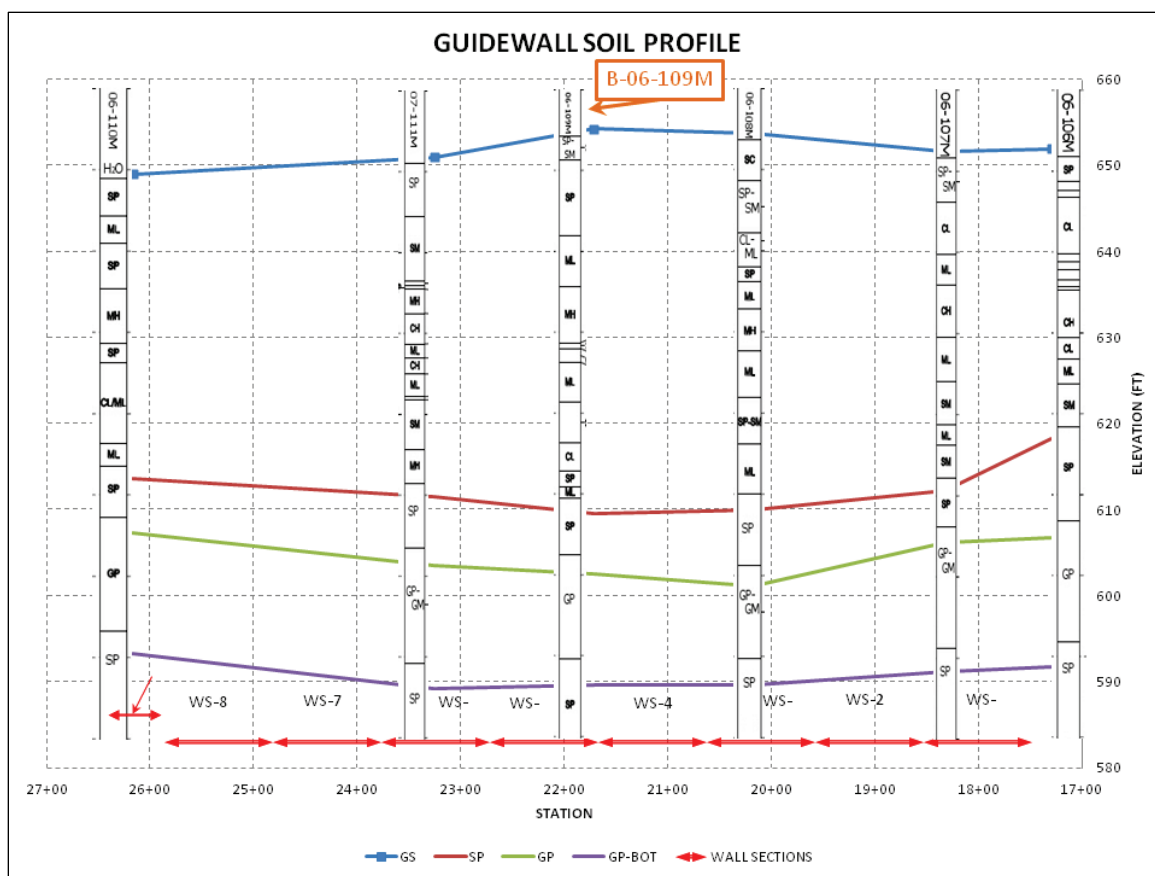


Table C.1. Lock and Dam 3 Guidewall extension Soil profile at station 21 + 72.

Layer #	Soil Type	Unified Soil Classification System	Elevation		Vertical Depth of Embedment			
			Top (ft)	Bottom (ft)	Top		Bottom	
					(ft)	(in)	(ft)	(in)
1	Riprap	GP	655	650	0	0	5	60
2	Loose sand	SP-SM	650	643	5	60	12	144
3	Silt and clay layers	ML-CL	643	621	12	144	34	408
4	Medium-dense sand	SP	621	616	34	408	39	468
5	Clay	CL	616	610	39	468	45	540
6	Medium-dense sand	SP	610	603	45	540	52	624
7	Dense sand	SP	603	-	52	624	-	-

Table C.2. Engineering material properties for the soil stratum at station 21 + 72.

Layer #	Soil Type	Unified Soil Classification System	$\gamma_{\text{saturated}}$		γ_{buoyant}		c		ϕ (deg)
			(pcf)	(pci)	(pcf)	(pci)	(psf)	(psi)	
1	Riprap	GP	140.16	0.081	77.76	0.045	0	0	43
2	Loose sand	SP-SM	121.15	0.070	58.75	0.034	0	0	28
3	Silt and clay layers	ML-CL	112.15	0.065	50.11	0.029	468	3.25	0
4	Medium-dense sand	SP	121.15	0.070	58.75	0.034	0	0	30
5	Clay	CL	112.51	0.065	50.11	0.029	631	4.38	0
6	Medium-dense sand	SP	122.88	0.071	60.48	0.035	0	0	33
7	Dense sand	SP	136.7	0.079	74.3	0.043	0	0	43

Table C.3 summarizes the calculation of the effective vertical stress, σ'_v , for equivalent batter elevations of the soil layers for a 4V:1H batter pile at Lock and Dam 3 Guidewall extension using the Soil profile at station 21 + 72. These equivalent batter pile elevations of the soil stratum help to facilitate the axial capacity evaluation of the 4V:1H batter pile.

Table C.3. Summary of the distribution of effective vertical stresses with elevation for an equivalent vertical batter pile soil profile of a 4V:1H batter compression pile at Lock and Dam 3 Guidewall extension for Soil profile at station 21 + 72.

Layer #	Soil Type	Vertical Depth		Equivalent Batter Length (in)	Equivalent Batter Elevation		γ_{buoyant}		σ'_v	
		(ft)	(in)		(ft)	(in)	(pcf)	(pci)	(psf)	(psi)
1	Riprap	0	0	0	0	0	77.76	0.045	0	0
		5	60	61.8	-5.15	-61.9			400.8	2.78
2	Loose sand	5	60	61.8	-5.15	-61.9	58.25	0.034	400.8	2.78
		12	144	148.4	-12.37	-148.4			821.1	5.73
3	Silt and clay layers	12	144	148.4	-12.37	-148.4	50.11	0.029	821.1	5.73
		34	408	420.6	-35.05	-420.6			1957.4	13.62
4	Medium dense sand	34	408	420.6	-35.05	-420.6	58.75	0.034	1957.4	13.62
		39	468	482.4	-40.2	-482.4			2260.2	15.72
5	Clay	39	468	482.4	-40.2	-482.4	50.11	0.029	2260.2	15.72
		45	540	556.6	-46.38	-556.6			2570.1	17.87
6	Medium dense sand	45	540	556.6	-46.38	-556.6	60.48	0.035	2570.1	17.87
		52	624	643.2	-53.6	-643.2			3006.5	20.90
7	Dense sand	52	624	643.2	-53.6	-643.2	74.3	0.043	3006.5	20.90

C.3 Axial capacity of the concrete-filled batter pile following EM 1110-2-2906 guidance

Table C.4 summarizes the calculation of the skin friction capacity of a 4V:1H batter compression pile at Lock and Dam 3 Guidewall extension for Soil profile at station 21 + 72 according to EM 1110-2-2906 (HQUSACE 1991) criteria. The critical depth, D_c , is set equal to 30 ft. This depth corresponds to 15 times the pile diameter, D_p , of 2 ft for a medium-dense sand (Table A.4). Calculation of the horizontal effective stress, σ'_h , is based on a horizontal earth pressure coefficient, K_h , value of 1 for all soil layers for a closed-end, driven pipe pile (Table A.3) and effective vertical stresses according to Equations A.5 and A.6. The vertical effective stress (used in the σ'_h computation) is restricted to being a value less than 1,705 psf. This value for effective overburden corresponds to the critical depth (D_c). The effective angle of the steel pipe pile-to-soil interface friction for the cohesionless layers is set equal to 0.83 times the effective angle of internal friction of the soil (Table A.1). The ultimate skin friction resistance is computed to be 171,991 lb for a compression batter pile in the layered strata by Equation A.8. Equation A.4 is used in these computations for the unit skin resistances, $(f_s)_i$, for the sand layers and Equations A.10 and A.11 for the silt and clay layers, respectively. The α values for the silt and clay layers are defined using the Figure A.1 relationships.

The unit tip capacity of the 24 in. diameter closed-end pipe bearing on (very) dense sand is computed to be 68,328 psf by Equation A.9, with N_q equal to 40 and using a limiting value for σ'_v set equal to 1,705 psf ($\sigma'_v < (\gamma_{buoy} * D_c)$, with D_c equal to 30 ft). By Equation A.3, the tip resistance of the pile due to end bearing equals 214,658 lb. The ultimate pipe pile capacity equals 386,649 lb (Equation A.1) by the EM 1110-2-2906 (HQUSACE 1991) design criteria. The end bearing provides 56% of the ultimate pipe pile capacity in this calculation.

EM 1110-2-2906 (HQUSACE 1991) suggests a value for the horizontal earth pressure coefficient, K_h , of 0.7 for tension piles in sand and silt strata (Table A.3) when computing effective vertical stresses by Equations A.5 and A.6. A K_h value of 0.7 is lower than the K_h value of 1 used for the compression piles calculation. The ultimate skin friction resistance is computed to be 147,273 lb for a tension batter pile in the layered soil strata.

Table C.4. Ultimate skin friction capacity calculations of a 4V:1H batter compression pile at Lock and Dam 3 Guidewall extension for Soil profile at station 21 + 72 according to EM 1110-2-2906 (HQUSACE 1991).

Layer #	Soil Type	Equivalent Batter ELEVATION (ft)	σ'_v (psf)	$\sigma'_v < (\gamma_{buoy} * D_c)$ (psf)	δ' (deg)	c (psf)	α (pcf)	$(f_s)_i$ (psf)	$(Q_s)_i$ (lb)
1	Riprap	0	0	0	36			0	4,661
		-5.15	400.8	400.8				288	
2	Loose sand	-5.15	400.8	400.8	23			172	11,929
		-12.37	821.1	821.1				353	
3	Silt and clay layers	-12.37	821.1	821.1	0	468	1	468	66,683
		-35.05	1957.4	1,705				468	
4	Medium dense sand	-35.05	1957.4	1,705	25			791	25,677
		-40.2	2260.2	1,705				791	
5	Clay	-40.2	2260.2	1,705	0	631	0.935	590	22,916
		-46.38	2570.1	1,705				590	
6	Medium dense sand	-46.38	2570.1	1,705	27			883	40,125
		-53.6	3006.5	1,705				883	
7	Dense sand	-53.6	3006.5	1,705	36			1,224	

C.4 Axial capacity of the concrete-filled batter pile following API (2000) guidelines

Table C.5 summarizes the calculation of the skin friction capacity of a 4V:1H batter compression pile at Lock and Dam 3 Guidewall extension for Soil profile at station 21 + 72 according to API guidelines. Calculation of the horizontal effective stress, σ'_h , is based on Equation A.4 and a horizontal earth pressure coefficient, K_h , value of 1 for all soil layers for a closed-end, driven pipe pile. With the availability of site-specific engineering data (Table C.2), the effective angle of the steel pipe pile-to-soil interface friction for the cohesionless layers is set equal to the effective angle of internal friction of the soil minus 5 degrees (Vijayvergia 1977). The ultimate skin friction resistance is computed to be 196,499 lb for the layered strata by Equation A.8 for piles in compression or in tension. Equation A.4 is used in these computations for unit skin friction values of $(f_s)_i$ for the sand layers and Equation A.15 for the silt and clay layers, respectively. The $(f_s)_i$ for the sand layers are all below the Table A.2 limiting skin friction values. The α values for the silt and clay layers are defined using the Equation A.16 relationship.

Table C.5. Ultimate skin friction capacity calculations of a 4V:1H batter compression pile at Lock and Dam 3 Guidewall extension for Soil profile at station 21 + 72 according to API (2000) guidelines.

Layer #	Soil Type	Equivalent Batter Elevation (ft)	σ'_v (psf)	δ' (deg)	c (psf)	c/σ'_v (psf)	α (pcf)	$(f_s)_l$ (psf)	$(Q_s)_l$ (lb)
1	Riprap	0	0	38				0	5,070
		-5.15	401.8					313	
2	Loose sand	-5.15	400.8	23				170	11,791
		-12.37	821.1					349	
3	Silt and clay layers	-12.37	821.1	0	468	0.34	0.86	404	57,520
		-35.05	1957.4					404	
4	Medium-dense sand	-35.05	1957.4	25				913	31,899
		-40.2	2260.2					1054	
5	Clay	-40.2	2260.2	0	631	0.26	0.935	590	22,916
		-46.38	2570.1					590	
6	Medium-dense sand	-46.38	2570.1	28				1,367	67,303
		-53.6	3006.5					1,599	
7	Dense sand	-53.6	3006.5	38				2,349	

The unit tip capacity of the 24 in. diameter, closed-end pipe bearing on dense sand is computed to be 150,510 psf by Equation A.9, with N_q equal to 50 (Table A.2) and a limiting unit end bearing value of 250,000 psf (Table A.2). By Equation A.3, the tip resistance of the pile due to end bearing equals 472,841 lb. The ultimate compression pipe pile capacity equals 669,340 lb (Equation A.1) by the API (2000) guidelines. The end bearing provides 71% of the ultimate pipe pile capacity in this calculation. The ultimate tension pipe pile capacity equals 196,499 lb.

C.5 Axial capacity of the concrete-filled batter pile using Castello skin friction and tip capacity curves for cohesionless soils

Table C.6 summarizes the calculation of the skin friction capacity of a 4V:1H batter compression pile at Lock and Dam 3 Guidewall extension for Soil profile at station 21 + 72 according to the Castello (1980) and Coyle and Castello (1981) sand curves and EM 1110-2-2906 (HQUSACE 1991) criteria for the silt and clay layers. Recall the diameter of pile, D_p , is 2 ft. The ultimate skin friction resistance is computed to be 176,385 lb for the layered strata by Equation A.8 for piles in compression or in tension. Equations A.10 and A.11 are used to compute f_s for the silt and clay layers with the α values for the silt and clay layers defined using the Figure A.1 (EM 1110-2-2906, HQUSACE [1991]) relationships.

Table C.6. Ultimate skin friction capacity calculations of a 4V:1H batter compression pile at Lock and Dam 3 Guidewall extension for Soil profile at station 21 + 72 according to the Castello sand curves and EM 1110-2-2906 (HQUSACE 1991) criteria for the silt and clay layers.

Layer #	Soil Type	Equivalent Batter Elevation (ft)	Depth/D _p	ϕ' (deg)	c (psf)	α (pcf)	(f _s) _i (psf)	(Q _s) _i (lb)
1	Riprap	0	0	43			0	12,953
		-5.15	2.5				800	
2	Loose sand	-5.15	2.5	28			140	6,800
		-12.37	6				280	
3	Silt and clay layers	-12.37	6	0	468	1	468	66,683
		-35.05	17				468	
4	Medium-dense sand	-35.05	17	30			500	17,163
		-40.2	19.5				560	
5	Clay	-40.2	19.5	0	631	0.935	590	22,916
		-46.38	22.5				590	
6	Medium-dense sand	-46.38	22.5	33			1060	49,870
		-53.6	26				1140	
7	Dense sand	-53.6	26	43			2400	

The unit tip capacity of the 24 in. diameter, closed-end pipe bearing on dense sand is estimated to be 250,000 psf by Figure A.3 for a Depth/D_p ratio equal to 26 and ϕ' equal to 43 degrees. By Equation A.3 the tip resistance of the pile due to end bearing equals 785,398 lb. The ultimate pipe pile capacity equals 961,783 lb (Equation A.1) using the Castello curves for the sand layers and the EM 1110-2-2906 (HQUSACE 1991) design criteria for the silt and clay layers. The end bearing provides 82% of the ultimate pipe pile capacity in this calculation.

C.6 Axial capacity of the concrete-filled batter pile using CAXPILE software with the Soil criteria

Table C.7 summarizes the input data to CAXPILE for a 4V:1H batter compression pile at Lock and Dam 3 Guidewall extension for Soil profile at station 21 + 72 using the Soil criteria. The effective angle of the steel pipe pile-to-soil interface friction for the cohesionless layers is specified in the CAXPILE data input and set equal to 0.83 times the effective angle of internal friction of the soil (Table A.1). The ultimate skin friction resistance is computed to be 160,334 lb for the layered strata by CAXPILE using the

Soil criteria for piles in compression or in tension. To compute the skin friction resistance, the CAXPILE Soil criteria uses the Castello curves for the sand layers and the Coyle and Reese (1966) curves for the clay (and silt) layers. The α values for the silt and clay layers are defined using the Figure A.1 relationships.

Table C.7. Summary of input data for computing the ultimate skin friction capacity of a 4V:1H batter compression pile at Lock and Dam 3 Guidewall extension for Soil profile at station 21 + 72 using the CAXPILE Soil criteria.

Layer #	Soil Type	Equivalent Batter Elevation (ft)	$\gamma_{\text{saturated}}$ (pcf)	ϕ' (deg)	δ' (deg)	c (psf)	α (pcf)	$(\epsilon)_{50}$
1	Riprap	0	140.16	43	36			
		-5.15						
2	Loose sand	-5.15	120.65	28	23			
		-12.37						
3	Silt and clay layers	-12.37	112.51	0	0	468	1	0.02
		-35.05						
4	Medium-dense sand	-35.05	121.15	30	25			
		-40.2						
5	Clay	-40.2	112.15	0	0	631	0.935	0.01
		-46.38						
6	Medium-dense sand	-46.38	122.88	33	27			
		-53.6						
7	Dense sand	-53.6	136.7	43	36			

The tip resistance of the 24 in. diameter, closed-end pipe bearing on dense sand (ϕ' equal to 43 degrees) is computed to be 762,970 lb by CAXPILE using the Soil criteria. The ultimate pipe pile capacity, Q_{ult} , equals 923,304 lb. The end bearing provides 83% of the ultimate pipe pile capacity according to the CAXPILE Soil criteria computation. The ultimate tension pipe pile capacity equals 160,334 lb.

The CAXPILE Soil criteria output was processed into C_{33} data using Equation 2.8:

$$C_{33} = \frac{P_A / w_A}{A * E / L_e} \quad (2.8 \text{ bis})$$

with P_A designating the applied compression load, w_A designating the displacement of the top of pile (at its start of embedment elevation), A designating the cross-sectional area of the concrete-filled pipe pile, E designating its (composite) Young's Modulus, and L_e being the length of pile embedment. The terms A , E , and L_e are constants: for this CAXPILE Soil criteria analysis of Lock and Dam 3 Soil profile at station 21 + 72, the cross-sectional area of the concrete-filled pipe pile is 452.4 in² (Equation B.1), the composite Young's Modulus is 5,124,000 psi (Equation B.12), and the length of embedded pile L_e , is 53.6 ft.

Recall C_{33} is a parameter used as input to a CPGA batter pile model. Because of the nonlinear response to increasing axial load, the C_{33} term is found to be a function of the magnitude of axial load P_A applied to the pile, and the magnitude P_A is being expressed as a fraction of the ultimate pile resistance, Q_{ult} , along the horizontal axis of the C_{33} versus $[P_A/Q_{ult}]$ data summarized in Figure C.2. Recall Q_{ult} equals 923,304 lb for the CAXPILE Soil criteria. The CAXPILE processed results are presented in this form so that comparisons can be made between the results from this CAXPILE SSI analysis and the other CAXPILE analyses in which the pile-to-soil constitutive model is changed to the WES criteria and to the VJ criteria. Figure C.1 shows the magnitude of C_{33} to be less than 1.0, and the value of C_{33} decreases as the capacity of the 24 in. diameter, batter pipe pile is mobilized. At one-half the ultimate pile capacity, C_{33} is approximately 0.44, and at full mobilization of its capacity, C_{33} is 0.18.

C.7 Axial capacity of the concrete-filled batter pile using CAXPILE software with the WES criteria

Table C.8 summarizes the input data to CAXPILE for a 4V:1H batter compression pile at Lock and Dam 3 Guidewall extension for Soil profile at station 21 + 72 using the WES criteria. The effective angle of the steel pipe pile-to-soil interface friction for the cohesionless layers is set equal to 0.83 times the effective angle of internal friction of the soil (Table A.1). The ultimate skin friction resistance is computed to be 137,285 lb for the layered strata by CAXPILE using the WES criteria for piles in compression or in tension. The α values for the silt and clay layers are defined using the Figure A.1 relationships. Constant cohesion values are specified in the silt and clay layer 3 and in the clay layer 5. Consequently, c/σ'_v is specified as zero for each of these uniform, undrained strength layers in the WES criteria data input. The value for $[E_u/c]$ was assigned based on the Duncan and Buchignani (1976) Figure 5 set of curves that correlates $[E_u/c]$ to the

values of over-consolidation ratio (OCR) and the plasticity index (PI) for the soil. This correlation figure is reproduced in Duncan and Bursey (2007) and in Pace et al. (2012).

Figure C.2. C_{33} versus axial load expressed as a fraction of the axial capacity of a 4V:1H batter compression pile at Lock and Dam 3 Guidewall extension for Soil profile at station 21 + 72 using the CAXPILE Soil criteria.

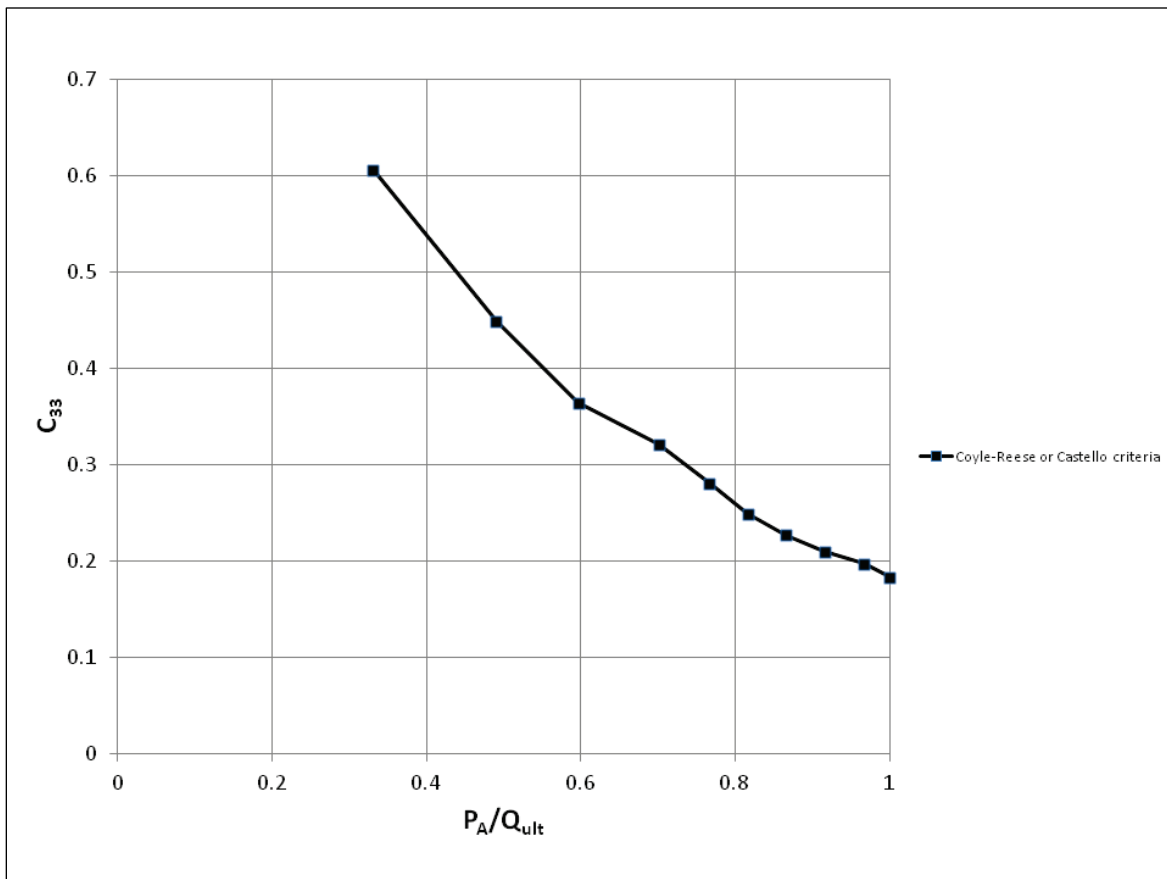


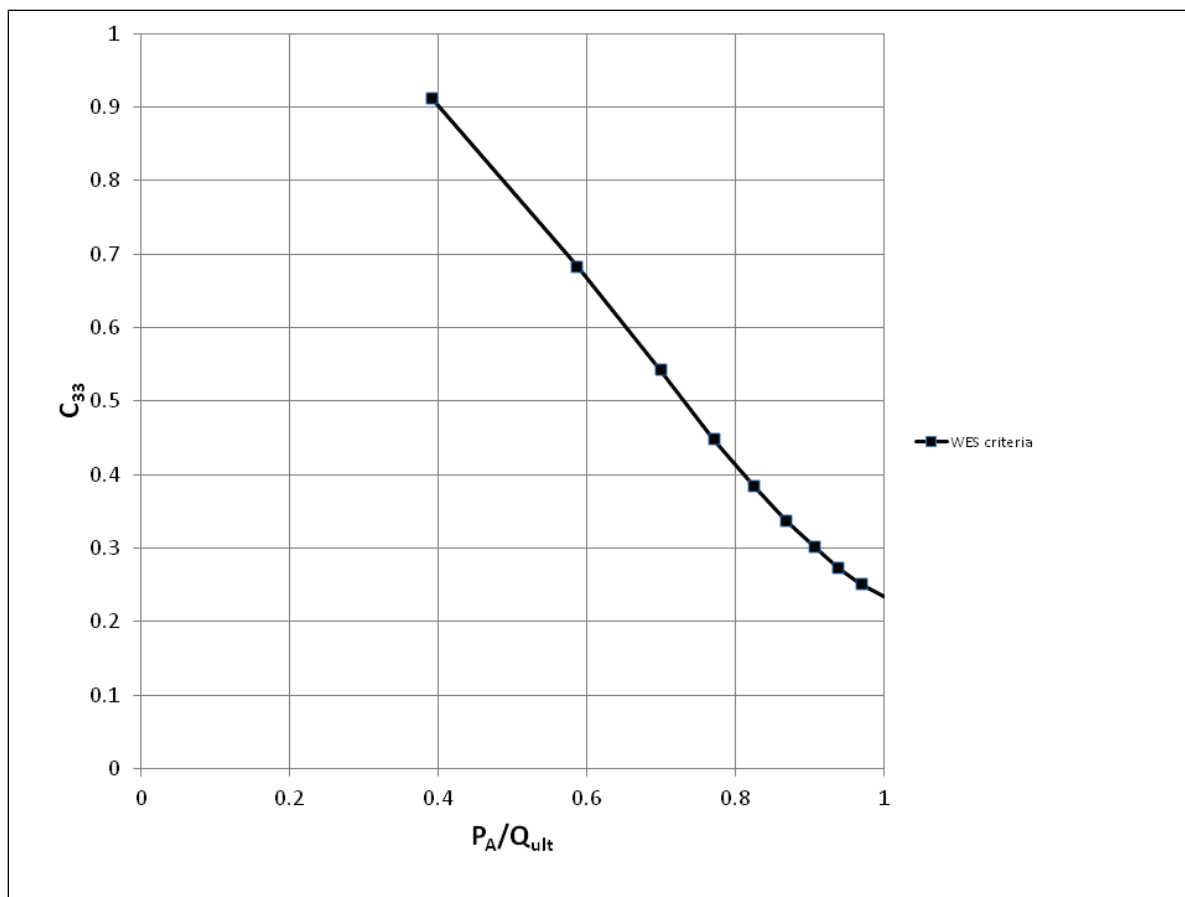
Table C.8. Summary of input data for computing the ultimate skin friction capacity of a 4V:1H batter compression pile at Lock and Dam 3 Guidewall extension for Soil profile at station 21 + 72 using the CAXPILE WES criteria.

Layer #	Soil Type	Equivalent Batter Elevation (ft)	$\gamma_{\text{saturated}}$ (pcf)	ϕ' (deg)	δ' (deg)	c (psf)	α (pcf)	E_u/c
1	Riprap	0	140.16	43	36			
		-5.15						
2	Loose sand	-5.15	120.65	28	23			
		-12.37						
3	Silt and clay layers	-12.37	112.51	0	0	468	1	600
		-35.05						
4	Medium-dense sand	-35.05	121.15	30	25			
		-40.2						
5	Clay	-40.2	112.15	0	0	631	0.935	800
		-46.38						
6	Medium-dense sand	-46.38	122.88	33	27			
		-53.6						
7	Dense sand	-53.6	136.7	43	36			

The tip resistance of the 24 in. diameter, closed-end pipe bearing on dense sand (ϕ' equal to 43 degrees) is computed to be 938,785 lb by CAXPILE using the WES criteria. The ultimate pipe pile capacity equals 1,076,070 lb. The end bearing provides 87% of the ultimate pipe pile capacity according to the CAXPILE WES criteria computation.

The CAXPILE WES criteria output was processed into C_{33} data using Equation 2.8 (with A equal to 452.4 in² [Equation B.1], a Young's Modulus of 5,124,000 psi [Equation B.12], and the length of embedded pile L_e , of 53.6 ft) and presented in Figure C.3 as a function of $[P_A/Q_{\text{ult}}]$. Recall Q_{ult} equals 1,076,070 lb for the CAXPILE WES criteria. Figure C.3 shows the magnitude of C_{33} to be less than 1.0, and the value of C_{33} decreases as the capacity of the 24 in. diameter batter pipe pile is mobilized. At one-half the ultimate pile capacity, C_{33} is approximately 0.77, and at full mobilization of its capacity, C_{33} is 0.23.

Figure C.3. C_{33} versus axial load expressed as a fraction of the axial capacity of a 4V:1H batter compression pile at Lock and Dam 3 Guidewall extension for Soil profile at station 21 + 72 using the CAXPILE WES criteria.



C.8 Axial capacity of the concrete-filled batter pile using CAXPILE software with the VJ criteria

Table C.9 summarizes the input data to CAXPILE for a 4V:1H batter compression pile at Lock and Dam 3 Guidewall extension for Soil profile at station 21 + 72 using the VJ criteria and values of ultimate skin friction calculated according to API (2000) guidelines. Calculation of the horizontal effective stress, σ'_h , is based on Equation A.4 and a horizontal earth pressure coefficient, K_h , value of 1 for all soil layers for a closed-end, driven pipe pile. With the availability of site-specific engineering data (Table A.7), the effective angle of the steel pipe pile-to-soil interface friction for the cohesionless layers is set equal to the effective angle of internal friction of the soil minus 5 degrees (Vijayvergia 1977). The API guidelines are used to compute the ultimate skin friction values in the various soil strata. The ultimate skin friction resistance is computed to be 194,007 lb for the layered strata by CAXPILE using the VJ criteria for piles

in compression or in tension. The parameter z_c is set equal to 0.25 in. in the VJ criteria input for all soils based on the guidance provided in Vijayvergia (1977). This recommendation for the value to be assigned to z_c is also given in Heydinger (1987). The α values for the silt and clay layers are defined using the Equation A.16 relationship.

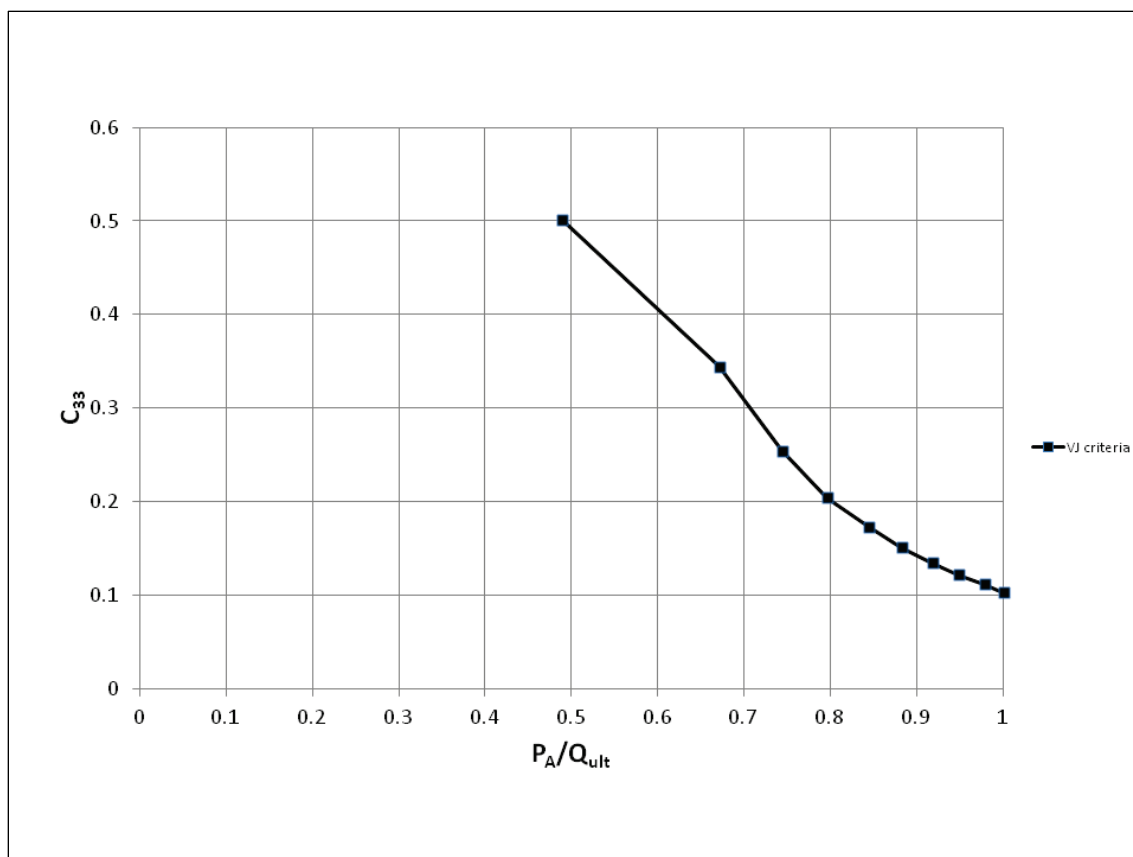
Table C.9. Summary of input data for computing the ultimate skin friction capacity of a 4V:1H batter compression pile at Lock and Dam 3 Guidewall extension for Soil profile at station 21 + 72 using the CAXPILE VJ criteria.

Layer #	Soil Type	Equivalent Batter Elevation (ft)	σ'_v (psf)	δ' (deg)	c (psf)	c/σ'_v (psf)	α (pcf)	$(f_s)_i$ (psf)	z_c (in)
1	Riprap	0	0	38				0	0.25
		-5.15	401.8					313	0.25
2	Loose sand	-5.15	400.8	23				170	0.25
		-12.37	821.1					349	0.25
3	Silt and clay layers	-12.37	821.1	0	468	0.34	0.86	404	0.25
		-35.05	1957.4					404	0.25
4	Medium-dense sand	-35.05	1957.4	25				913	0.25
		-40.2	2260.2					1054	0.25
5	Clay	-40.2	2260.2	0	631	0.26	0.935	590	0.25
		-46.38	2570.1					590	0.25
6	Medium-dense sand	-46.38	2570.1	28				1,367	0.25
		-53.6	3006.5					1,599	0.25
7	Dense sand	-53.6	3006.5	38				2,349	0.25

The unit tip capacity of the 24 in. diameter, closed-end pipe bearing on dense sand is computed to be 150,325 psf by Equation A.9, with N_q equal to 50 (Table A.2) and a limiting unit end bearing value of 250 psf (Table A.2). The tip resistance of the 24 in. diameter, closed-end pipe bearing on dense sand (ϕ' equal to 43 degrees) is computed to be 472,251 lb by CAXPILE using the VJ criteria. The tip movement parameter z_t for use in the SSI calculations made at the pile tip is set equal to 1.6 in. in the VJ criteria. This value for z_t is based on the average of the data provided in Table 2 of Vijayvergia (1977); z_t is approximately 0.065 times the diameter of the pile tip bearing on sands. The ultimate pipe pile capacity equals 666,258 lb. The end bearing provides 71% of the ultimate pipe pile capacity according to the CAXPILE VJ criteria computation.

The CAXPILE VJ criteria output was processed into C_{33} data using Equation 2.8 (with A equal to 452.4 in.² [Equation B.1], a Young's Modulus of 5,124,000 psi [Equation B.12] and the length of embedded pile L_e , of 53.6 ft) and presented in Figure C.4 as a function of $[P_A/Q_{ult}]$. Recall Q_{ult} equals 666,258 lb for the CAXPILE VJ criteria. Figure C.4 shows the magnitude of C_{33} to be less than 1.0, and the value of C_{33} decreases as the capacity of the 24 in. diameter batter pipe pile is mobilized. At one-half the ultimate pile capacity, C_{33} is 0.5, and at full mobilization of its capacity, C_{33} is 0.1.

Figure C.4. C_{33} versus axial load expressed as a fraction of the axial capacity of a 4V:1H batter compression pile at Lock and Dam 3 Guidewall extension for Soil profile at station 21 + 72 using the CAXPILE VJ criteria.



Appendix D: Axial Capacity of a Lock and Dam 3 Concrete-Filled Batter Pile Founded in Medium-Dense Sand and Evaluation of the Value of the CPGA C_{33} Term

D.1 Introduction

This appendix continues the Appendix C investigation of axial batter pile capacity and appropriate value(s) for the axial stiffness modifier term C_{33} for use in pushover analyses of batter pile group configured flexible approach walls. This appendix summarizes the first series of six analyses in a parametric investigation study of the influence that the density of cohesionless soil comprising the foundation has on the magnitude of the C_{33} term. This parametric investigation makes use of the Figure 1.2 Lock and Dam 3 batter pile geometry but founded in homogenous medium-dense sand. Recall that the actual foundation is a layered soil site consisting of sands of different densities, silts, and clays (Figure C.1). The 5 ft of riprap on top of the foundation soil is maintained in this parametric model. All pile geometry is the same as was discussed in Appendix C.

Six axial capacity calculations are made for a concrete-filled batter pipe in axial compression of the Lock and Dam 3 pile group configuration founded in medium-dense sand. One set of three hand calculations is made for its axial compression capacity following EM 1110-2-2906 (HQUSACE 1991) guidance, API (2000) guidelines, and using the Castello (1980) and Coyle and Castello (1981) curves for skin friction and tip resistance for cohesionless soils. The second set of three compression pile capacity calculations was made using the CASE software CAXPILE (Dawkins 1984) with the Soil criteria, the WES criteria, and the VJ criteria. Additionally, data generated by these three CAXPILE analyses provide a basis for determining the value of the C_{33} term to be used for batter piles founded in medium-dense sand in a CPGA (Hartman et al. 1989) software analysis of the Figure 1.2 batter pile groups.

Hand calculations for the pile-to-soil tension capacity calculations are also reported in this appendix. Recall that for a pipe pile being subjected to tension loading, the tip resistance of the pile due to end bearing is not engaged.

D.2 Engineering property characterization for a medium-dense sand foundation

The engineering material properties of the 5 ft of riprap (el 650 to 655) and a hypothetical medium-dense foundation sand are summarized in Table D.1. The top of riprap is at el 655. All elevations mirror those discussed in Appendix C for a Figure 1.2 batter pile group configuration.

Table D.1. Engineering material properties for the riprap and medium-dense sand foundation.

Soil Type	Unified Soil Classification System	$\gamma_{\text{saturated}}$		γ_{buoyant}		ϕ (deg)
		(pcf)	(pci)	(pcf)	(pci)	
Riprap	GP	140.16	0.081	77.76	0.045	43
Medium-dense sand	SP	122	0.071	59.6	0.034	32

Table D.2 summarizes the calculation of the effective vertical stress, σ'_v , for select, equivalent batter elevations within the hypothetical medium-dense sand foundation for a 4V:1H batter pile configuration like that used at the Lock and Dam 3 Guidewall extension. These elevations facilitate the axial capacity evaluation of the 4V:1H batter pile. The elevations at which these computations are made mirror those listed in Table C.3 for the seven soil layer boundaries found at the Lock and Dam 3 site. The layer numbers are maintained in this appendix for bookkeeping purposes and to conveniently relate back to Appendix C information.

Table D.2. Summary of the distribution of effective vertical stresses with elevation of an equivalent vertical batter pile in medium-dense sand for a 4V:1H batter compression pile type configuration used at Lock and Dam 3 Guidewall extension.

Layer #	Soil Type	Vertical Depth		Equivalent Batter Length (in.)	Equivalent Batter Elevation		γ_{buoyant}		σ'_v	
		(ft)	(in.)		(ft)	(in.)	(pcf)	(pci)	(psf)	(psi)
1	Riprap	0	0	0	0	0	77.76	0.045	0	0
		5	60	61.8	-5.15	-61.9			400.8	2.78
2	Medium-dense sand	5	60	61.8	-5.15	-61.9	59.6	0.034	400.8	2.78
		12	144	148.4	-12.37	-148.4			830.8	5.77
3	Medium-dense sand	12	144	148.4	-12.37	-148.4	59.6	0.034	830.8	5.77
		34	408	420.6	-35.05	-420.6			2182.4	15.16
4	Medium-dense sand	34	408	420.6	-35.05	-420.6	59.6	0.034	2182.4	15.16
		39	468	482.4	-40.2	-482.4			2489.5	17.29
5	Medium-dense sand	39	468	482.4	-40.2	-482.4	59.6	0.034	2489.5	17.29
		45	540	556.6	-46.38	-556.6			2858.1	19.85

Layer #	Soil Type	Vertical Depth		Equivalent Batter Length	Equivalent Batter Elevation		γ_{buoyant}		σ'_v	
		(ft)	(in.)	(in.)	(ft)	(in.)	(pcf)	(pci)	(psf)	(psi)
6	Medium-dense sand	45	540	556.6	-46.38	-556.6	59.6	0.034	2858.1	19.85
		52	624	643.2	-53.6	-643.2			3288.2	22.83
7	Medium-dense sand	52	624	643.2	-53.6	-643.2	59.6	0.034	3288.2	22.83

D.3 Axial capacity of the concrete-filled batter pile following EM 1110-2-2906 guidance

Table D.3 summarizes the EM 1110-2-2906 (HQUSACE 1991) based calculation of the skin friction capacity of an equivalent vertical batter pile in medium-dense sand for a 4V:1H batter compression pile type configuration used at Lock and Dam 3 Guidewall extension. The critical depth, D_c , is set equal to 30 ft. This depth corresponds to 15 times the pile diameter, D_p , of 2 ft for a medium-dense sand (Table A.4). Calculation of the horizontal effective stress, σ'_h , is based on a horizontal earth pressure coefficient, K_h , value of 1 for all soil layers for a closed-end, driven pipe pile (Table A.3) and effective vertical stresses according to Equations A.5 and A.6. The vertical effective stress (used in the σ'_h computation) is restricted to being a value less than 1,882 psf. This value for effective overburden corresponds to the critical depth (D_c). The effective angle of the steel pipe pile-to-soil interface friction for the cohesionless layers is set equal to 0.83 times the effective angle of internal friction of the soil (Table A.1). The ultimate skin friction resistance is computed to be 224,866 lb for a batter pile under axial compression in a homogenous medium-dense sand by Equation A.8. Equation A.4 is used in these computations for the unit skin resistances, $(f_s)_i$, for the sand layers.

Table D.3. Ultimate skin friction capacity calculations according to EM 1110-2-2906 (HQUSACE 1991) of an equivalent vertical batter pile in medium-dense sand for a 4V:1H batter compression pile type configuration used at Lock and Dam 3 Guidewall extension.

Layer #	Soil Type	Equivalent Batter Elevation (ft)	σ'_v (psf)	$\sigma'_v < (\gamma_{\text{buoy}} * D_c)$ (psf)	δ' (deg)	$(f_s)_i$ (psf)	$(Q_s)_i$ (lb)
1	Riprap	0	0	0	36	0	4,661
		-5.15	400.8	400.8		288	
2	Medium-dense sand	-5.15	400.8	400.8	27	200	13,956
		-12.37	830.8	830.8		415	

Layer #	Soil Type	Equivalent Batter Elevation (ft)	σ'_v (psf)	$\sigma'_v < (\gamma_{buy} * D_c)$ (psf)	δ' (deg)	$(f_s)_i$ (psf)	$(Q_s)_i$ (lb)
3	Medium-dense sand	-12.37	830.8	830.8	27	415	96,597
		-35.05	2182.4	1881.6		941	
4	Medium-dense sand	-35.05	2182.4	1881.6	27	941	30,459
		-40.2	2489.5	1881.6		941	
5	Medium-dense sand	-40.2	2489.5	1881.6	27	941	36,551
		-46.38	2858.1	1881.6		941	
6	Medium-dense sand	-46.38	2858.1	1881.6	27	941	42,643
		-53.6	3288.2	1881.6		941	
7	Medium-dense sand	-53.6	3288.2	1881.6	27	941	

The unit tip capacity of the 24 in. diameter, closed-end pipe bearing on medium-dense sand is computed to be 75,264 psf by Equation A.9, with N_q equal to 40 and using a limiting value for σ'_v set equal to 1,882 psf ($\sigma'_v < (\gamma_{buy} * D_c)$, with D_c equal to 30 ft). By Equation A.3, the tip resistance of the pile due to end bearing equals 236,448 lb. The ultimate pipe pile capacity equals 461,314 lb (Equation A.1) by the EM 1110-2-2906 (HQUSACE 1991) design criteria. The end bearing provides 51% of the ultimate pipe pile capacity in this calculation.

EM 1110-2-2906 (HQUSACE 1991) suggests a value for the horizontal earth pressure coefficient, K_h , of 0.7 for tension piles in sand and silt strata (Table A.3) when computing effective vertical stresses by Equations A.5 and A.6. A K_h value of 0.7 is lower than the K_h value of 1 used for the axial compression pile calculation. The ultimate skin friction resistance is computed to be 157,406 lb for a tension batter pile in the layered soil strata.

D.4 Axial capacity of the concrete-filled batter pile following API (2000) guidelines

Table D.4 summarizes the calculation of the skin friction capacity according to API guidelines of an equivalent vertical batter pile in medium-dense sand for a 4V:1H batter compression pile type configuration used at Lock and Dam 3 Guidewall extension. Calculation of the horizontal effective stress, σ'_h , is based on Equation A.4 and a horizontal earth pressure coefficient, K_h , value of 1 for all soil layers for a closed-end, driven pipe pile. The effective angle of the steel pipe pile-to-soil interface friction for the cohesionless

layers is set equal to the effective angle of internal friction of the medium-dense sand, which is 27 degrees (Table A.2). The ultimate skin friction resistance is computed to be 291,145 lb by Equation A.8 for piles in compression or in tension. Equation A.4 is used in these computations for unit skin friction values of $(f_s)_i$ for the sand layers. The $(f_s)_i$ for the sand layers are all below the Table A.2 limiting skin friction value of 1,850 psf.

Table D.4. Ultimate skin friction capacity calculations according to API (2000) guidelines of an equivalent vertical batter pile in medium-dense sand for a 4V:1H batter compression pile type configuration used at Lock and Dam 3 Guidewall extension.

Layer #	Soil Type	Equivalent Batter Elevation (ft)	σ'_v (psf)	δ' (deg)	$(f_s)_i$ (psf)	$(Q_s)_i$ (lb)
1	Riprap	0	0	38	0	5,070
		-5.15	400.8		313	
2	Medium-dense sand	-5.15	400.8	27	204	14,225
		-12.37	830.8		423	
3	Medium-dense sand	-12.37	830.8	27	423	109,377
		-35.05	2182.4		1112	
4	Medium-dense sand	-35.05	2182.4	27	1112	38,543
		-40.2	2489.5		1268	
5	Medium-dense sand	-40.2	2489.5	27	1268	52,941
		-46.38	2858.1		1456	
6	Medium-dense sand	-46.38	2858.1	27	1456	70,989
		-53.6	3288.2		1675	
7	Medium-dense sand	-53.6	3288.2	27	1675	

The unit tip capacity of the 24 in. diameter, closed-end pipe bearing on dense sand is computed to be 98,645 psf by Equation A.9, with N_q equal to 30 (Table A.2) and a limiting unit end bearing value of 150,000 psf (Table A.2). By Equation A.3, the tip resistance of the pile due to end bearing equals 309,903 lb. The ultimate pipe pile compression capacity equals 601,048 lb (Equation A.1) by the API (2000) guidelines. The end bearing provides 52% of the ultimate pipe pile capacity in this calculation. The ultimate tension pipe pile capacity equals 291,145 lb.

D.5 Axial capacity of the concrete-filled batter pile using Castello skin friction and tip capacity curves for cohesionless soils

Table D.5 summarizes the calculation of the skin friction capacity according to the Castello (1980) and Coyle and Castello (1981) sand curves of an equivalent vertical batter pile in medium-dense sand for a 4V:1H batter compression pile type configuration used at Lock and Dam 3 Guidewall extension. Recall the diameter of pile, D_p , is 2 ft. The ultimate skin friction resistance is computed to be 136,591 lb for the layered strata by Equation A.8 for piles in compression or in tension.

Table D.5. Ultimate skin friction capacity calculations according to the Castello sand curves of an equivalent vertical batter pile in medium-dense sand for a 4V:1H batter compression pile type configuration used at Lock and Dam 3 Guidewall extension.

Layer #	Soil Type	Equivalent Batter Elevation (ft)	Depth/ D_p	ϕ' (deg)	$(f_s)_i$ (psf)	$(Q_s)_i$ (lb)
1	Riprap	0	0	43	0	2,914
		-5.15	2.5		180	
2	Medium-dense sand	-5.15	2.5	32	180	9,067
		-12.37	6		380	
3	Medium-dense sand	-12.37	6	32	380	26,748
		-35.05	17		800	
4	Medium-dense sand	-35.05	17	32	800	26,878
		-40.2	19.5		860	
5	Medium-dense sand	-40.2	19.5	32	860	28,821
		-46.38	22.5		920	
6	Medium-dense sand	-46.38	22.5	32	920	42,162
		-53.6	26		940	
7	Medium-dense sand	-53.6	26	32	940	

The unit tip capacity of the 24 in. diameter closed-end pipe bearing on dense sand is computed to be 52,000 psf by Figure A.3 for a Depth/ D_p ratio equal to 26 and ϕ' equal to 32 degrees. By Equation A.3 the tip resistance of the pile due to end bearing equals 163,363 lb. The ultimate pipe pile capacity equals 299,954 lb (Equation A.1) using the Castello curves for the sand layer. The end bearing provides 54% of the ultimate pipe pile capacity in this calculation.

D.6 Axial capacity of the concrete-filled batter pile using CAXPILE software with the Soil criteria

Table D.6 summarizes the input data to a CAXPILE analysis with Soil criteria of an equivalent vertical batter pile in medium-dense sand for a 4V:1H batter compression pile type configuration used at Lock and Dam 3 Guidewall extension. The effective angle of the steel pipe pile-to-soil interface friction for the cohesionless layers is specified in the CAXPILE data input and set equal to 0.83 times the effective angle of internal friction of the soil (Table A.1). The ultimate skin friction resistance is computed to be 104,274 lb for the layered strata by CAXPILE using the Soil criteria for piles in compression or in tension. To compute the skin friction resistance, the CAXPILE Soil criteria uses the Castello (Castello 1980) curves for the sand layers and the Coyle and Reese (1966) curves for the clay and/or silt layers, if present.

Table D.6. Summary of CAXPILE, Soil criteria, input data for computing the ultimate skin friction capacity curves of an equivalent vertical batter pile in medium-dense sand for a 4V:1H batter compression pile type configuration used at Lock and Dam 3 Guidewall extension.

Layer #	Soil Type	Equivalent Batter Elevation (ft)	$\gamma_{\text{saturated}}$ (pcf)	ϕ' (deg)	δ' (deg)
1	Riprap	0	140.16	43	36
		-5.15			
2	Medium-dense sand	-5.15	122	32	27
		-12.37			
3	Medium-dense sand	-12.37	122	32	27
		-35.05			
4	Medium-dense sand	-35.05	122	32	27
		-40.2			
5	Medium-dense sand	-40.2	122	32	27
		-46.38			
6	Medium-dense sand	-46.38	122	32	27
		-53.6			
7	Medium-dense sand	-53.6	122	32	27

The tip resistance of the 24 in. diameter, closed-end pipe bearing on medium-dense sand (ϕ' equal to 32 degrees) is computed to be 241,467 lb by CAXPILE using the Soil criteria. The ultimate pipe pile capacity, Q_{ult} , equals 345,741 lb. The end bearing provides 70% of the ultimate pipe pile

capacity according to the CAXPILE Soil criteria computation. The ultimate tension pipe pile capacity equals 104,274 lb.

The CAXPILE Soil criteria output was processed into C_{33} data using Equation 2.8:

$$C_{33} = \frac{P_A / w_A}{A * E / L_e} \quad (2.8 \text{ bis})$$

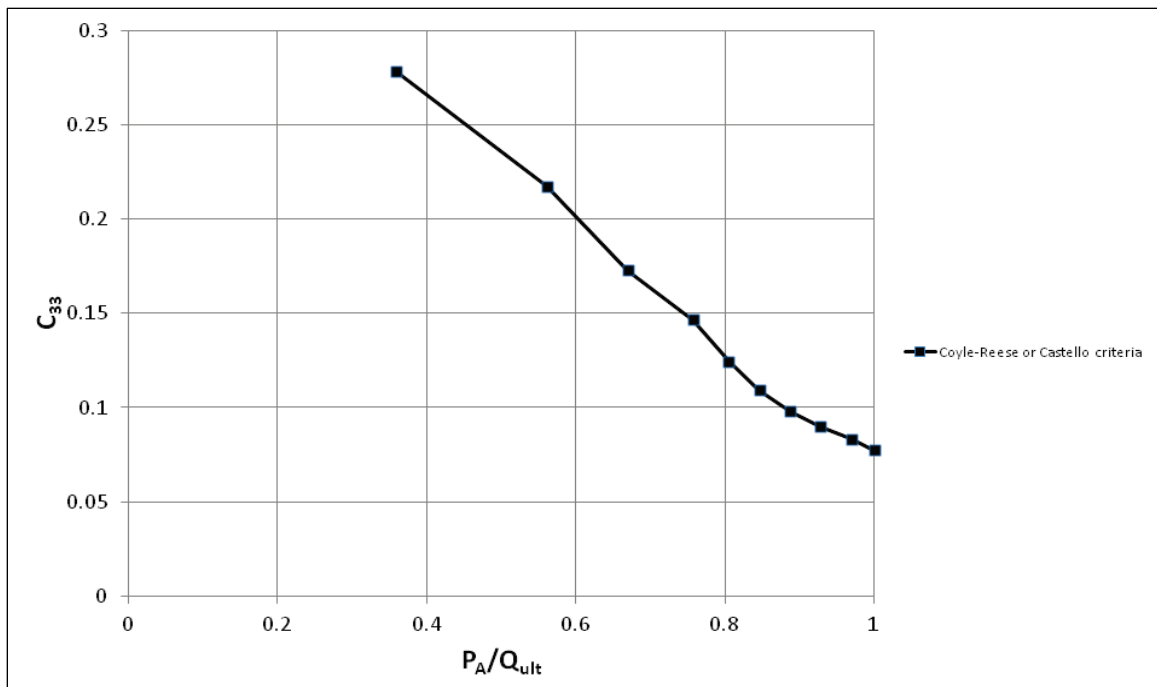
with P_A designating the applied compression load, w_A designating the displacement of the top of pile (at its start of embedment elevation), A designating the cross-sectional area of the concrete-filled pipe pile, E designating its (composite) Young's Modulus, and L_e being the length of pile embedment. The three terms A , E , and L_e are constants; the cross-sectional area of the concrete-filled pipe pile is 452.4 in.² by Equation B.1; the composite Young's Modulus is 5,124,000 psi by Equation B.12; and the length of embedded pile L_e , is 53.6 ft.

Because of the nonlinear response to increasing axial load, the C_{33} term is found to be a function of the magnitude of axial load P_A applied to the pile. In Figure D.1, P_A is being expressed as a fraction of the ultimate pile resistance, Q_{ult} , along the horizontal axis of the C_{33} versus $[P_A/Q_{ult}]$ CAXPILE output data. Recall Q_{ult} equals 345,741 lb for the CAXPILE Soil criteria. Figure D.1 shows the magnitude of C_{33} to be less than 1.0, and the value of C_{33} decreases as the capacity of the 24 in. diameter, batter pipe pile is mobilized. At one-half the ultimate pile capacity, C_{33} is approximately 0.24, and at full mobilization of its capacity, C_{33} is 0.08.

D.7 Axial capacity of the concrete-filled batter pile using CAXPILE software with the WES criteria

Table D.7 summarizes the input data to a CAXPILE analysis with WES criteria of an equivalent vertical batter pile in medium-dense sand for a 4V:1H batter compression pile type configuration used at Lock and Dam 3 Guidewall extension. The effective angle of the steel pipe pile-to-soil interface friction for the cohesionless foundation is set equal to 0.83 times the effective angle of internal friction of the soil (Table A.1). The ultimate skin friction resistance is computed to be 92,230 lb for the medium-dense sand strata by CAXPILE using the WES criteria for piles in compression or in tension.

Figure D.1. C_{33} versus axial load expressed as a fraction of the axial capacity of an equivalent vertical batter pile in medium-dense sand for a 4V:1H batter compression pile type configuration used at Lock and Dam 3 Guidewall extension computed using the CAXPILE Soil criteria.



The tip resistance of the 24 in. diameter, closed-end pipe bearing on dense sand (ϕ' equal to 32 degrees) is computed to be 317,147 lb by CAXPILE using the WES criteria. The ultimate pipe pile capacity equals 409,377 lb. The end bearing provides 77% of the ultimate pipe pile capacity according to the CAXPILE WES criteria computation.

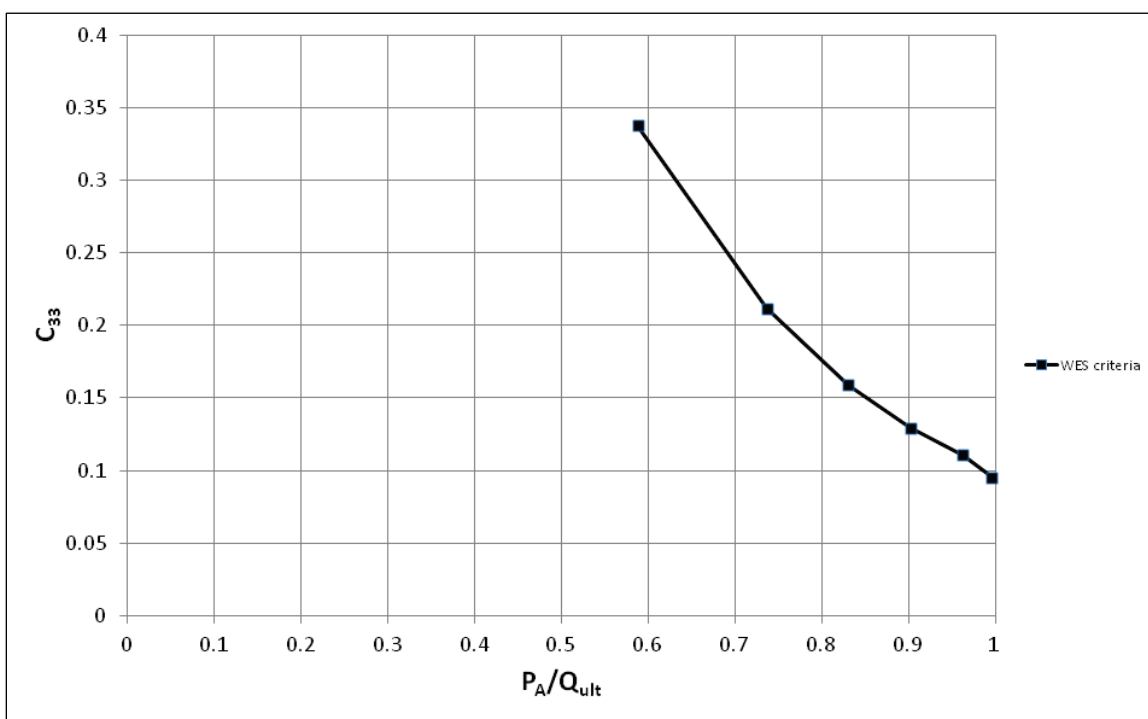
Table D.7. Summary of CAXPILE, WES criteria, input data for computing the ultimate skin friction capacity curves of an equivalent vertical batter pile in medium-dense sand for a 4V:1H batter compression pile type configuration used at Lock and Dam 3 Guidewall extension.

Layer #	Soil Type	Equivalent Batter Elevation (ft)	$\gamma_{saturated}$ (pcf)	ϕ' (deg)	δ' (deg)
1	Riprap	0	140.16	43	36
		-5.15			
2	Medium-dense sand	-5.15	122	32	27
		-12.37			
3	Medium-dense sand	-12.37	122	32	27
		-35.05			
4	Medium-dense sand	-35.05	122	32	27
		-40.2			
5	Medium-dense sand	-40.2	122	32	27
		-46.38			

Layer #	Soil Type	Equivalent Batter Elevation (ft)	$\gamma_{\text{saturated}}$ (pcf)	ϕ' (deg)	δ' (deg)
6	Medium-dense sand	-46.38	122	32	27
		-53.6			
7	Medium-dense sand	-53.6	122	32	27

The CAXPILE WES criteria output was processed into C_{33} data using Equation 2.8 (with A equal to 452.4 in² [Equation B.1], a Young's Modulus of 5,124,000 psi [Equation B.12] and the length of embedded pile L_e , of 53.6 ft) and presented in Figure D.2 as a function of $[P_A/Q_{\text{ult}}]$. Recall Q_{ult} equals 409,377 lb for the CAXPILE WES criteria. Figure D.2 shows the magnitude of C_{33} to be less than 1.0, and the value of C_{33} decreases as the capacity of the 24 in. diameter, batter pipe pile is mobilized. At one-half the ultimate pile capacity, C_{33} is approximated to be equal to 0.4 and at full mobilization of its capacity, C_{33} is 0.1.

Figure D.2. C_{33} versus axial load expressed as a fraction of the axial capacity of an equivalent vertical batter pile in medium-dense sand for a 4V:1H batter compression pile type configuration used at Lock and Dam 3 Guidewall extension computed using the CAXPILE WES criteria.



D.8 Axial capacity of the concrete-filled batter pile using CAXPILE software with the VJ criteria

Table D.8 summarizes the input data to a CAXPILE analysis with VJ criteria of an equivalent vertical batter pile in medium-dense sand for a 4V:1H batter compression pile type configuration used at Lock and Dam 3 Guidewall extension. The values for ultimate skin friction used as input to CAXPILE are calculated following API (2000) guidelines. Calculation of the horizontal effective stress, σ'_h , is based on Equation A.4 and a horizontal earth pressure coefficient, K_h , value of 1 for all soil layers for a closed-end, driven pipe pile. The effective angle of the steel pipe pile-to-soil interface friction for the cohesionless layers is set equal to 27 degrees (Table A.2). The ultimate skin friction resistance is computed to be 290,565 lb for the medium-dense sand site by CAXPILE using the VJ criteria for piles in compression or in tension. The parameter z_c is set equal to 0.25 in. in the VJ criteria input for all soils based on the guidance provided in Vijayvergia (1977). This recommendation for the value to be assigned to z_c is also given in Heydinger (1987).

Table D.8. Summary of CAXPILE, VJ criteria, input data for computing the ultimate skin friction capacity curves of an equivalent vertical batter pile in medium-dense sand for a 4V:1H batter compression pile type configuration used at Lock and Dam 3 Guidewall extension.

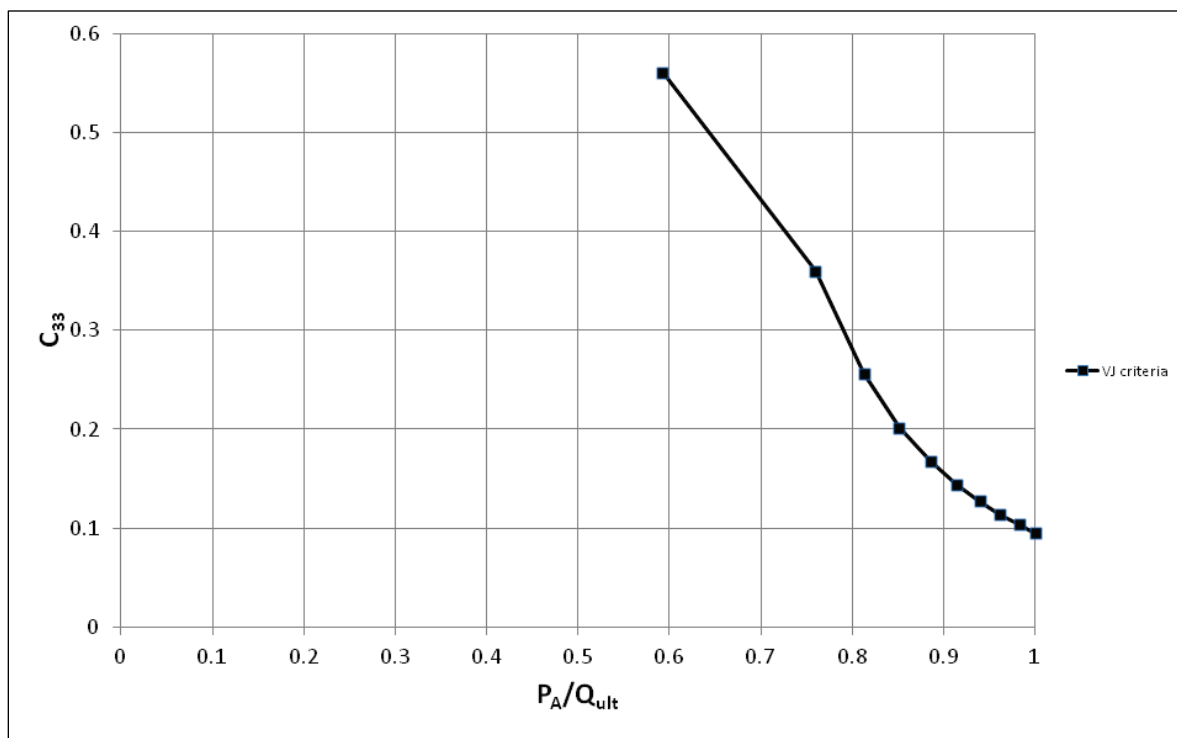
Layer #	Soil Type	Equivalent Batter Elevation (ft)	σ'_v (psf)	δ' (deg)	$(f_s)_i$ (psf)	z_c (in.)
1	Riprap	0	0	38	0	0.25
		-5.15	400.8		313	0.25
2	Medium-dense sand	-5.15	400.8	27	204	0.25
		-12.37	821.1		423	0.25
3	Medium-dense sand	-12.37	821.1	27	423	0.25
		-35.05	1957.4		1112	0.25
4	Medium-dense sand	-35.05	1957.4	27	1112	0.25
		-40.2	2260.2		1268	0.25
5	Medium-dense sand	-40.2	2260.2	27	1268	0.25
		-46.38	2570.1		1456	0.25
6	Medium-dense sand	-46.38	2570.1	27	1456	0.25
		-53.6	3006.5		1675	0.25
7	Medium-dense sand	-53.6	3006.5	27	1675	0.25

The unit tip capacity of the 24 in. diameter, closed-end pipe bearing on medium-dense sand is computed to be 98,645 psf by Equation A.9, with N_q equal to 30 (Table A.2) and a limiting unit end bearing value of

150,000 psf (Table A.2). The tip resistance of the 24 in. diameter, closed-end pipe bearing on dense sand (ϕ' equal to 32 degrees) is computed to be 309,903 lb by CAXPILE using the VJ criteria. The tip movement parameter z_t for use in the SSI calculations made at the pile tip is set equal to 1.6 in. in the VJ criteria. This value for z_t is based on the average of the data provided in Table 2 of Vijayvergia (1977); z_t is approximately 0.065 times the diameter of the pile tip bearing on sands. The ultimate pipe pile capacity equals 601,048 lb. The end bearing provides 52% of the ultimate pipe pile capacity according to the CAXPILE VJ criteria computation.

The CAXPILE VJ criteria output was processed into C_{33} data using Equation 2.8 (with A equal to 452.4 in.² [Equation B.1], a Young's Modulus of 5,124,000 psi [Equation B.12] and the length of embedded pile L_e , of 53.6 ft) and presented in Figure D.3 as a function of $[P_A/Q_{ult}]$. Recall Q_{ult} equals 601,048 lb for the CAXPILE VJ criteria. Figure D.3 shows the magnitude of C_{33} to be less than 1.0, and the value of C_{33} decreases as the capacity of the 24 in. diameter, batter pipe pile is mobilized. At one-half the ultimate pile capacity, C_{33} is estimated to be 0.66, and at full mobilization of its capacity, C_{33} is 0.1.

Figure D.3. C_{33} versus axial load expressed as a fraction of the axial capacity of an equivalent vertical batter pile in medium-dense sand for a 4V:1H batter compression pile type configuration used at Lock and Dam 3 Guidewall extension computed using the CAXPILE VJ criteria.



Appendix E: Axial Capacity of Lock and Dam 3 Concrete-Filled Batter Pile Founded in Dense Sand and Evaluation of the Value of the CPGA C_{33} Term

E.1 Introduction

This appendix continues the Appendix C investigation of axial batter pile capacity and appropriate value(s) for the axial stiffness modifier term C_{33} for use in pushover analyses of batter pile group configured flexible approach walls. This appendix summarizes the second series of six analyses in a parametric investigation study of the influence that the density of cohesionless soil comprising the foundation has on the magnitude of the C_{33} term. This parametric investigation made use of the Figure 1.2 Lock and Dam 3 batter pile geometry but founded in homogenous dense sand. Recall that the actual foundation is a layered soil site consisting of sands of different densities, silts, and clays (Figure C.1). The 5 ft of riprap on top of the foundation soil is maintained in this parametric model. All pile geometry is the same as was discussed in Appendix C.

Six axial capacity calculations were made for a concrete-filled batter pipe under axial compression of the Lock and Dam 3 pile group configuration founded in dense sand. One set of three hand calculations was made for its axial compression capacity following EM 1110-2-2906 (HQUSACE 1991) guidance, API (2000) guidelines, and the Castello (1980) and Coyle and Castello (1981) curves for skin friction and tip resistance for cohesionless soils. The second set of three pile compression capacity calculations was made using the CASE software CAXPILE (Dawkins 1984) with the Soil criteria, the WES criteria, and the VJ criteria. Additionally, data generated by these three CAXPILE analyses provide a basis for determining the value of the C_{33} term to be used for batter piles founded in dense sand in a CPGA (Hartman et al. 1989) software analysis of the Figure 1.2 batter pile groups.

Hand calculations for the pile-to-soil tension capacity calculations are also reported in this appendix. Recall that for a pipe pile being subjected to tension loading, the tip resistance of the pile due to end bearing is not engaged.

E.2 Engineering property characterization for a dense sand foundation

The engineering material properties of the 5 ft of riprap (el 650 to 655) and a hypothetical dense foundation sand are listed in Table E.1. The top of riprap is at el 655. All elevations mirror those discussed in Appendix C for a Figure 1.2 batter pile group configuration.

Table E.1. Engineering material properties for the riprap and dense sand foundation.

Soil Type	Unified Soil Classification System	$\gamma_{\text{sat}}_{\text{urated}}$		γ_{buoyant}		ϕ (deg)
		(pcf)	(pci)	(pcf)	(pci)	
Riprap	GP	140.16	0.081	77.76	0.045	43
Dense sand	SP	127	0.073	64.6	0.037	36

Table E.2 summarizes the calculation of the effective vertical stress, σ'_v , for select, equivalent batter elevations within the hypothetical dense sand foundation for a 4V:1H batter pile configuration like that used at the Lock and Dam 3 Guidewall extension. These elevations facilitate the axial capacity evaluation of the 4V:1H batter pile. The elevations at which these computations are made mirror those listed in Table C.3 for the seven soil layer boundaries found at the Lock and Dam 3 site. The layer numbers are maintained in this appendix for bookkeeping purposes and to conveniently relate back to Appendix C information.

Table E.2. Summary of the distribution of effective vertical stresses with elevation of an equivalent vertical batter pile in dense sand for a 4V:1H batter compression pile type configuration used at Lock and Dam 3 Guidewall extension.

Layer #	Soil Type	Vertical Depth		Equivalent Batter Length (in.)	Equivalent Batter Elevation		γ_{buoyant}		σ'_v	
		(ft)	(in.)		(ft)	(in.)	(pcf)	(pci)	(psf)	(psi)
1	Riprap	0	0	0	0	0	77.76	0.045	0	0
		5	60	61.8	-5.15	-61.9			400.8	2.78
2	Dense sand	5	60	61.8	-5.15	-61.9	64.6	0.037	400.8	2.78
		12	144	148.4	-12.37	-148.4			866.9	6.02
3	Dense sand	12	144	148.4	-12.37	-148.4	64.6	0.037	866.9	6.02
		34	408	420.6	-35.05	-420.6			2331.8	16.19
4	Dense sand	34	408	420.6	-35.05	-420.6	64.6	0.037	2331.8	16.19
		39	468	482.4	-40.2	-482.4			2664.8	18.51
5	Dense sand	39	468	482.4	-40.2	-482.4	64.6	0.037	2664.8	18.51
		45	540	556.6	-46.38	-556.6			3064.3	21.28
6	Dense sand	45	540	556.6	-46.38	-556.6	64.6	0.037	3064.3	21.28
		52	624	643.2	-53.6	-643.2			3530.4	24.52
7	Dense sand	52	624	643.2	-53.6	-643.2	64.6	0.037	3530.4	24.52

E.3 Axial capacity of the concrete-filled batter pile following EM 1110-2-2906 guidance

Table E.3 summarizes the EM 1110-2-2906 (HQUSACE 1991) based calculation of the skin friction capacity of an equivalent vertical batter pile in dense sand for a 4V:1H batter compression pile type configuration used at Lock and Dam 3 Guidewall extension. The critical depth, D_c , is set equal to 40 ft. This depth corresponds to 20 times the pile diameter, D_p , of 2 ft for a dense sand (Table A.4). Calculation of the horizontal effective stress, σ'_h , is based on a horizontal earth pressure coefficient, K_h , value of 1 for all soil layers for a closed-end, driven pipe pile (Table A.3) and effective vertical stresses according to Equations A.5 and A.6. The vertical effective stress (used in the σ'_h computation) is restricted to being a value less than approximately 2,665 psf. This value for effective overburden corresponds to the critical depth (D_c). The effective angle of the steel pipe pile-to-soil interface friction for the cohesionless layers is set equal to 0.83 times the effective angle of internal friction of the soil (Table A.1). The ultimate skin friction resistance is computed to be 327,495 lb for a batter pile under axial compression in a homogenous dense sand by Equation A.8. Equation A.4 is used in these computations for the unit skin resistances, $(f_s)_i$, for the sand layers.

Table E.3. Ultimate skin friction capacity calculations according to EM 1110-2-2906 (HQUSACE 1991) of an equivalent vertical batter pile in dense sand for a 4V:1H batter compression pile type configuration used at Lock and Dam 3 Guidewall extension.

Layer #	Soil Type	Equivalent Batter Elevation (ft)	σ'_v (psf)	$\sigma'_v < (\gamma_{buoy} * D_c)$ (psf)	δ' (deg)	$(f_s)_i$ (psf)	$(Q_s)_i$ (lb)
1	Riprap	0	0	0	36	0	4,661
		-5.15	400.8	400.8		288	
2	Dense sand	-5.15	400.8	400.8	30	230	16,510
		-12.37	866.9	866.9		498	
3	Dense sand	-12.37	866.9	866.9	30	498	130,933
		-35.05	2331.8	2331.8		1340	
4	Dense sand	-35.05	2331.8	2331.8	30	1340	46,483
		-40.2	2664.8	2664.8		1531	
5	Dense Sand	-40.2	2664.8	2664.8	30	1531	59,496
		-46.38	3064.3	2664.8		1531	
6	Dense sand	-46.38	3064.3	2664.8	30	1531	69,412
		-53.6	3530.4	2664.8		1531	
7	Dense sand	-53.6	3530.4	2664.8	30	1531	

The unit tip capacity of the 24 in. diameter, closed-end pipe bearing on dense sand is computed to be 106,591 psf by Equation A.9, with N_q equal to 40 and using a limiting value for σ'_v set equal to approximately 2,665 psf ($\sigma'_v < (\gamma_{\text{buoy}} * D_c)$, with D_c equal to 40 ft). By Equation A.3, the tip resistance of the pile due to end bearing equals 334,864 lb. The ultimate pipe pile capacity equals 662,359 lb (Equation A.1) by the EM 1110-2-2906 (HQUSACE 1991) design criteria. The end bearing provides 51% of the ultimate pipe pile capacity in this calculation.

EM 1110-2-2906 (HQUSACE 1991) suggests a value for the horizontal earth pressure coefficient, K_h , of 0.7 for tension piles in sand and silt strata (Table A.3) when computing effective vertical stresses by Equations A.5 and A.6. A K_h value of 0.7 is lower than the K_h value of 1 used for the piles axial compression calculation. The ultimate skin friction resistance is computed to be 229,247 lb for a tension batter pile in the layered soil strata.

E.4 Axial capacity of the concrete-filled batter pile following API (2000) guidelines

Table E.4 summarizes the calculation of the skin friction capacity according to API guidelines of an equivalent vertical batter pile in dense sand for a 4V:1H batter compression pile type configuration used at Lock and Dam 3 Guidewall extension. Calculation of the horizontal effective stress, σ'_h , is based on Equation A.4 and a horizontal earth pressure coefficient, K_h , value of 1 for all soil layers for a closed-end, driven pipe pile. The effective angle of the steel pipe pile-to-soil interface friction for the cohesionless layers is set equal to the effective angle of internal friction of the dense sand is set equal to 31 degrees (Table A.2). The ultimate skin friction resistance is computed to be 364,095 lb by Equation A.8 for piles in compression or in tension. Equation A.4 is used in these computations for unit skin friction values of $(f_s)_i$ for the sand layers. The $(f_s)_i$ for the sand layers are all below the Table A.2 limiting skin friction value of 2,100 psf.

Table E.4. Ultimate skin friction capacity calculations according to API (2000) guidelines of an equivalent vertical batter pile in dense sand for a 4V:1H batter compression pile type configuration used at Lock and Dam 3 Guidewall extension.

Layer #	Soil Type	Equivalent Batter Elevation (ft)	σ'_v (psf)	δ' (deg)	$(f_s)_i$ (psf)	$(Q_s)_i$ (lb)
1	Riprap	0	0	38	0	5,070
		-5.15	400.8		313	
2	Dense sand	-5.15	400.8	31	241	17,266
		-12.37	866.9		521	

Layer #	Soil Type	Equivalent Batter Elevation (ft)	σ'_v (psf)	δ' (deg)	$(f_s)_i$ (psf)	$(Q_s)_i$ (lb)
3	Dense sand	-12.37	866.9	31	521	136,926
		-35.05	2331.8		1401	
4	Dense sand	-35.05	2331.8	31	1401	48,611
		-40.2	2664.8		1601	
5	Dense sand	-40.2	2664.8	31	1601	66,884
		-46.38	3064.3		1841	
6	Dense sand	-46.38	3064.3	31	1841	89,339
		-53.6	3530.4		2100	
7	Dense sand	-53.6	3530.4	31	2100	

The unit tip capacity of the 24 in. diameter, closed-end pipe bearing on dense sand is computed to be 148,277 psf by Equation A.9, with N_q equal to 42 (Table A.2) and a limiting unit end bearing value of 210,000 psf (Table A.2). By Equation A.3, the tip resistance of the pile due to end bearing equals 465,827 lb. The ultimate pipe pile axial compression capacity equals 829,922 lb (Equation A.1) by the API (2000) guidelines. The end bearing provides 56% of the ultimate pipe pile capacity in this calculation. The ultimate tension pipe pile capacity equals 364,095 lb.

E.5 Axial capacity of the concrete-filled batter pile using Castello skin friction and tip capacity curves for cohesionless soils

Table E.5 summarizes the calculation of the skin friction capacity according to the Castello (1980) and Coyle and Castello (1981) sand curves of an equivalent vertical batter pile in dense sand for a 4V:1H batter compression pile type configuration used at Lock and Dam 3 Guidewall extension. Recall the diameter of pile, D_p , is 2 ft. The ultimate skin friction resistance is computed to be 267,288 lb for the layered strata by Equation A.8 for piles in compression or in tension.

Table E.5. Ultimate skin friction capacity calculations according to the Castello sand curves of an equivalent vertical batter pile in dense sand for a 4V:1H batter compression pile type configuration used at Lock and Dam 3 Guidewall extension.

Layer #	Soil Type	Equivalent Batter Elevation (ft)	Depth/ D_p	ϕ' (deg)	$(f_s)_i$ (psf)	$(Q_s)_i$ (lb)
1	Riprap	0	0	43	0	6,315
		-5.15	2.5		390	
2	Dense sand	-5.15	6	36	390	19,268
		-12.37	6		800	

Layer #	Soil Type	Equivalent Batter Elevation (ft)	Depth/ D_p	ϕ' (deg)	$(f_s)_i$ (psf)	$(Q_s)_i$ (lb)
3	Dense sand	-12.37	17	36	800	53,496
		-35.05	17		1560	
4	Dense sand	-35.05	19.5	36	1560	52,298
		-40.2	19.5		1670	
5	Dense sand	-40.2	22.5	36	1670	55,213
		-46.38	22.5		1740	
6	Dense sand	-46.38	26	36	1740	80,698
		-53.6	26		1820	
7	Dense sand	-53.6	26	36	1820	

The unit tip capacity of the 24 in. diameter, closed-end pipe bearing on dense sand is computed to be 136,000 psf by Figure A.3 for a Depth/ D_p ratio equal to 26 and ϕ' equal to 36 degrees. By Equation A.3, the tip resistance of the pile due to end bearing equals 427,257 lb. The ultimate pipe pile capacity equals 694,545 lb (Equation A.1) using the Castello curves for the sand layer. The end bearing provides 62% of the ultimate pipe pile capacity in this calculation.

E.6 Axial capacity of the concrete-filled batter pile using CAXPILE software with the Soil criteria

Table E.6 summarizes the input data to a CAXPILE analysis with Soil criteria of an equivalent vertical batter pile in dense sand for a 4V:1H batter compression pile type configuration used at Lock and Dam 3 Guidewall extension. The effective angle of the steel pipe pile-to-soil interface friction for the cohesionless layers is specified in the CAXPILE data input and set equal to 0.83 times the effective angle of internal friction of the soil (Table A.1). The ultimate skin friction resistance is computed to be 103,363 lb for the layered strata by CAXPILE using the Soil criteria for piles in compression or in tension. To compute the skin friction resistance, the CAXPILE Soil criteria uses the Castello (1980) curves for the sand layers and the Coyle and Reese (1966) curves for the clay and/or silt layers, if present.

Table E.6. Summary of CAXPILE, Soil criteria, input data for computing the ultimate skin friction capacity curves of an equivalent vertical batter pile in dense sand for a 4V:1H batter compression pile type configuration used at Lock and Dam 3 Guidewall extension.

Layer #	Soil Type	Equivalent Batter Elevation (ft)	$\gamma_{\text{sat}} (\text{pcf})$	$\phi' (\text{deg})$	$\delta' (\text{deg})$
1	Riprap	0	140.16	43	36
		-5.15			
2	Dense sand	-5.15	127	36	30
		-12.37			
3	Dense sand	-12.37	127	36	30
		-35.05			
4	Dense sand	-35.05	127	36	30
		-40.2			
5	Dense sand	-40.2	127	36	30
		-46.38			
6	Dense sand	-46.38	127	36	30
		-53.6			
7	Dense sand	-53.6	127	36	30

The tip resistance of the 24 in. diameter closed-end pipe bearing on dense sand (ϕ' equal to 36 degrees) is computed to be 528,658 lb by CAXPILE using the Soil criteria. The ultimate pipe pile capacity, Q_{ult} , equals 632,021 lb. The end bearing provides 84% of the ultimate pipe pile capacity according to the CAXPILE Soil criteria computation. The ultimate tension pipe pile capacity equals 103,363 lb.

The CAXPILE Soil criteria output was processed into C_{33} data using Equation 2.8:

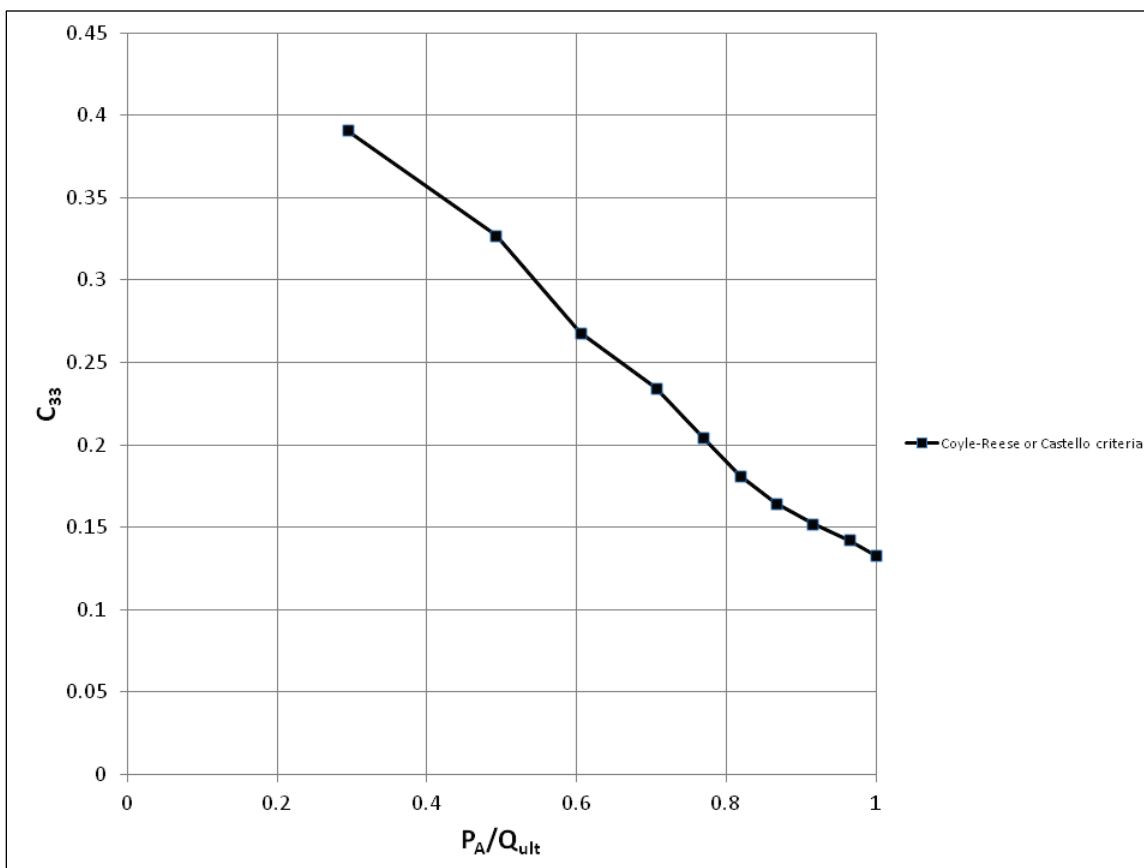
$$C_{33} = \frac{P_A / w_A}{A * E / L_e} \quad (2.8 \text{ bis})$$

with P_A designating the applied compression load, w_A designating the displacement of the top of pile (at its start of embedment elevation), A designating the cross-sectional area of the concrete-filled pipe pile, E designating its (composite) Young's Modulus, and L_e being the length of pile embedment. The three terms A , E , and L_e are constants; the cross-sectional area of the concrete-filled pipe pile is 452.4 in.² by Equation B.1;

the composite Young's Modulus is 5,124,000 psi by Equation B.12; and the length of embedded pile L_e , is 53.6 ft.

Because of the nonlinear response to increasing axial load, the C_{33} term is found to be a function of the magnitude of axial load P_A applied to the pile. In Figure E.1, P_A is being expressed as a fraction of the ultimate pile resistance, Q_{ult} , along the horizontal axis of the C_{33} versus $[P_A/Q_{ult}]$ CAXPILE output data. Recall Q_{ult} equals 632,021 lb for the CAXPILE Soil criteria. Figure E.1 shows the magnitude of C_{33} to be less than 1.0, and the value of C_{33} decreases as the capacity of the 24 in. diameter, batter pipe pile is mobilized. At one-half the ultimate pile capacity, C_{33} is approximately 0.33, and at full mobilization of its capacity, C_{33} is 0.13.

Figure E.1. C_{33} versus axial load expressed as a fraction of the axial capacity of an equivalent vertical batter pile in dense sand for a 4V:1H batter compression pile type configuration used at Lock and Dam 3 Guidewall extension computed using the CAXPILE Soil criteria.



E.7 Axial capacity of the concrete-filled batter pile using CAXPILE software with the WES criteria

Table E.7 summarizes the input data to a CAXPILE analysis with WES criteria of an equivalent vertical batter pile in dense sand for a 4V:1H batter compression pile type configuration used at Lock and Dam 3 Guidewall extension. The effective angle of the steel pipe pile-to-soil interface friction for the cohesionless foundation is set equal to 0.83 times the effective angle of internal friction of the soil (Table A.1). The ultimate skin friction resistance is computed to be 101,329 lb for the dense sand strata by CAXPILE using the WES criteria for piles in compression or in tension.

Table E.7. Summary of CAXPILE, WES criteria, input data for computing the ultimate skin friction capacity curves of an equivalent vertical batter pile in dense sand for a 4V:1H batter compression pile type configuration used at Lock and Dam 3 Guidewall extension.

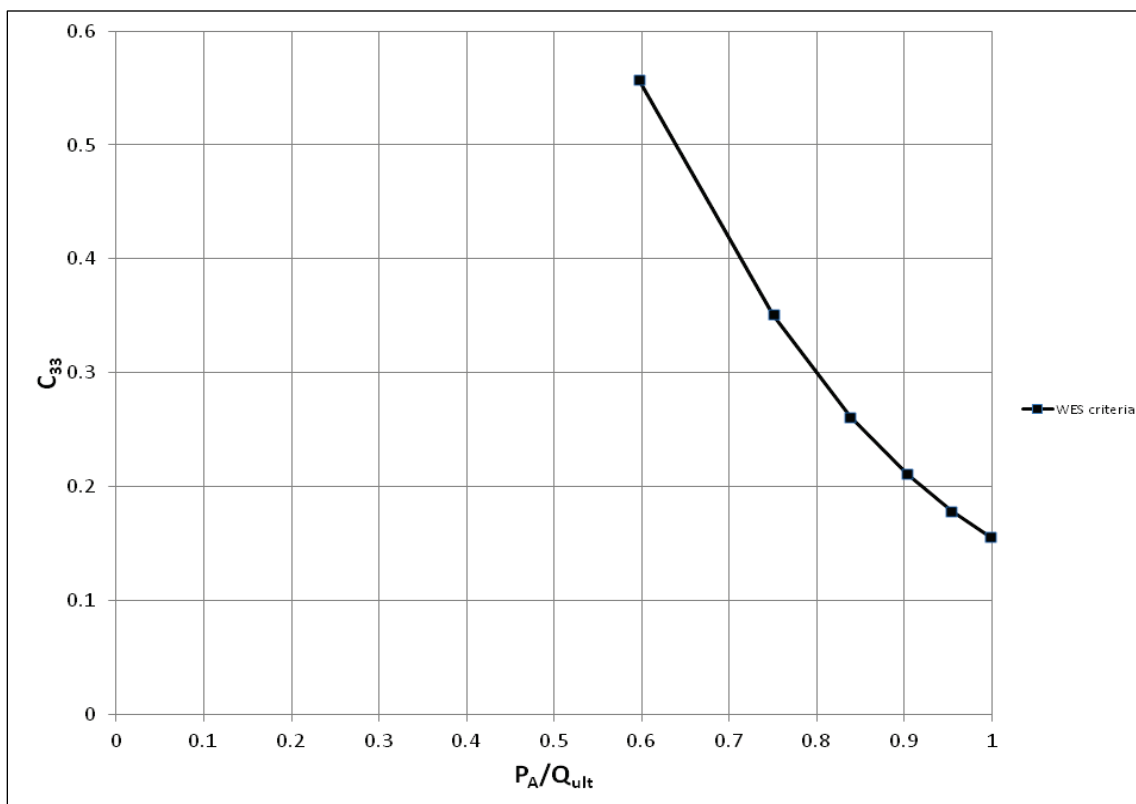
Layer #	Soil Type	Equivalent Batter Elevation (ft)	$\gamma_{\text{sat}} (\text{pcf})$	$\phi' (\text{deg})$	$\delta' (\text{deg})$
1	Riprap	0	140.16	43	36
		-5.15			
2	Dense sand	-5.15	127	36	30
		-12.37			
3	Dense sand	-12.37	127	36	30
		-35.05			
4	Dense sand	-35.05	127	36	30
		-40.2			
5	Dense sand	-40.2	127	36	30
		-46.38			
6	Dense sand	-46.38	127	36	30
		-53.6			
7	Dense sand	-53.6	127	36	30

The tip resistance of the 24 in. diameter, closed-end pipe bearing on dense sand (ϕ' equal to 36 degrees) is computed to be 566,208 lb by CAXPILE using the WES criteria. The ultimate pipe pile capacity equals 667,537 lb. The end bearing provides 85% of the ultimate pipe pile capacity according to the CAXPILE WES criteria computation.

The CAXPILE WES criteria output was processed into C_{33} data using Equation 2.8 (with A equal to 452.4 in.² [Equation B.1], a Young's Modulus of 5,124,000 psi [Equation B.12] and the length of embedded pile

L_e , of 53.6 ft) and presented in Figure E.2 as a function of $[P_A/Q_{ult}]$. Recall Q_{ult} equals 667,537 lb for the CAXPILE WES criteria. Figure E.2 shows the magnitude of C_{33} to be less than 1.0, and the value of C_{33} decreases as the capacity of the 24 in. diameter, batter pipe pile is mobilized. At one-half the ultimate pile capacity, C_{33} is approximated to be equal to 0.69, and at full mobilization of its capacity, C_{33} is 0.15.

Figure E.2. C_{33} versus axial load expressed as a fraction of the axial capacity of an equivalent vertical batter pile in dense sand for a 4V:1H batter compression pile type configuration used at Lock and Dam 3 Guidewall extension computed using the CAXPILE WES criteria.



E.8 Axial capacity of the concrete-filled batter pile using CAXPILE software with the VJ criteria

Table E.8 summarizes the input data to a CAXPILE analysis with VJ criteria of an equivalent vertical batter pile in dense sand for a 4V:1H batter compression pile type configuration used at Lock and Dam 3 Guidewall extension. The values for ultimate skin friction used as input to CAXPILE are calculated following to API (2000) guidelines. Calculation of the horizontal effective stress, σ'_h , is based on Equation A.4 and a horizontal earth pressure coefficient, K_h , value of 1 for all soil layers for a closed-end, driven pipe pile. The effective angle of the steel pipe pile-to-

soil interface friction for the cohesionless layers is set equal to 31 degrees (Table A.2). The ultimate skin friction resistance is computed to be 363,424 lb for the dense sand site by CAXPILE using the VJ criteria for piles in compression or in tension. The parameter z_c is set equal to 0.25 in. in the VJ criteria input for all soils based on the guidance provided in Vijayvergia (1977). This recommendation for the value to be assigned to z_c is also given in Heydinger (1987).

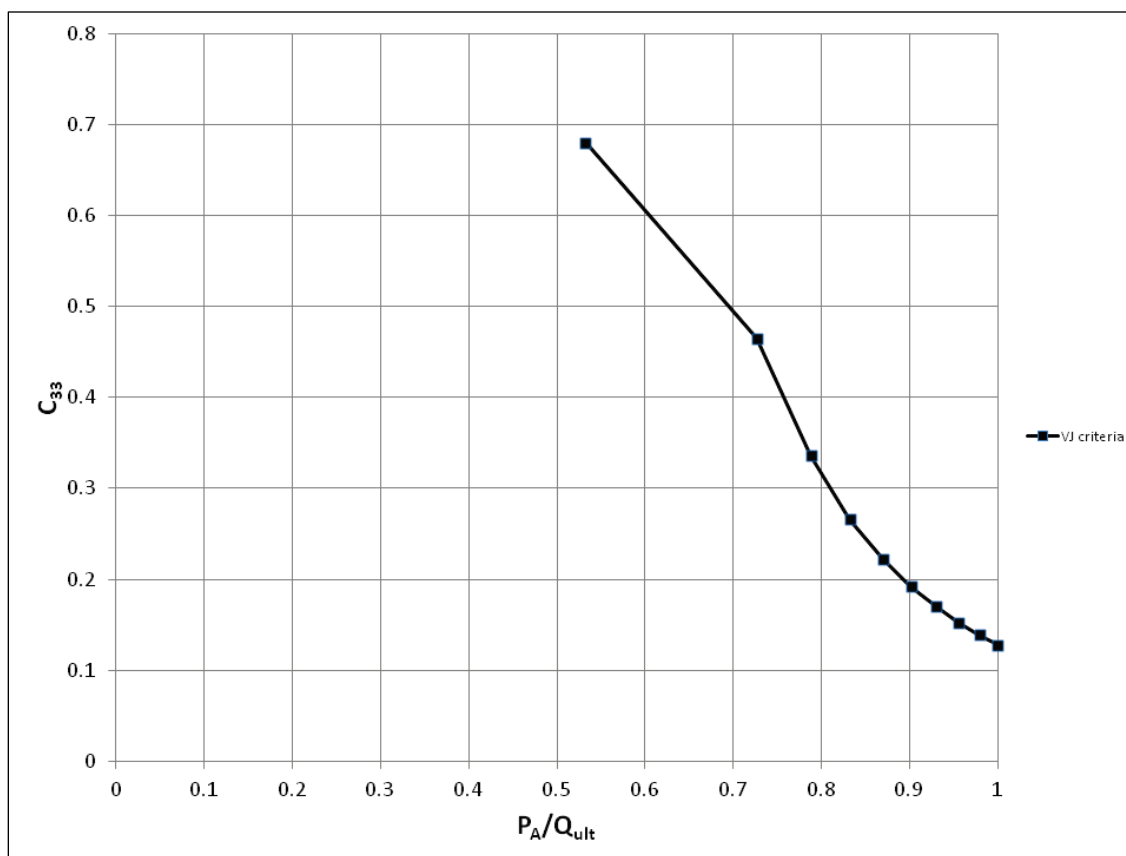
Table E.8. Summary of CAXPILE, VJ criteria, input data for computing the ultimate skin friction capacity curves of an equivalent vertical batter pile in dense sand for a 4V:1H batter compression pile type configuration used at Lock and Dam 3 Guidewall extension.

Layer #	Soil Type	Equivalent Batter Elevation (ft)	σ'_v (psf)	δ' (deg)	$(f_s)_i$ (psf)	z_c (in.)
1	Riprap	0	0	38	0	0.25
		-5.15	400.8		313	0.25
2	Dense sand	-5.15	400.8	31	241	0.25
		-12.37	866.9		521	0.25
3	Dense sand	-12.37	866.9	31	521	0.25
		-35.05	2331.8		1401	0.25
4	Dense sand	-35.05	2331.8	31	1401	0.25
		-40.2	2664.8		1601	0.25
5	Dense sand	-40.2	2664.8	31	1601	0.25
		-46.38	3064.3		1841	0.25
6	Dense sand	-46.38	3064.3	31	1841	0.25
		-53.6	3530.4		2100	0.25
7	Dense sand	-53.6	3530.4	31	2100	0.25

The unit tip capacity of the 24 in. diameter, closed-end pipe bearing on dense sand is computed to be 148,277 psf by Equation A.9, with N_q equal to 42 (Table A.2) and a limiting unit end bearing value of 210,000 psf (Table A.2). The tip resistance of the 24 in. diameter, closed-end pipe bearing on dense sand (ϕ' equal to 36 degrees) is computed to be 465,837 lb by CAXPILE using the VJ criteria. The tip movement parameter z_t for use in the SSI calculations made at the pile tip is set equal to 1.6 in. in the VJ criteria. This value for z_t is based on the average of the data provided in Table 2 of Vijayvergia (1977); z_t is approximately 0.065 times the diameter of the pile tip bearing on sands. The ultimate pipe pile capacity equals 829,261 lb. The end bearing provides 59% of the ultimate pipe pile capacity according to the CAXPILE VJ criteria computation.

The CAXPILE VJ criteria output was processed into C_{33} data using Equation 2.8 (with A equal to 452.4 in² [Equation B.1]), a Young's Modulus of 5,124,000 psi [Equation B.12] and the length of embedded pile L_e , of 53.6 ft) and presented in Figure E.3 as a function of $[P_A/Q_{ult}]$. Recall Q_{ult} equals 829,261 lb for the CAXPILE VJ criteria. Figure E.3 shows the magnitude of C_{33} to be less than 1.0, and the value of C_{33} decreases as the capacity of the 24 in. diameter, batter pipe pile is mobilized. At one-half the ultimate pile capacity, C_{33} is estimated to be approximately 0.71, and at full mobilization of its capacity, C_{33} is 0.13.

Figure E.3. C_{33} versus axial load expressed as a fraction of the axial capacity of an equivalent vertical batter pile in dense sand for a 4V:1H batter compression pile type configuration used at Lock and Dam 3 Guidewall extension computed using the CAXPILE VJ criteria.



Appendix F: Final CPGA Input Files and Associated Output for Each Incremental Stage of Pushover Analysis Number 1 for a Lock and Dam 3 Approach Wall Batter Pile Group in Its Layered Soil Site

Note: All output results are a subset of the total output.

F.1 Increment 1: Initial dead load

F.1.1 Pile Cap Output File

```

10 Lock and Dam 3 - Dead Loads - Pile Cap Output
20 PIL 1 0 0 0
30 ANG 0 1
40 PIL 2 7 0 0
50 BAT 4 2
60 ANG 0 2
70 PIL 3 14 0 0
80 BAT 4 3
90 ANG 0 3
100 PRO 5124 16286 16286 452.4 0.35 0 1 2 3
110 SOI NH 0.025 L 72 24 1
120 RED 1 1 1
130 SOI NH 0.025 L 74.2 24.7 2 3
140 RED 1 1 2
150 ALL R 1000 242 1485 933 8544 8544 1 2 3
160 UNS S 0.6 0.6 1000 1000 N 1 2 3
170 FUN 355 355 1 2 3
180 FIX 1 2 3
190 LOA 1 0 0 200 0 0 0
200 TOUT 1 2 3 4 5 6 7
210 PLB ALL

```

F.1.2 Pile cap output results

```

*****
*****
PILE CAP DISPLACEMENTS
LOAD
CASE DX DY DZ RX RY RZ
IN IN IN RAD RAD RAD
1 -0.2530E+00 0.0000E+00 0.1533E+00 0.0000E+00 0.6577E-03 0.0000E+00
*****
*****

```

```

PILE FORCES IN LOCAL GEOMETRY
M1 & M2 NOT AT PILE HEAD FOR PINNED PILES
* INDICATES PILE FAILURE
# INDICATES CBF BASED ON MOMENTS DUE TO
(F3*EMIN) FOR CONCRETE PILES
B INDICATES BUCKLING CONTROLS
LOAD CASE - 1
PILE F1 F2 F3 M1 M2 M3 ALF CBF
K K K IN-K IN-K IN-K
1 -1.3 0.0 183.7 0.0 -158.0 0.0 0.18 0.14
FUNSMOM 0.0 312.3 0.16
2 -1.4 0.0 39.2 0.0 -183.7 0.0 0.04 0.05
FUNSMOM 0.0 315.2 0.06
3 -1.3 0.0 -23.1 0.0 -150.4 0.0 0.10 0.04
FUNSMOM 0.0 294.8 0.06

```

```

*****
*****

```

F.1.3 Mudline output file

```

10 Lock and Dam 3 - Dead Loads - Mudline Output
20 PIL 1 0 0 0
30 ANG 0 1
40 PIL 2 7 0 0
50 BAT 4 2
60 ANG 0 2
70 PIL 3 14 0 0
80 BAT 4 3
90 ANG 0 3
100 PRO 5124 16286 16286 452.4 0.35 0 1 2 3
110 SOI NH 0.025 L 72 24 1
120 RED 1 1 1
130 SOI NH 0.025 L 74.2 24.7 2 3
140 RED 1 1 2
150 ALL R 1000 242 1485 933 8544 8544 1 2 3
160 UNS S 0.6 0.6 1000 1000 N 1 2 3
170 PMA 335 335 1 2 3
180 FUN 355 355 1 2 3
190 FIX 1 2 3
200 LOA 1 0 0 200 0 0 0
210 TOUT 1 2 3 4 5 6 7
220 PLB ALL

```

F.1.4 Mudline output results

```

*****
*****
PILE CAP DISPLACEMENTS
LOAD
CASE DX DY DZ RX RY RZ
IN IN IN RAD RAD RAD
1 -0.2530E+00 0.0000E+00 0.1533E+00 0.0000E+00 0.6577E-03 0.0000E+00

```

```

*****
*****
PILE FORCES IN LOCAL GEOMETRY
M1 & M2 NOT AT PILE HEAD FOR PINNED PILES
* INDICATES PILE FAILURE
# INDICATES CBF BASED ON MOMENTS DUE TO
(F3*EMIN) FOR CONCRETE PILES
B INDICATES BUCKLING CONTROLS
LOAD CASE - 1
PILE F1 F2 F3 M1 M2 M3 ALF CBF
K K K IN-K IN-K IN-K
1 -1.3 0.0 183.7 0.0 -158.0 0.0 0.18 0.14
FUNSMOM 0.0 312.3 0.16
2 -1.4 0.0 39.2 0.0 -183.7 0.0 0.04 0.05
FUNSMOM 0.0 315.2 0.06
3 -1.3 0.0 -23.1 0.0 -150.4 0.0 0.10 0.04
FUNSMOM 0.0 294.8 0.06
*****
*****

```

F.2 Increment 2: Loss of pile cap fixity: Pile 1

F.2.1 Pile Cap Output File

```

10 Lock and Dam 3 - Increment 2 - Pile Cap Output
20 PIL 1 0 0 0
30 ANG 0 1
40 PIL 2 7 0 0
50 BAT 4 2
60 ANG 0 2
70 PIL 3 14 0 0
80 BAT 4 3
90 ANG 0 3
100 PRO 5124 16286 16286 452.4 0.35 0 1 2 3
110 SOI NH 0.025 L 72 24 1
120 RED 1 1 1
130 SOI NH 0.025 L 74.2 24.7 2 3
140 RED 1 1 2
150 ALL R 1000 242 1485 933 8544 8544 1 2 3
160 UNS S 0.6 0.6 1000 1000 N 1 2 3
170 FUN 355 355 1 2 3
180 FIX 1 2 3
190 LOA 1 170 0 0 0 0 0
200 TOUT 1 2 3 4 5 6 7
210 PFO ALL
220 PLB ALL

```

F.2.2 Pile cap output results

```

*****
*****
PILE CAP DISPLACEMENTS
LOAD

```

```

CASE DX DY DZ RX RY RZ
IN IN IN RAD RAD RAD
1 0.2483E+01 0.0000E+00 -0.2151E+00 0.0000E+00 0.2225E-02 0.0000E+00

*****
*****
PILE FORCES IN LOCAL GEOMETRY
M1 & M2 NOT AT PILE HEAD FOR PINNED PILES
* INDICATES PILE FAILURE
# INDICATES CBF BASED ON MOMENTS DUE TO
(F3*EMIN) FOR CONCRETE PILES
B INDICATES BUCKLING CONTROLS
LOAD CASE - 1
PILE F1 F2 F3 M1 M2 M3 ALF CBF
K K K IN-K IN-K IN-K
1 35.3 0.0 -257.8 0.0 8060.1 0.0 1.07 1.22 *
FUNSMOM 0.0 -4484.0 0.80
2 33.8 0.0 246.8 0.0 7860.9 0.0 0.25 1.22 *
FUNSMOM 0.0 -4137.3 0.72
3 34.3 0.0 36.0 0.0 7973.4 0.0 0.04 0.96
FUNSMOM 0.0 -4206.3 0.52

*****
*****

```

F.2.3 Mudline output file

```

10 Lock and Dam 3 - Increment 2 - Mudline Output
20 PIL 1 0 0 0
30 ANG 0 1
40 PIL 2 7 0 0
50 BAT 4 2
60 ANG 0 2
70 PIL 3 14 0 0
80 BAT 4 3
90 ANG 0 3
100 PRO 5124 16286 16286 452.4 0.35 0 1 2 3
110 SOI NH 0.025 L 72 24 1
120 RED 1 1 1
130 SOI NH 0.025 L 74.2 24.7 2 3
140 RED 1 1 2
150 ALL R 1000 242 1485 933 8544 8544 1 2 3
160 UNS S 0.6 0.6 1000 1000 N 1 2 3
170 PMA 335 335 1 2 3
180 FUN 355 355 1 2 3
190 FIX 1 2 3
200 LOA 1 170 0 0 0 0 0
210 TOUT 1 2 3 4 5 6 7
220 PFO ALL
230 PLB ALL

```

F.2.4 Mudline output results

```

*****
*****

```

```

PILE CAP DISPLACEMENTS
LOAD
CASE DX DY DZ RX RY RZ
IN IN IN RAD RAD RAD
1 0.2483E+01 0.0000E+00 -0.2151E+00 0.0000E+00 0.2225E-02 0.0000E+00

*****
*****
PILE FORCES IN LOCAL GEOMETRY
M1 & M2 NOT AT PILE HEAD FOR PINNED PILES
* INDICATES PILE FAILURE
# INDICATES CBF BASED ON MOMENTS DUE TO
(F3*EMIN) FOR CONCRETE PILES
B INDICATES BUCKLING CONTROLS
LOAD CASE - 1
PILE F1 F2 F3 M1 M2 M3 ALF CBF
K K K IN-K IN-K IN-K
1 35.3 0.0 -257.8 0.0 8060.1 0.0 1.07 1.22 *
FUNSMOM 0.0 -4484.0 0.80
2 33.8 0.0 246.8 0.0 7860.9 0.0 0.25 1.22 *
FUNSMOM 0.0 -4137.3 0.72
3 34.3 0.0 36.0 0.0 7973.4 0.0 0.04 0.96
FUNSMOM 0.0 -4206.3 0.52

*****
*****

```

F.3 Increment 3: Loss of pile cap fixity: Piles 2 & 3

F.3.1 Pile cap output file

```

10 Lock and Dam 3 - Increment 3 - Pile Cap Output
20 PIL 1 0 0 0
30 ANG 0 1
40 PIL 2 7 0 0
50 BAT 4 2
60 ANG 0 2
70 PIL 3 14 0 0
80 BAT 4 3
90 ANG 0 3
100 PRO 5124 16286 16286 452.4 0.35 0 1 2 3
110 SOI NH 0.025 L 72 24 1
120 RED 1 1 1
130 SOI NH 0.025 L 74.2 24.7 2 3
140 RED 1 1 2
150 ALL R 1000 242 1485 933 8544 8544 1 2 3
160 UNS S 0.6 0.6 1000 1000 N 1 2 3
170 FUN 355 355 1 2 3
180 FIX 2 3
190 PIN 1
200 LOA 1 10 0 0 0 0 0
210 TOUT 1 2 3 4 5 6 7
220 PFO ALL
230 PLB ALL

```

F.3.2 Pile cap output results

```

*****
*****
PILE CAP DISPLACEMENTS
LOAD
CASE DX DY DZ RX RY RZ
IN IN IN RAD RAD RAD
1 0.1858E+00 0.0000E+00 -0.1331E-01 0.0000E+00 0.2004E-03 0.0000E+00

*****
*****
PILE FORCES IN LOCAL GEOMETRY
M1 & M2 NOT AT PILE HEAD FOR PINNED PILES
* INDICATES PILE FAILURE
# INDICATES CBF BASED ON MOMENTS DUE TO
(F3*EMIN) FOR CONCRETE PILES
B INDICATES BUCKLING CONTROLS
LOAD CASE - 1
PILE F1 F2 F3 M1 M2 M3 ALF CBF
K K K IN-K IN-K IN-K
1 0.6 0.0 -16.0 0.0 0.0 0.0 0.07 0.02
2 2.6 0.0 18.4 0.0 613.3 0.0 0.02 0.08
FUNSMOM 0.0 -314.5 0.05
3 2.7 0.0 -0.6 0.0 623.4 0.0 0.00 0.07
FUNSMOM 0.0 -320.7 0.04

*****
*****

```

F.3.3 Mudline output file

```

10 Lock and Dam 3 - Increment 3 - Mudline Output
20 PIL 1 0 0 0
30 ANG 0 1
40 PIL 2 7 0 0
50 BAT 4 2
60 ANG 0 2
70 PIL 3 14 0 0
80 BAT 4 3
90 ANG 0 3
100 PRO 5124 16286 16286 452.4 0.35 0 1 2 3
110 SOI NH 0.025 L 72 24 1
120 RED 1 1 1
130 SOI NH 0.025 L 74.2 24.7 2 3
140 RED 1 1 2
150 ALL R 1000 242 1485 933 8544 8544 1 2 3
160 UNS S 0.6 0.6 1000 1000 N 1 2 3
170 PMA 335 335 1 2 3
180 FUN 335 335 1 2 3
190 FIX 2 3
200 PIN 1
210 LOA 1 10 0 0 0 0 0
220 TOUT 1 2 3 4 5 6 7
230 PFO ALL

```

240 PLB ALL

F.3.4 Mudline output results

```
*****
*****
PILE CAP DISPLACEMENTS
LOAD
CASE DX DY DZ RX RY RZ
IN IN IN RAD RAD RAD
1 0.1858E+00 0.0000E+00 -0.1331E-01 0.0000E+00 0.2004E-03 0.0000E+00
*****
*****
PILE FORCES IN LOCAL GEOMETRY
M1 & M2 NOT AT PILE HEAD FOR PINNED PILES
* INDICATES PILE FAILURE
# INDICATES CBF BASED ON MOMENTS DUE TO
(F3*EMIN) FOR CONCRETE PILES
B INDICATES BUCKLING CONTROLS
LOAD CASE - 1
PILE F1 F2 F3 M1 M2 M3 ALF CBF
K K K IN-K IN-K IN-K
1 0.6 0.0 -16.0 0.0 -192.5 0.0 0.07 0.04
2 2.6 0.0 18.4 0.0 613.3 0.0 0.02 0.08
FUNSMOM 0.0 -262.2 0.04
3 2.7 0.0 -0.6 0.0 623.4 0.0 0.00 0.07
FUNSMOM 0.0 -267.5 0.03
*****
*****
```

F.4 Increment 4: Loss of tensile capacity: Pile 1

F.4.1 Mudline output file

```
10 Lock and Dam 3 - Increment 4 - Mudline Output
20 PIL 1 0 0 0
30 ANG 0 1
40 PIL 2 7 0 0
50 BAT 4 2
60 ANG 0 2
70 PIL 3 14 0 0
80 BAT 4 3
90 ANG 0 3
100 PRO 5124 16286 16286 452.4 0.35 0 1 2 3
110 SOI NH 0.025 L 72 24 1
120 RED 1 1 1
130 SOI NH 0.025 L 74.2 24.7 2 3
140 RED 1 1 2
150 ALL R 1000 242 1485 933 8544 8544 1 2 3
160 UNS S 0.6 0.6 1000 1000 N 1 2 3
170 PMA 335 335 1 2 3
180 PIN 1 2 3
190 LOA 1 38 0 0 0 0 0
```

```

200 TOUT 1 2 3 4 5 6 7
210 PFO ALL
220 PLB ALL

```

F.4.2 Mudline output results

```

*****
*****
PILE CAP DISPLACEMENTS
LOAD
CASE DX DZ R
IN IN RAD
1 0.1826E+01 -0.7032E-01 0.2750E-02

*****
*****
ELASTIC CENTER INFORMATION
ELASTIC CENTER IN PLANE X-Z X Z
FT FT
1.10 -35.30
LOAD MOMENT IN
CASE X-Z PLANE
1 0.00000E+00

*****
*****
PILE FORCES IN LOCAL GEOMETRY
M1 & M2 NOT AT PILE HEAD FOR PINNED PILES
* INDICATES PILE FAILURE
# INDICATES CBF BASED ON MOMENTS DUE TO
(F3*EMIN) FOR CONCRETE PILES
B INDICATES BUCKLING CONTROLS
LOAD CASE - 1
PILE F1 F2 F3 M1 M2 M3 ALF CBF
K K K IN-K IN-K IN-K
1 5.6 0.0 -84.3 0.0 -1892.2 0.0 0.35 0.31
2 5.4 0.0 175.1 0.0 -1805.3 0.0 0.18 0.33
3 5.6 0.0 -85.5 0.0 -1860.1 0.0 0.35 0.31

*****
*****

```

F.5 Increment 5: Mudline hinge: Pile 1

F.5.1 Mudline output file

```

10 Lock and Dam 3 - Increment 5 - Mudline Output
20 PIL 1 0 0 0
30 ANG 0 1
40 PIL 2 7 0 0
50 BAT 4 2
60 ANG 0 2
70 PIL 3 14 0 0
80 BAT 4 3
90 ANG 0 3
100 PRO 5124 16286 16286 452.4 0.35 0 2 3

```

```

110 PRO 5124 16286 16286 452.4 0.0001 0 1
120 SOI NH 0.025 L 72 24 1
130 RED 1 1 1
140 SOI NH 0.025 L 74.2 24.7 2 3
150 RED 1 1 2
160 ALL R 1000 242 1485 933 8544 8544 1 2 3
170 UNS S 0.6 0.6 1000 1000 N 1 2 3
180 PMA 335 335 1 2 3
190 PIN 1 2 3
200 LOA 1 6 0 0 0 0 0
210 TOUT 1 2 3 4 5 6 7
220 PFO ALL
230 PLB ALL

```

F.5.2 Mudline output results

```

*****
*****
PILE CAP DISPLACEMENTS
LOAD
CASE DX DZ R
IN IN RAD
1 0.6435E+00 -0.1602E+00 0.2103E-05

*****
*****
ELASTIC CENTER INFORMATION
ELASTIC CENTER IN PLANE X-Z X Z
FT FT
10.47 -0.11
LOAD MOMENT IN
CASE X-Z PLANE
1 0.00000E+00

*****
*****
PILE FORCES IN LOCAL GEOMETRY
M1 & M2 NOT AT PILE HEAD FOR PINNED PILES
* INDICATES PILE FAILURE
# INDICATES CBF BASED ON MOMENTS DUE TO
(F3*EMIN) FOR CONCRETE PILES
B INDICATES BUCKLING CONTROLS
LOAD CASE - 1
PILE F1 F2 F3 M1 M2 M3 ALF CBF
K K K IN-K IN-K IN-K
1 2.0 0.0 -0.1 0.0 -666.7 0.0 0.00 0.08
2 1.9 0.0 0.6 0.0 -649.0 0.0 0.00 0.08
3 1.9 0.0 0.4 0.0 -649.0 0.0 0.00 0.08

*****
*****

```

F.6 Increment 6: Mudline hinge: Pile 3

F.6.1 Mudline output file

```

10 BATTER PILE BENT FIXED TOP FILE:BF7
20 PIL 1 7 0 0
30 BAT 4 1
40 ANG 0 1
50 PIL 2 14 0 0
60 BAT 4 2
70 ANG 0 2
80 PRO 5124 16286 16286 452.4 0.35 0 1 2
90 SOI NH 0.025 L 74.2 24.7 1 2
100 RED 1 1 1
110 ALL R 1000 242 1485 933 8544 8544 1 2
120 UNS S 0.6 0.6 1000 1000 N 1 2
130 PMA 335 335 1 2
140 PIN 1 2
150 LOA 1 7 0 0 0 0 0
160 TOUT 1 2 3 4 5 6 7
170 PFO ALL
180 PLB ALL

```

F.6.2 Mudline output results

```

*****
*****
PILE CAP DISPLACEMENTS
LOAD
CASE DX DZ R
IN IN RAD
1 0.1128E+01 -0.2812E+00 0.2446E-17

*****
*****
ELASTIC CENTER INFORMATION
ELASTIC CENTER IN PLANE X-Z X Z
FT FT
10.50 0.00
LOAD MOMENT IN
CASE X-Z PLANE
1 0.00000E+00

*****
*****
PILE FORCES IN LOCAL GEOMETRY
M1 & M2 NOT AT PILE HEAD FOR PINNED PILES
* INDICATES PILE FAILURE
# INDICATES CBF BASED ON MOMENTS DUE TO
(F3*EMIN) FOR CONCRETE PILES
B INDICATES BUCKLING CONTROLS
LOAD CASE - 1
PILE F1 F2 F3 M1 M2 M3 ALF CBF

```

```

K K K IN-K IN-K IN-K
1 3.4 0.0 0.8 0.0 -1137.5 0.0 0.00 0.13
2 3.4 0.0 0.8 0.0 -1137.5 0.0 0.00 0.13
*****
*****

```

F.7 Increment 7: Mudline hinge: Pile 2

F.7.1 Mudline output file

```

10 BATTER PILE BENT FIXED TOP FILE:BF7
20 PIL 1 7 0 0
30 BAT 4 1
40 ANG 0 1
50 PIL 2 14 0 0
60 BAT 4 2
70 ANG 0 2
80 PRO 5124 16286 16286 452.4 0.35 0 1 2
90 SOI NH 0.025 L 74.2 24.7 1
100 RED 1 1 1
110 SOI NH 0.025 L 28 24.7 2
120 RED 1 1 2
130 ALL R 1000 242 1485 933 8544 8544 1 2
140 UNS S 0.6 0.6 1000 1000 N 1 2
150 PMA 335 335 1 2
160 PIN 1 2
170 LOA 1 3.5 0 0 0 0 0
180 TOUT 1 2 3 4 5 6 7
190 PFO ALL
200 PLB ALL

```

F.7.2 Mudline output results

```

*****
*****
PILE CAP DISPLACEMENTS
LOAD
CASE DX DZ R
IN IN RAD
1 0.5639E+00 -0.1403E+00 0.3559E-05
*****
*****
ELASTIC CENTER INFORMATION
ELASTIC CENTER IN PLANE X-Z X Z
FT FT
12.67 -0.54
LOAD MOMENT IN
CASE X-Z PLANE
1 0.00000E+00
*****
*****
PILE FORCES IN LOCAL GEOMETRY
M1 & M2 NOT AT PILE HEAD FOR PINNED PILES
* INDICATES PILE FAILURE
# INDICATES CBF BASED ON MOMENTS DUE TO
(F3*EMIN) FOR CONCRETE PILES

```

B INDICATES BUCKLING CONTROLS
 LOAD CASE - 1
 PILE F1 F2 F3 M1 M2 M3 ALF CBF
 K K K IN-K IN-K IN-K
 1 1.7 0.0 0.4 0.0 -568.7 0.0 0.00 0.07

2 1.7 0.0 0.4 0.0 -568.8 0.0 0.00 0.07

F.8 Results tables

Table F.1. Global displacements and forces at the impact deck for the Lock and Dam 3 structural system at each incremental analysis step with $C_{33}=0.35$.

Increment Number	Incremental		Cumulative		Notes
	Lateral Load (kip)	Displacement (in.)	Lateral Load (kip)	Displacement (in.)	
1	0.0	-0.253	0.0	-0.253	-200 kips vertical load [1] Fig. 4.1
2	170.0	2.483	170.0	2.23	[2] Fig. 4.1
3	10.0	0.1858	180.0	2.4158	[3][4] Fig. 4.1
4	38.0	1.826	218.0	4.2418	[5] Fig. 4.1
5	6.0	0.6435	224.0	4.8853	[6] Fig. 4.1
6	7	1.128	231	6.0133	[7] Fig. 4.1
7	3.5	0.564	234.5	6.5773	[8] Fig. 4.1

Table F.2. Axial force, pile cap moment, and mudline moment for the three piles in the Lock and Dam 3 structural system at each incremental analysis step with $C_{33}=0.35$.

Increment Number	Pile Number	Incremental			Cumulative			Notes
		Axial Force (kips)	Pile Cap Moment (in.-kips)	Mudline Moment (in.-kips)	Axial Force (kips)	Pile Cap Moment (in.-kips)	Mudline Moment (in.-kips)	
1	1	183.7	-158	312	183.7	-158	312	
	2	39.2	-184	315	39.2	-184	315	
	3	-23.1	-150	295	-23.1	-150	295	
2	1	-257.8	8060	-4484	-74.1	7902	-4172	
	2	246.8	7861	-4137	286	7677	-3822	
	3	36	7973	-4206	12.9	7823	-3911	
3	1	-16		-193	-90.1		-4365	Loss of Pile Cap Fixity for Pile #1
	2	18.4	613	-262	304.4	8290	-4084	
	3	-0.6	623	-268	12.3	8446	-4179	
4	1	-84.3		-1892	-174.4		-6257	Loss of Pile Cap
	2	175.1		-1805	479.5		-5889	

Increment Number	Pile Number	Incremental			Cumulative			Notes
		Axial Force (kips)	Pile Cap Moment (in.-kips)	Mudline Moment (in.-kips)	Axial Force (kips)	Pile Cap Moment (in.-kips)	Mudline Moment (in.-kips)	
	3	-85.5		-1860	-73.2		-6039	Fixity for Piles #2 and #3
5	1	-0.1		-667	-174.5		-6924	
	2	0.6		-649	480.1		-6538	
	3	0.4		-649	-72.8		-6688	
6	1	0		0	0		0	
	2	0.8		-1137.5	480.9		-7675.5	
	3	0.8		1137.5	-72.0		-7825.5	
7	1	0		0	0		0	
	2	0.4		-567.7	481.3		-8244.2	
	3	0.4		-567.8	-71.6		-8394.3	

REPORT DOCUMENTATION PAGE					Form Approved OMB No. 0704-0188	
<p>The public reporting burden for this collection of information is estimated to average 1 hour per response, including the time for reviewing instructions, searching existing data sources, gathering and maintaining the data needed, and completing and reviewing the collection of information. Send comments regarding this burden estimate or any other aspect of this collection of information, including suggestions for reducing the burden, to Department of Defense, Washington Headquarters Services, Directorate for Information Operations and Reports (0704-0188), 1215 Jefferson Davis Highway, Suite 1204, Arlington, VA 22202-4302. Respondents should be aware that notwithstanding any other provision of law, no person shall be subject to any penalty for failing to comply with a collection of information if it does not display a currently valid OMB control number.</p> <p>PLEASE DO NOT RETURN YOUR FORM TO THE ABOVE ADDRESS.</p>						
1. REPORT DATE November 2016		2. REPORT TYPE Technical Report			3. DATES COVERED (From - To)	
4. TITLE AND SUBTITLE Characterizing Axial Stiffness of Individual Batter Piles with Emphasis on Elevated, Laterally Loaded, Clustered Pile Groups				5a. CONTRACT NUMBER		
				5b. GRANT NUMBER		
				5c. PROGRAM ELEMENT NUMBER		
6. AUTHOR(S) Robert M. Ebeling, Barry C. White				5d. PROJECT NUMBER		
				5e. TASK NUMBER		
				5f. WORK UNIT NUMBER 448769		
7. PERFORMING ORGANIZATION NAME(S) AND ADDRESS(ES) Information Technology Laboratory U.S. Army Engineer Research and Development Center 3909 Halls Ferry Road Vicksburg, MS 39180-6199				8. PERFORMING ORGANIZATION REPORT NUMBER ERDC/ITL TR-16-5		
9. SPONSORING/MONITORING AGENCY NAME(S) AND ADDRESS(ES) U.S. Army Corps of Engineers Washington, DC 20314-1000				10. SPONSOR/MONITOR'S ACRONYM(S)		
				11. SPONSOR/MONITOR'S REPORT NUMBER(S) HQUSACE		
12. DISTRIBUTION/AVAILABILITY STATEMENT Approved for public release; distribution is unlimited.						
13. SUPPLEMENTARY NOTES						
14. ABSTRACT <p>This report focuses on an investigation into the engineering characterization of the axial stiffness of individual compression piles embedded within soil. This characterization of axial stiffness is used in the analysis of a clustered pile group's deformation and load distribution response. Its impact on the computed pile group response is most pronounced among a clustered pile group containing batter piles.</p> <p>This characterization is important because the Corps is moving toward low-cost, pile-founded flexible lock approach walls. These walls absorb kinetic energy of barge-train impacts, which occur as the barge train aligns itself to enter the lock. One type of wall is comprised of an elevated impact deck supported by groups of clustered piles, some with batter. These impact decks are supported tens of feet above the mudline.</p> <p>A pushover analysis technique is used to establish the potential energy (PE) capacity and displacement capacity of individual batter pile groups accounting for the various pile failure mechanisms. An appropriate axial stiffness characterization will increase the accuracy of this computation. The total stored energy (PE) of the approach wall system will be the sum of the stored energy of all the pile groups reacting to the barge impact. The study concludes with a pushover analysis of a batter pile configuration used at Lock and Dam 3 flexible approach wall extension.</p> <p>Batter pile groups are constructed of steel pipe or H-piling, which are conducive to in-the-wet construction. This type of construction leads to a cost savings for Corps projects.</p>						
15. SUBJECT TERMS (see reverse)						
16. SECURITY CLASSIFICATION OF:			17. LIMITATION OF ABSTRACT	18. NUMBER OF PAGES	19a. NAME OF RESPONSIBLE PERSON	
a. REPORT	b. ABSTRACT	c. THIS PAGE			Robert M. Ebeling	
Unclassified	Unclassified	Unclassified	SAR	158	19b. TELEPHONE NUMBER (Include area code) 601-634-3458	

15. SUBJECT TERMS (concluded)

Axial pile stiffness
Batter piles
Pushover analysis
Pile Groups
Clustered pile groups
Pile hinge
Flexural yielding
Pile buckling
Barge impact
Barge train impact
Flexible lock approach wall
Flexible approach wall
Guide wall
Guard wall
Elevated deck
Impact deck
Balance of energy
Energy balance